

ASSEMBLY'S EDGE Somerville, Massachusetts

Fresh Air Filtration and Indoor Air Quality
Management Design Concepts

Mike Zimmerman, PE & Rae Nistler
mikez@alliedconsulting.net; rae@alliedconsulting.net

December 28, 2017

Fresh Air Filtration and Indoor Air Quality Management Design Concepts

Assembly's Edge – Somerville Massachusetts

The Residential Building

The Massachusetts Mechanical Code requires that "Living Areas" in residential buildings other than single family and two-family dwelling units be provided with 0.35 air changes per hour of outdoor air or 15 CFM per person, whichever is greater, or approximately 40-60 CFM per apartment. The Massachusetts Energy Code requires that outdoor air units that operate continuously must utilize energy recovery. To meet this fresh air and energy recovery requirement, we propose to employ an Energy Recovery Ventilator (ERV) to recovery heating or cooling energy from the building exhaust, including toilet exhaust and general exhaust to preheat or precool and pre-dehumidify the fresh air brought into the building by the outdoor air unit.

The Energy Recovery Ventilator we have selected will have a MERV 13 filter. The MERV 13 filter was selected based on its commercial availability and price, as well as, its energy and filtration efficiency on particulates in the 3-70 nanometer size range as reported by P. Karjalainen et al. (Karjalainen et al., 2017) in a paper published in Aerosol Science and Technology entitled "Performance of ventilation filtration technologies on characteristic traffic related aerosol down to nanocluster size", a copy of the report is attached. Karjalainen reported that F7 filters, the European classification standard equivalent to MERV 13, efficiently removed nanocluster sized particles below ~3 nm. It was efficient across all particle sizes, but over 99% efficient at removing particles smaller than 30 nm. The fresh air will be heated or cooled and supplied via a galvanized sheetmetal duct system to the common corridors, amenity spaces and each individual apartment, thus assuring that all fresh air introduced into the building and apartments will be provided with pre-filtered fresh air.

Each apartment will have a compressorized heating and cooling unit or units, depending upon the apartment size and orientation, located within the apartment in a centralized location(s). Warm air or cool air will be supplied to the entire apartment via a ducted system within the apartment that utilizes galvanized sheetmetal ductwork to distribute air to each room within the apartment. The heating and cooling unit will be provided with a MERV 13 filter that will filter all the air recirculated within the apartment. The fan of the unit will be allowed to run continuously to maintain the air within the apartment at a very high level of cleanliness. The filtered fresh air system will run constantly and pressurize the building. This system is similar to the Exhaust Ventilation System "E" and Supply Ventilation System "A" described by Brett Singer et al. in "Measured performance of filtration and ventilation systems for fine and ultrafine particles and ozone in an unoccupied modern California house" published in the International Journal of Indoor Environment and Health (copy attached). System "E" achieved more than a 90% reduction in the number of particles in the size range of 6-100 nanometer between the indoor air and the outdoor air. System "A" of the Singer report provided approximately a 70% reduction in the mass of nanoparticles in the indoor air versus the unfiltered outdoor air. This

reduction was achieved without MERV 13 filtration in the recirculated air. The addition of a MERV 13 filter in the recirculation air should yield an even higher level of assurance and greater reduction in nanoparticles.

In addition to the foregoing, all heated and cooled common areas, corridors, storage rooms, etc., will be provided with compressorized heating and cooling units equipped with similar MERV 13 filters in the recirculation air.

The Hotel Building

The Massachusetts Mechanical Code requires that hotel “bedrooms/living rooms” be provided with 5 CFM per person + .06 CFM per sq.ft. of fresh air or approximately 20-40 CFM per hotel room. The Massachusetts Energy Code requires that outdoor air units that operate continuously must utilize energy recovery. To meet this fresh air and energy recovery requirement, we propose to employ an Energy Recovery Ventilator (ERV) to recovery heating or cooling energy from the building exhaust, including toilet exhaust and general exhaust to preheat or precool and pre-dehumidify the fresh air brought into the building by the outdoor air unit.

The Energy Recovery Ventilator we have selected will have a MERV 13 filter. The fresh air will be heated or cooled and supplied via a galvanized sheetmetal duct system to the common corridors, amenity spaces and each individual hotel room, thus assuring that all fresh air introduced into the building and hotel rooms will be provided with pre-filtered fresh air.

Each hotel room or suite will have a compressorized heating and cooling unit located within the unit. Warm air or cool air will be supplied to the unit via supply air grilles installed in the unit discharge plenum. The heating and cooling unit will be provided with a MERV 13 filter.

In addition to the foregoing, all heated and cooled common areas, lobby spaces, offices, corridors, dining rooms and back of house spaces (with the exception of mechanical rooms, laundry rooms, kitchens and similar specialized use spaces), etc., will be provided with compressorized heating and cooling units equipped with MERV 13 filters.

Using the same logic presented in the design of the apartment building at Assembly's Edge, the constant pressurization with outdoor air filtered through MERV 13 filters combined with the recirculated air filtered with MERV 13 filters in the compressorized units in each space, should achieve high levels of nanoparticle reductions in the occupied space.

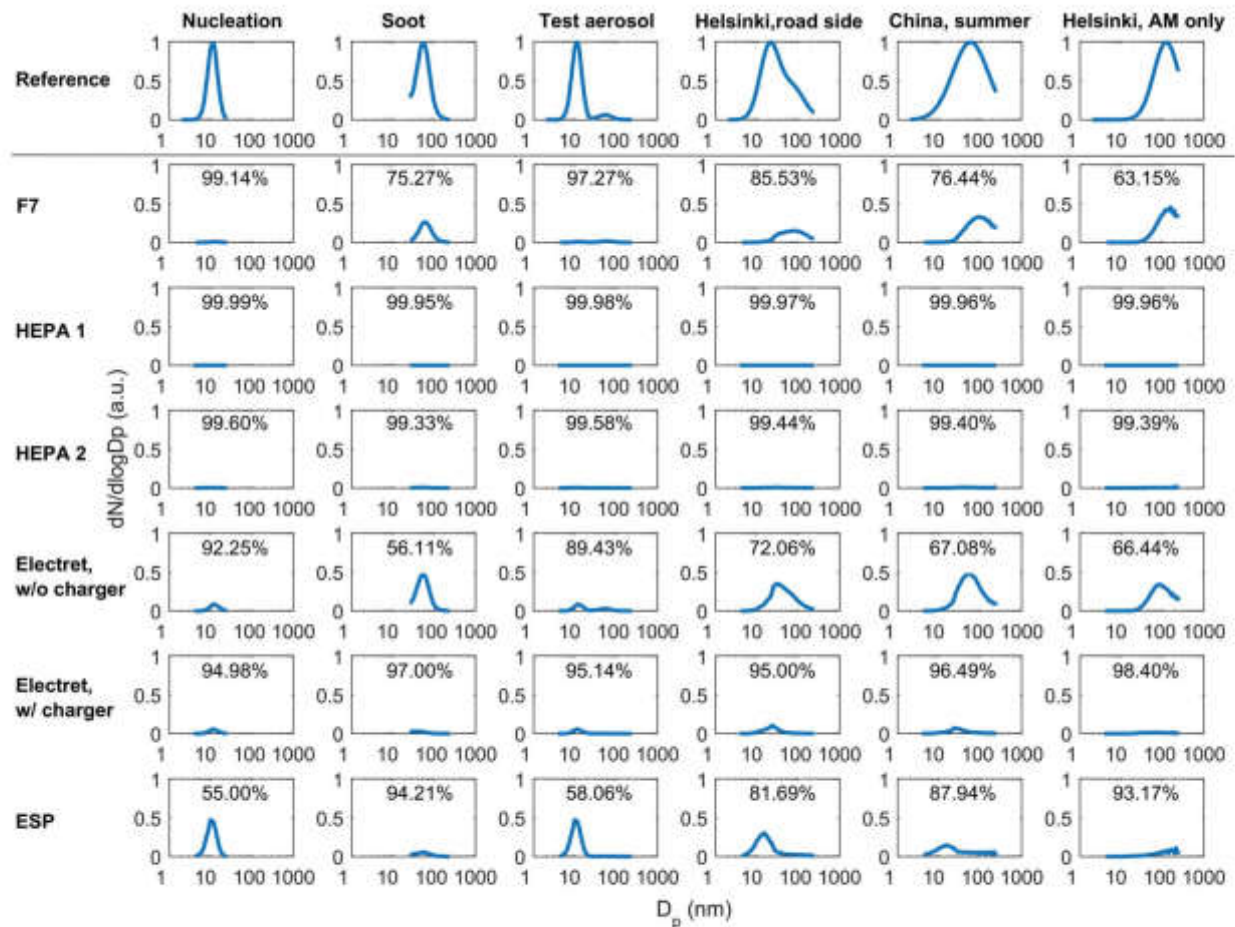
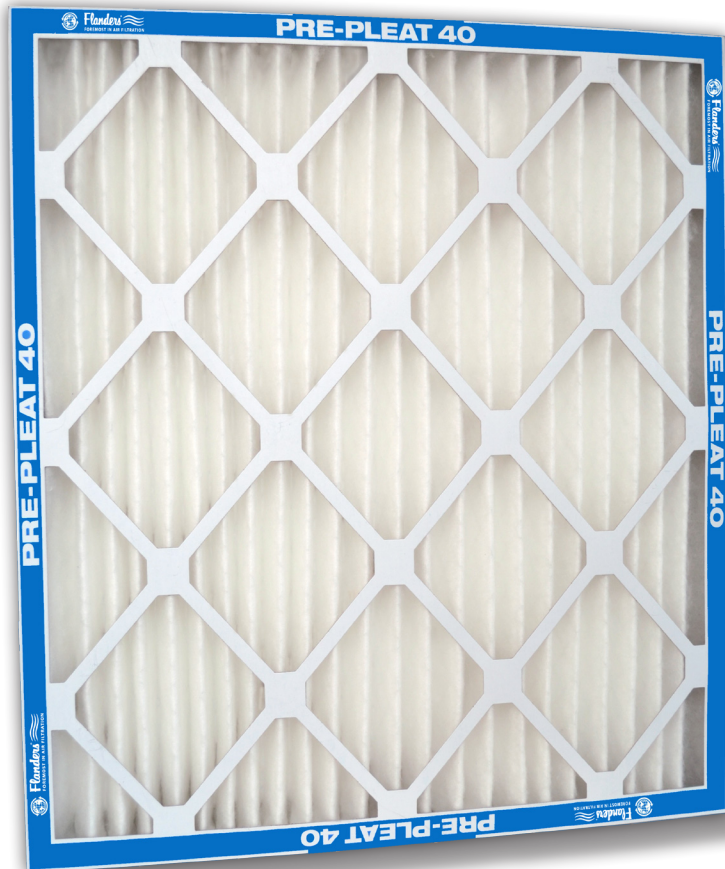


Figure 5. Uppermost row shows the normalized particle size distributions from the left: NM (this study), SM (this study), test aerosol (this study), Helsinki road side (Virtanen et al. 2006), Peking (Wu et al. 2008), Helsinki accumulation mode (AM) only (Hussein et al. 2004). The rows below indicate what size distribution exists indoor after row corresponding filtration, and the percentages indicate the total number filtration efficiency for the corresponding aerosol.

ASHRAE Standard 52.2-1999				ASHRAE 52.1		EN	EN779:2012			EN 1822
Minimum Eff Reporting Value	Composite Average Particle Size Efficiency % in Size Range, µm			Average Arrestance	Average Dust Spot Efficiency	Filter Class	Av. Arrestance of Syn. Dust	Average Eff at 0.4 µm	Min. Eff at 0.4 µm	Average Eff at MPPS
	Range 1	Range 2	Range 3	NB. This standard is obsolete and here for reference only. Performances are not equivalent to ASHREA 52:2 or EN779.			Test Final DP 250Pa	Test Final DP 450Pa		
(MERV)	0.30 - 1.0	1.0 - 3.0	3.0 - 10.0	%	%		%	%	%	%
1	n/a	n/a	E3<20	Aavg<65	<20	G1	50≤Am≤65			
2	n/a	n/a	E3<20	Aavg<65	<20	G2	65≤Am≤80			
3	n/a	n/a	E3<20	Aavg<70	<20					
4	n/a	n/a	E3<20	Aavg<75	<20					
5	n/a	n/a	E3≥20	80	20	G3	80≤Am≤90			
6	n/a	n/a	E3≥35	85	20-25					
7	n/a	n/a	E3≥50	90	25-30	G4	90Am≤			
8	n/a	n/a	E3≥70	92	30-35					
9	n/a	n/a	E3≥85	95	40-45	M5		40≤Em≤60		
10	n/a	E2≥50	E3≥85	96	50-55					
11	n/a	E2≥65	E3≥85	97	60-65	M6		60≤Em≤80		
12	n/a	E2≥80	E3≥90	98	70-75					
13	n/a	E2≥90	E3≥90	98	80-85	F7		80≤Em≤90	35	
14	E1≥75	E2≥90	E3≥90	99	90-95	F8		90≤Em≤95	55	
15	E1≥85	E2≥90	E3≥90	99	95	F9		95≤Em	70	
16	E1≥95	E2≥95	E3≥95	100	99	E10				<85
N/A	N/A	N/A	N/A	N/A	N/A	E11				<95
						E12				<99.5
						H13				<99.95
						H14				<99.995
						U15				<99.9995
						U16				<99.99995
						U17				<99.999995

Note: The final MERV value is the highest MERV where the filter data meets all requirements of that MERV.



Pre Pleat M13

- Complies with the Air Filter requirements of Credits 1.4 and 1.5 under LEED® IEQ Version 3
- Contributes to satisfying the following LEED® Version 3 Credits:
 - Energy & Atmosphere:
Credit 1.0
 - Materials & Resources:
Credit 1.0
 - Indoor Environmental Quality:
Credits 1.1 and 3.2
 - Innovation:
Credit: 1.0

Pre Pleat® M13

MERV 13 Pleated Filter

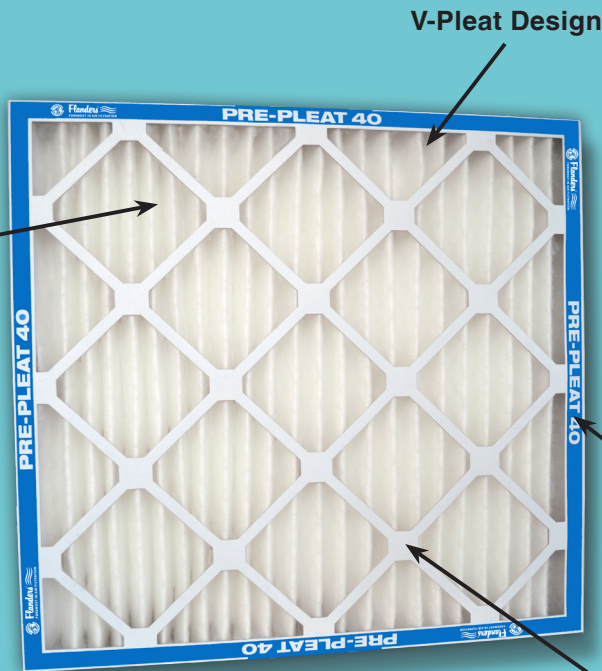
Low Initial Resistance for Reducing Energy



Flanders has led the world in filter media development and the application of high efficiency filtration for over 60-years. Pre Pleat M13 pleated panel filters can be an ideal choice to achieve the compliance requirements of LEED® V3 IEQ Credits 1.4 and 1.5. The low initial resistance of the M13 can also contribute an overall strategy of reducing energy consumption. Its one, two and four inch depths makes MERV 13 upgrades as trouble-free as a direct replacement for most commercial and industrial applications.

Construction / Physical Data

**100% Synthetic
Recyclable High-Loft
Media**



Additional Features:

- 2-Piece heavy duty die-cut frame
- New designed expanded metal backing

Double-Wall Frame

**Diagonal grid supports for
maximum strength**

Airflow Resistance

- 1" Depth: .25" w.g. @ 300 FPM
- 2" Depth: .30" w.g. @ 500 FPM
- 4" Depth: .23" w.g. @ 500 FPM

Media

100% Non-woven synthetic media manufactured from recyclable material.

Media Support

Diamond-shaped expanded metal maintains maximum support while avoiding air by-pass.

Pleat Design

V-Pleat design minimizes resistance keeping consistent pleat count, height and shape.

Frame

Heavy-duty two piece moisture-resistant frame includes diagonal and horizontal support members bonded to the media on the air entering and leaving sides. Durable for any commercial and industrial application.

General

The Pre Pleat M13 provides an initial efficiency of MERV 13 per ASHRAE 52.2-2007 (80-85%) at a resistance of only .20" w.g. (2" depth) when operating at approach velocity of 375 FPM - only 0.30 at 500 FPM.

Installation Considerations

Distinctions can be made in air filter technology. Flanders is committed to continuously developing new and improved products to assist in an environmentally responsible, healthy, and prosperous environment.

The Pre Pleat M13 pleated panel filters are suitable as pre filters but are best suited for heavy duty commercial, industrial, and pharmaceutical applications. The Pre Pleat M13 can be installed in PF-1 Holding Frames, K-Trac Framing Modules, Surepleat Side Access Housings and Bag-In / Bag-Out Containment housings.

Operating Temperature Limits

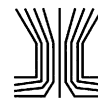
Maximum operating temperature is 180°F (82.22°C).

Capacities and Dimensions

Nominal Depth (in.)	Nominal Size WxHxD (in.)	Air Flow Capacity				Media Area (sq. ft.)	Wt. Each (lbs.)
		300 FPM		500 FPM			
		CFM	PD	CFM	PD		
1” Air Flow Capacity 15 ppf	10x20x1	417	0.25	694	-	2.7	0.3
	12x20x1	500	0.25	833	-	3.1	0.3
	12x24x1	600	0.25	1000	-	3.7	0.4
	14x20x1	583	0.25	972	-	3.7	0.4
	14x25x1	729	0.25	1215	-	4.6	0.5
	15x20x1	625	0.25	1042	-	3.9	0.4
	16x20x1	667	0.25	1111	-	4.1	0.4
	16x24x1	800	0.25	1333	-	4.9	0.5
	16x25x1	833	0.25	1389	-	5.2	0.5
	18x20x1	750	0.25	1250	-	4.7	0.5
	18x24x1	900	0.25	1500	-	5.7	0.6
	18x25x1	938	0.25	1563	-	5.9	0.6
	20x20x1	833	0.25	1389	-	5.1	0.5
	20x24x1	1000	0.25	1667	-	6.2	0.6
	20x25x1	1042	0.25	1736	-	6.4	0.6
	24x24x1	1200	0.25	2000	-	7.4	0.7
	25x25x1	1302	0.25	2170	-	8.3	0.8
2” Air Flow Capacity 15 ppf	10x20x2	417	0.15	694	0.30	6.1	0.6
	12x20x2	500	0.15	833	0.30	7.3	0.7
	12x24x2	600	0.15	1000	0.30	8.8	0.8
	14x20x2	583	0.15	972	0.30	8.5	0.8
	14x25x2	729	0.15	1215	0.30	10.6	1.0
	15x20x2	625	0.15	1042	0.30	9.1	0.8
	16x20x2	667	0.15	1110	0.30	9.7	0.9
	16x24x2	800	0.15	1335	0.30	11.2	1.0
	16x25x2	833	0.15	1390	0.30	12.2	1.1
	18x20x2	750	0.15	1250	0.30	10.9	1.2
	18x24x2	900	0.15	1500	0.30	13.1	1.3
	18x25x2	938	0.15	1563	0.30	13.7	1.1
	20x20x2	833	0.15	1390	0.30	12.2	1.3
	20x24x2	1000	0.15	1667	0.30	14.6	1.3
	20x25x2	1042	0.15	1735	0.30	15.2	1.5
	24x24x2	1200	0.15	2000	0.30	17.5	1.6
	25x25x2	1302	0.15	2170	0.30	19.0	1.6
4” Air Flow Capacity 9 ppf	12x24x4	600	0.13	1000	0.23	11.3	.09
	16x20x4	667	0.13	1110	0.23	12.5	1.0
	16x25x4	833	0.13	1390	0.23	15.6	1.3
	18x24x4	900	0.13	1500	0.23	17.5	1.4
	20x20x4	833	0.13	1390	0.23	15.6	1.3
	20x24x4	1000	0.13	1667	0.23	18.8	1.5
	20x25x4	1042	0.13	1735	0.23	19.6	1.6
	24x24x4	1200	0.13	2000	0.23	22.6	1.8
	28x30x4	1750	0.13	2915	0.23	32.6	2.8

Notes:

1. PD represents clean pressure drop in inches w.g. The recommended final pressure drop for all models is 1.0 in. w.g. System design may dictate a lower change-out point.
2. Actual filter face size for 12x24 and 24x24 filters is 5/8 inch under on height and width. Actual face size on all other sizes is 1/2 inch under on height and width.
3. Actual filter depth is 1/4 inch under for these nominal 1-inch, 2-inch and 4-inch deep filters. For capacities other than those shown, ratio the face velocities.



Performance of ventilation filtration technologies on characteristic traffic related aerosol down to nanocluster size

Panu Karjalainen^a, Sampo Saari^a, Heino Kuuluvainen^a, Tapio Kalliohaka^b, Aimo Taipale^b, and Topi Rönkkö^a

^aAerosol Physics Laboratory, Faculty of Natural Sciences, Tampere University of Technology, Tampere, Finland; ^bClean Air Solutions, VTT Technical Research Centre of Finland Ltd., Tampere, Finland

ABSTRACT

Near traffic routes and urban areas, the outdoor air particle number concentration is typically dominated by ultrafine particles. These particles can enter into the nearby buildings affecting the human exposure on ultrafine particles indoors. In this study, we demonstrate an aerosol generation system which mimics the characteristic traffic related aerosol. The aerosol generation system was used to determine the size-resolved particle filtration efficiencies of five typical commercial filters in the particle diameter range of 1.3–240 nm. Two different HEPA filters were observed to be efficient in all particle sizes. A fibrous filter (F7) was efficient at small particle sizes representing the nucleation mode of traffic related aerosol, but its efficiency decreased down to 60% with the increasing particle size. In contrast, the filtration efficiency of an electrostatic precipitator (ESP) increased as a function of the particle size, being more efficient for the soot mode of traffic related aerosol than for the nucleation mode. An electret filter with a charger was relatively efficient (filtration efficiency >85%) at all the observed particle sizes. The HEPA, F7 and electret filters were found to practically remove the particles/nanoclusters smaller than 3 nm. All in all, the filtration efficiencies were observed to be strongly dependent on the particle size and significant differences were found between different filters. Based on these results, we suggest that the particulate filter test standards should be extended to cover the ultrafine particles, which dominate the particle concentrations in outdoor air and are hazardous for public health.

ARTICLE HISTORY

Received 21 December 2016
Accepted 11 July 2017

EDITOR

Jing Wang

Introduction

Inhalable fine particulate matter, PM_{2.5} (mass of particles below 2.5 μm in diameter) has been observed to be a hazardous air pollutant in outdoor environments (Pope III 1995; Lelieveld et al. 2015) and in indoor environments (Hänninen et al. 2011). Also ultrafine particles (UFP, defined as having a diameter of 0.1 μm or less) have been suggested to pose health risks due to their ability to reach the alveolar area of lungs (Wichmann and Peters 2000; Oberdörster et al. 2001, 2005; Li et al. 2003). Often majority of the vehicle exhaust particle number belongs to the UFP. On the other hand, World Health Organization (2012) reported that there was sufficient evidence of the carcinogenicity of diesel engine exhaust for humans. In general, large human populations are exposed to traffic related particles in everyday life.

In several studies, the urban air particle number size distribution measurements have shown that near traffic routes and in city centers the particle number is

dominated by the UFP (Kittelson et al. 2004; Wehner et al. 2002; Ketzel et al. 2003; Longley et al. 2003; Virtanen et al. 2006; Pirjola et al. 2012; Lähde et al. 2014; Rönkkö et al. 2017). In these cases, the mean particle size in urban air has been observed to be even smaller than 30 nm. Especially in traffic environments the UFP are emitted to the urban air mainly from traffic, by both gasoline (Karjalainen et al. 2014a) and diesel vehicles (Rönkkö et al. 2006). In addition to nanoparticles containing mainly semi-volatile sulphur compounds and organics (Tobias et al. 2001; Schneider et al. 2005; Rönkkö et al. 2007), diesel and gasoline vehicles can emit metallic nanoparticles (Rönkkö et al. 2014; Karjalainen et al. 2014a) and soot particles (Heywood 1989; Harris and Maricq 2001), both contributing also on the UFP size range. In the vehicle exhaust particle number size distribution, particles with different structure and chemical composition are typically seen in different modes, which are a nucleation mode (NM) and a soot mode

CONTACT Panu Karjalainen ✉ panu.karjalainen@tut.fi Aerosol Physics Laboratory, Faculty of Natural Sciences, Tampere University of Technology, P.O. Box 692, Tampere FI-33101, Finland.

Color versions of one or more of the figures in the article can be found online at www.tandfonline.com/uast.

Supplemental data for this article can be accessed on the [publisher's website](#).

© 2017 American Association for Aerosol Research

(SM). These traffic-related modes have been observed also in urban air quality studies near traffic routes. In addition to these modes, the urban aerosol is also affected by other sources and atmospheric aging. However, the traffic-related modes have been shown to dominate the lung deposited surface area (LDSA) size distributions in urban environments (Kuuluvainen et al. 2016). The LDSA is a metric for the potential negative health effects of aerosol particles.

In polluted areas, the outdoor particle concentration can affect significantly the indoor air particle concentrations in buildings (Quang et al. 2013; Morawska et al. 2013; Hussein et al. 2005, 2015). Due to that, especially in the buildings near heavy traffic areas, indoor air may contain significant amounts of vehicle exhaust originated UFP. Particle filtration in ventilation systems can be seen as a key technology to prevent health risks of these particles (Nazaroff et al. 2004). According to the classical filtration theory, the mechanical fibrous filters are relatively effective for removing very small particles due to the diffusion mechanism (Friedlander 1958; Hinds 1982). Shi et al. (2013) reported that the filtration efficiency of UFP varied between different intermediate bag filters, designed for general ventilation applications, and was influenced, for instance, by the air velocity and the electrical properties of the filter media. However, it is not very well known how the building ventilation and filtration systems or the room air cleaners affect the UFP concentrations. Especially, the number of studies focusing on the size dependency of filtration efficiencies in the UFP size range is limited.

The optical particle measurement technologies utilized in filter standards, such as EN779-2012, ASTM F1471-2009, EN 1822-2009 and ASHRAE 52.2-2012, cannot detect particles in the UFP size range, which means that the filtration efficiency for the UFP is not measured in the standard tests. The standard test particle generators producing DEHS particles (EN779-2012) or KCl particles (ASHRAE 52.2-2012) are not typically used in the UFP size range, although these methods can be used to generate particles in the ultrafine particle size range. An exception is the HEPA test standard (ISO 29463), where DEHS is one of the test materials, for which the particle size range is down to $0.04\ \mu\text{m}$. Loading aerosols used in laboratory measurements (ISO Fine and ASHRAE test dust) mainly consist of particles above $1000\ \text{nm}$, and therefore the standard tests are not able to predict properly the filter performance under real operation conditions. While the DEHS and KCl particles are typically used in filter testing, few studies for the filter loading characteristics have been also with real soot particles (Kim et al. 2009; Valmari et al. 2006; Chen et al. 2017).

In this study, we demonstrate a test aerosol generation system which mimics the characteristics of engine exhaust aerosol dominating the particle number concentration in urban environments. The test aerosol generation system produces not only the typical particle size distribution but also the physical and chemical characteristics of particles. In addition, the generation system is used in this study to determine the ultrafine particle filtration efficiencies down to $1.3\ \text{nm}$ in particle size of typical commercial filtration solutions, including a fibrous filter, HEPA filter, electrostatic fibrous filter and an electrostatic precipitator.

Methods

Test aerosol generation system

The test aerosol generation system consists of a nucleation mode (NM) particle generator and soot mode (SM) particle generator (Figure 1). The NM generator aims to reproduce the sulphur driven nucleation particle formation process (Arnold et al. 2012) by a controllable way. In the generator, SO_2 gas is oxidized to SO_3 at high temperature in a catalytic converter (Giechaskiel et al. 2007; Karjalainen et al. 2014b). Oxidized SO_3 then reacts with water molecules forming gaseous sulphur acid (GSA) (Arnold et al. 2012). This high temperature gas is further mixed with cool air, which leads to the formation of nucleation mode particles. The size of these particles is typically in the range of $3\text{--}30\ \text{nm}$. The SM generator is a common small sized boat diesel engine (Yanmar L40E-D operated at $750\ \text{W}$ power). The initial NM formation occurs upstream of the SM generator inlet in order to minimize condensation losses to existing soot particles. In our system, the NM particles and SM particles are mixed, and the resulted aerosol is stabilized in the mixing chamber with the volume of $\sim 5\ \text{m}^3$. The particle generation system enables the filter tests with typical flow rates of ventilation filters.

Test filters

The particle generation system was applied to study the filtration efficiency of five different commercial particle filters. The first filter was a mechanical bag-type glass fiber filter graded to the class F7 according to EN779. The second and third test filters were high-efficiency particulate arrestance (HEPA) filters, called HEPA 1 (graded to the class H12) and HEPA 2 (graded to the class 13) here. The fourth test filter was an electret filter including a wire-type particle charger and an electrostatic filter media. The electret filter was studied both with (w/) and without (w/o)

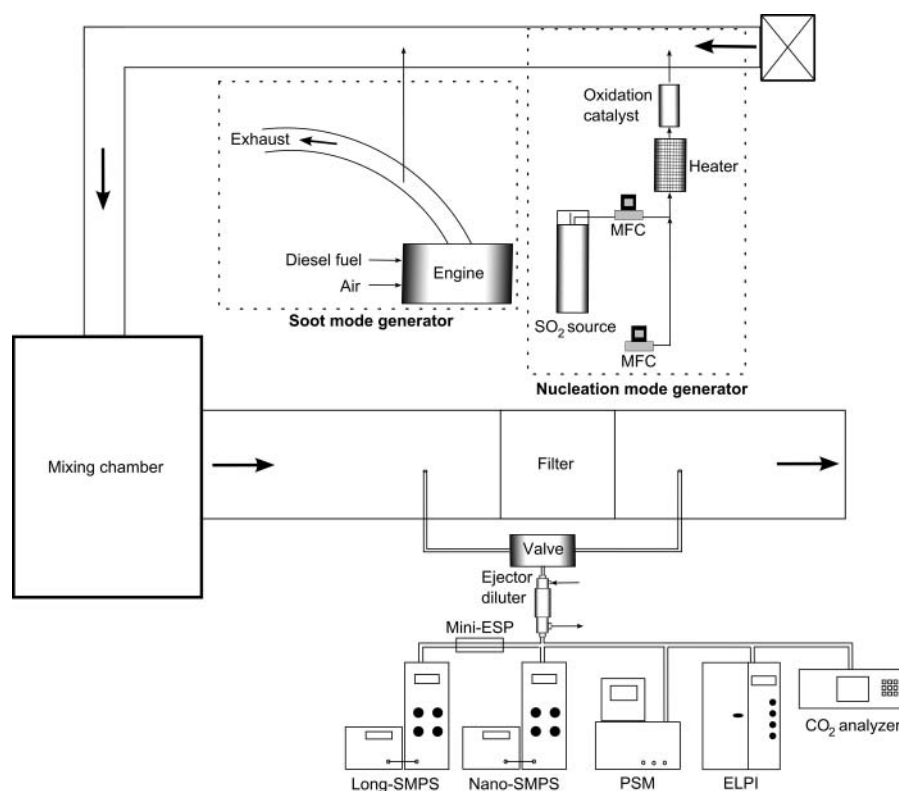


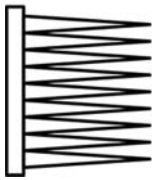
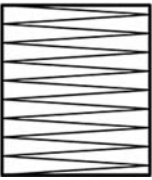
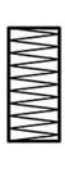
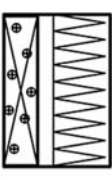
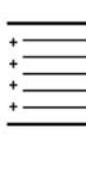
Figure 1. Experimental setup consisting of aerosol particle generators (both nucleation and soot), mixing chamber, ventilation channel, test filters, dilution, and aerosol measurement instruments.

the charger. The fifth test filter was a two-stage electrostatic precipitator (ESP), including a wire-type particle charger region and a collection stage made of aluminum plates. The charger and collection voltages in the ESP were 7.5 kV and 4.0 kV, respectively, and the corona current was 1 mA. Schematic figures and details of the test filters are shown in Table 1.

The tested filters were fixed tightly in the duct downstream of the mixing chamber and the air flow through the filter was fixed to the desired value. In these tests, the

face velocity was varying according to designed application resulting flow rates between 50 l/s and 500 l/s through the filters 1–5. With these flow rates, pressure drops over the filters varied between 3 Pa and 152 Pa, respectively. Since both the particle generators are thermal systems that require stabilized temperatures, the generators were turned on at least one hour before the actual efficiency measurements to ensure a constant concentration and a stable particle size distribution during the measurement.

Table 1. Description of the tested filters: F7, HEPA 1, HEPA 2, Electret, ESP. Errors for pressure drop, volumetric flow and face velocities have been determined by the information provided by the device manufacturers.

	F7	HEPA 1	HEPA 2	Electret	ESP
					
Dimensions (mm)	610 × 610 × 620	610 × 610 × 580	295 × 295 × 120	610 × 610 × 600	525 × 325 × 205
Pressure drop (Pa)	43 ± 0.5	152 ± 0.5	90 ± 0.5	115 ± 0.5	3 ± 0.5
Volumetric flow (l/s)	500 ± 25	500 ± 25	53 ± 2.6	500 ± 25	170 ± 8.5
Face velocity (m/s)	1.34 ± 0.07	1.34 ± 0.07	0.61 ± 0.03	1.34 ± 0.07	1 ± 0.05

Sampling and measurements

The test aerosol sample was taken from the ventilation channel via two sampling probes, one upstream and the other downstream of the test filter (Figure 1). An automated valve was used to switch the sampling lines at a 12-minute interval. The sequential upstream and downstream measurement cycle was repeated three times for every test filter. After sampling, the aerosol was diluted by an ejector type diluter (Dekati Diluter, dilution ratio of c. 8) and then conducted to measurement instruments. The filtration efficiencies were studied in a wide particle size range, but especially with ultrafine particles down to 1.3 nm. A particle size magnifier (PSM, Airmodus A10) (Vanhänen et al. 2011) and two scanning mobility particle sizers (Nano-SMPS and Long-SMPS, TSI Inc.) were used to measure particle number size distribution in the size ranges of 1.3–2.9 nm (PSM), 3–65 nm (Nano-SMPS) and 10–450 nm (Long-SMPS). A small-scale ESP (Mini-ESP, similar as used, e.g., in Karjalainen et al. 2014b) was applied to study the subsets of charged and uncharged particles. The Mini-ESP was installed upstream of the Long-SMPS, and it operated with the flow of 0.6 lpm. Using a voltage of 3 kV in the Mini-ESP, based on the experimental data, charged particles below 100 nm in diameter were removed. An electrical low pressure impactor (ELPI, manufactured by Dekati Oy) (Keskinen et al. 1992) was used to monitor the particle concentration with a high time resolution. A CO₂ analyzer (SICK Maihak, Sidor) was used in the

setup in order to monitor that the dilution ratio in the ejector diluter was constant, so that it did not change when the aerosol flow was changed between the upstream and downstream sampling. Simultaneously, the stability of CO₂ concentration was used to monitor the stability of the SM generator.

Results and discussion

Test aerosol

Figure 2 shows a typical particle size distribution of the generated aerosol measured from the upstream of the test filter after the dilution (dilution ratio ~8). The mean particle sizes (mean particle diameters) of the nucleation mode (NM) and soot mode (SM) were 11 nm and 55 nm, respectively. There were measurable but small particle concentrations of NM particles also in the PSM particle size range (inside panel in Figure 3). The relative concentrations in the modes were adjusted by controlling the exhaust flow of the SM generator. When compared, e.g., to the typical real-world fresh diesel exhaust aerosol (Rönkkö et al. 2006; Karjalainen et al. 2014b), it can be seen that the generation system reproduced the exhaust particle size distribution and the relative concentrations of the two particle modes well.

It should be noted that also the characteristics of particles were, at least qualitatively, similar than in real exhaust; generated nanoparticles were semivolatile and consisted of sulphur compounds whereas the larger

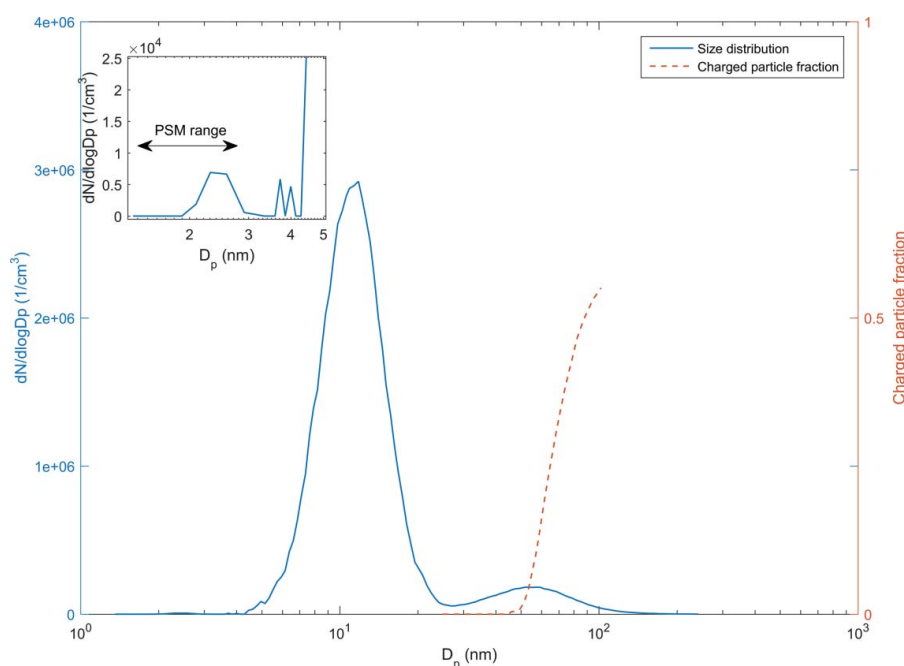


Figure 2. Example of the upstream particle size distribution used in the experiments (solid [blue] line) and the fraction of electrically charged particles (dashed [orange] line). Zoomed size distribution shows the particle concentrations in the PSM detection size range.

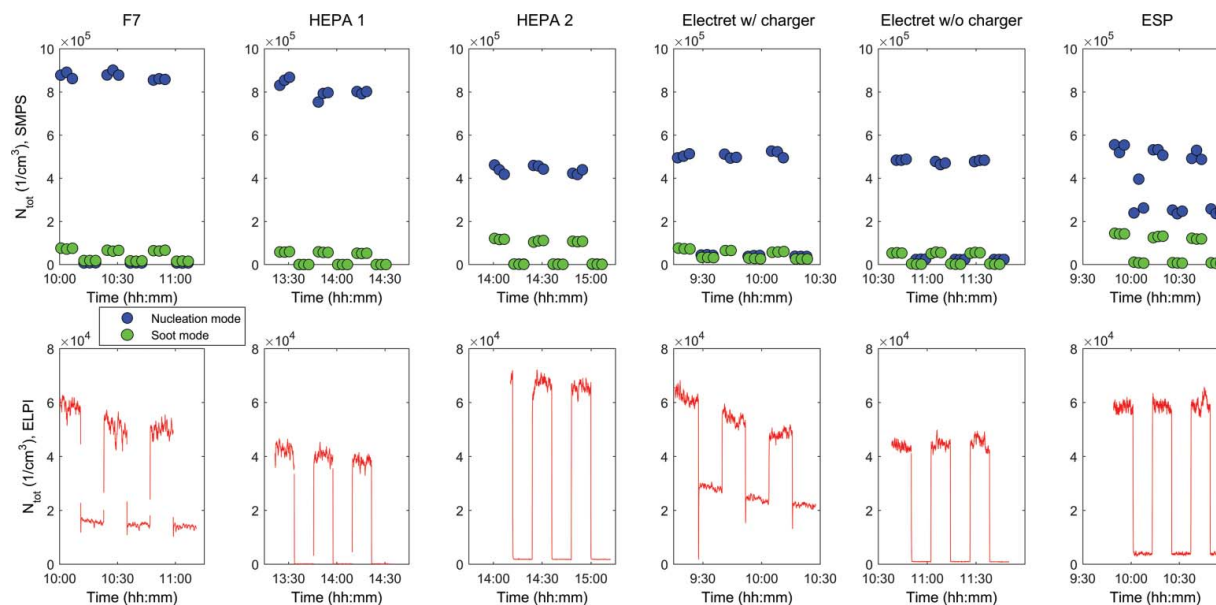


Figure 3. Stability of the aerosol generation system measured by the Nano-SMPS (dark gray [blue], $D_p < 20$ nm) and Long-SMPS (light gray [green], $D_p > 20$ nm) (top), and by the ELPI (total particle concentration, $D_a > 30$ nm) (bottom).

particles were mainly solid soot particles. Based on the size distribution data and the usage of the Mini-ESP, the particles smaller than 50 nm were electrically neutral, but the larger soot particles were partially charged so that over a half of the particles at 100 nm was electrically charged. Therefore, basically the whole NM was uncharged, similarly as in Karjalainen et al. (2014b), but large soot particles were partially charged (Maricq 2006). The effects of the original charging state of particles on the filtration efficiency are discussed below.

Figure 3, the upper pane, shows the time series of the particle number concentrations for the nucleation and soot modes calculated from the size distributions upstream and downstream of the tested filters (Nano-SMPS, $D_p < 20$ nm, for nucleation mode and Long-SMPS, $D_p > 20$ nm, for soot mode). The lower pane of Figure 3 shows the total particle concentrations measured by the ELPI. For all instruments, the higher concentrations were measured upstream of the test filter, while the lower concentrations were measured downstream. When sampled upstream of the filter, the NM number concentrations were 4–10 times the SM concentrations. This is also seen from the ELPI data which only measured particles larger than 30 nm. For F7 and HEPA 1 filters, the NM concentration was higher compared to other filter tests because of different flow rates and dilution ratios used in the generator part. The particle concentration remained relatively stable through each test. However, there were decreasing trends in the soot mode concentrations in the cases of F7 and the electret filter with a charger. However, the variation in the particle concentration was not significant in larger time scales.

The sampling was periodically performed both upstream and downstream of the filter to avoid systematic error, and hence the particle filtration tests produced reliable and comparable results.

Filtration efficiency

Differences in filtration efficiency between the tested filters were observed to be significant (Figure 4). Almost all the particles smaller than 3 nm in diameter were removed in all the filters. This is explained by the rapid diffusion motion of these nanoparticles and thus the particle losses in the filters were remarkably high regardless of the different filtration techniques. However, for the particles larger than 3 nm, the general trends of the filtration efficiency as a function of the particle size showed significant differences between the different filtration techniques. In general the relative error increased towards the lower and upper detectable particle sizes (shown in Figure S1) but the error levels were in general low. Most relative error values were below 5%-points even though especially for the ESP values were greater below 5 nm and above 150 nm. There was also an increased relative error in the particle size area between NM and SM (~ 20 nm). The relative error (as percentage points) was naturally dependent on the filtration efficiency values, so that, e.g., for HEPA 1 the values were below 0.1%-points below 100 nm particle sizes.

In the case of F7, the collection efficiency was practically 100% up to the particle diameter of 10 nm and decreased steeply in the particle size range above 20 nm. Hence, the F7 was efficient filter for the NM particles but

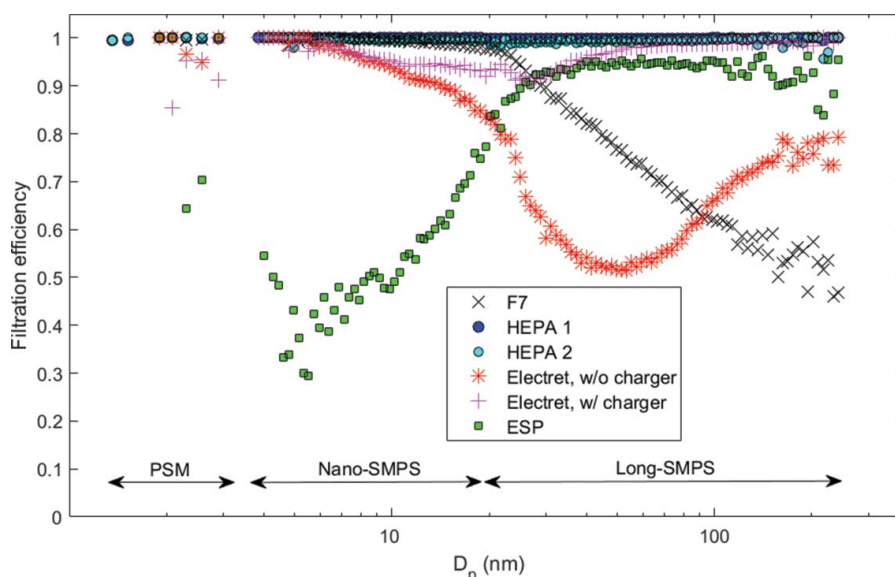


Figure 4. Particle filtration efficiencies for the tested filters calculated from upstream and downstream size distributions measured by the PSM (D_p 1.3–2.9 nm), Nano-SMPS (D_p 3–20 nm), and Long-SMPS (D_p > 20 nm).

less efficient for the SM particles. The particle filtration efficiency of F7 type filters is typically dominated by the diffusion, impaction and interception processes of the particles in the filter media (Friedlander 1958; Shi et al. 2012). The F7 filtration efficiency curve observed in Figure 4 was in line with the previous studies (Shi et al. 2012; Goodfellow et al. 2001) having the most penetrating particle size (MPPS) roughly at 200 nm wherein filtration efficiency was around 50%. The diffusion motion of particles increases in smaller particle sizes, and therefore the observed filtration efficiency was high for the particles below 20 nm. Kim et al. (2006, 2007) reported also that the particle penetration in glass fiber filters decreases continuously down to 3 nm as expected from the classical filtration theory. They suggest that the thermal rebound phenomena would be operative for nanoparticles with diameters below 2 nm, even though it would depend on the states of both the particles and the filter media (Kim et al. 2006). In this study, we did not find the thermal rebound of NM particles although our measurement range covered particle diameters down to 1.3 nm.

Compared to the F7 filter, the ESP was not that efficient at small particle sizes but the particle filtration efficiency increased as a function of particle size; in particle sizes 4–10 nm the collection efficiency was lower than 50%, at 20 nm it was 70% and at 40 nm it reached a level of 95%, so the ESP was efficient for the SM particles but less efficient for the NM particles. It should be noted that, for the ESP, a collection efficiency of 100% was not observed at any particle sizes. This is probably due to the charging efficiency of the ESP charger (part of the

particles remains electrically neutral in all particle sizes). The functioning of the ESP is based on the electrical charging of particles using a corona charger and collecting the charged particles using an electric field (Jaworek et al. 2007). The collection efficiency of ESP depends on the charging efficiency, number of elemental charges and electrical mobility of particles as well as the geometry of the device. The charging efficiency of corona chargers typically decreases in smaller particle sizes (Kulkarni et al. 2011), and thus the filtration efficiency was low for particles below 30 nm in this study. The low filtration efficiency of the ESP devices for small nanoparticles was also reported by Huang et al. (2002). They stated that aerosol penetration through the single- and two-stage ESPs increased significantly for particles below 20 and 50 nm, respectively. The observation that the filtration efficiency again increased when the particle size decreased below 3 nm is likely due to the diffusional filtration mechanisms of neutral particles, not because of electrical filtration since particle charging probability is likely very small. Note however that there was a high relative error in the determination of filtration efficiency for the ESP in particle sizes below c. 6 nm.

The electret filter represents a modern filter type including both a wire-type particle charger and an electrostatic filter media. The filtration efficiency of the electret filter with a charger was above 90% for both the NM and the SM in the size range of 4.5–200 nm (Figure 4). Both the ESP and F7 filter characteristics are combined in the electret resulting in high particle removal performance in a wide size range with relatively low pressure drop. The filtration efficiency without a

charger represents the performance of the electrostatic filter alone. In this case, particles below 20 nm are removed by diffusion similarly as in the F7 but with lower performance. The filtration efficiency decreased for the particles larger than 20 nm but increased again for the particles larger than 50 nm. This can be explained by increasing fraction of the originally charged SM particles in the size range above 50 nm, as shown in Figure 2. Electrostatic filter media have typically higher filtration efficiency for charged particles compared to neutral particles (Shi 2012; Romay et al. 1998).

The filtration efficiencies of both HEPA filters were above 99% in the test particle size range. The HEPA 1 collected 99.99% of NM particles and 99.95% of SM particles, whereas the filtration efficiencies of the HEPA 2 were 99.60% and 99.33% for the NM and the SM particles, respectively. The results showed that both the HEPA filters worked very well, even though the penetrated particle number for the HEPA 1 was over 10 times less than for the HEPA 2.

The most penetrating particle size (MPPS) was calculated for the test filters based on the filtration efficiency curves (Figure 4). For each filter, the filtration efficiency was converted to the penetration and a quadratic function was fitted to the data at the neighborhood of the local maximum of the penetration. The obtained MPPS values were >200 nm, 34 nm, 32 nm, 20 nm, 50 nm and 6.2 nm for the F7, HEPA1, HEPA2, Electret w/ charger, Electret w/o charger and ESP, respectively. With the exception of F7, all the test filters had the MPPS in the ultrafine particle size range. The MPPS results are reasonable if compared to previous studies. Chang et al. (2015) reported MPPS values between 10 and 30 nm for pleated HVAC electret filters at face velocities between 0.05 and 1 m/s. A previous study by Sinclair (1976) showed that the typical MPPS value for a HEPA filter was about 40 nm at a flow rate of 70 cm/s. Alderman et al. (2008) reported the MPPS values of 110–130 nm for HEPA filters at low face velocities (2.0–4.5 cm/s). The MPPS values typically increase with lower face velocities (Lee and Liu 1980). Chen et al. (2017) reported that MPPS values were about 200 nm for two fiber filter types, however the MPPS values were sensitive of filter loading so that with increased loading the size decreased by 20–50 nm depending on the filter type. It should be noticed that most of the filters tested in this study had the MPPS at the same particle size range as the dominant outdoor aerosol.

While the particle size resolved filtration efficiencies are highly beneficial in the evaluation of filtration technologies, the final effectiveness of the technologies can be evaluated only if the aerosol, especially the aerosol particle size distribution, is known. In urban areas the particle size distribution varies significantly; while the smallest particle

sizes are typically measured near traffic, the mean particle size of urban background aerosol is often larger. Figure 5 simulates the effectiveness of the filter types studied above for different urban aerosols, simultaneously aiming to show how the studied filter technologies can affect indoor air particles in different environments. Figure 5 includes both total filtration efficiencies (TFE) for particles and the size distributions of particles penetrated the studied filters. The TFE and size distributions were calculated for test aerosols used in this study (nucleation mode, soot mode, both modes), and then with real ambient aerosols measured next to a major road in Helsinki (Helsinki, road side, Virtanen et al. 2006), at an urban background station in Beijing (Beijing summer, Wu et al. 2008) and at an urban background station in Helsinki representing long range transported aerosol (Hussein et al. 2005). The size distribution of the test aerosol used in this study represents well the ambient aerosol measured next to a major road in Helsinki having similar mean particle sizes (NM 10–20 nm, SM 50–70 nm), thus, the TFE for these aerosols are also almost equal. The filtering technologies effective for the smallest particle sizes were observed to produce the highest TFE. Size distribution of the ambient background aerosol in Helsinki is dominated by the accumulation mode and the mean particle size is clearly larger than next to a major road in Helsinki. This affects the TFE of the filters so that the diffusion based filters, such as the F7 and electret filter w/o charger, have the lowest TFE, whereas the electrical separation based filters (electret filter and ESP) remove particles relatively well. In Beijing, the ambient aerosol size distribution has a mean particle size at around 60 nm and the filtration efficiencies calculated for different filters varied between 67.06–99.96%. With the exception of the HEPA filters, the most efficient filter (96.49%) in Beijing would be the electret filter with a charger.

Ultrafine particles (UFP) typically dominate number concentration of ambient aerosols. The major contributors of these aerosols are the combustion aerosols emitted from traffic. The combustion aerosols may contain many carcinogenic compounds such as heavy metals and PAHs (Schauer et al. 1999; Shi et al., 2000). UFP can produce toxic effects even at low concentrations due to their small size and surface characteristics (Johnston et al., 2000). In addition, the non-soluble UFP deposited in the pulmonary region have sufficient time to penetrate into interstitial region and ultimately accumulate there for years (Hussain et al. 2011). The filter technology affects significantly the particle removal efficiency in the UFP size range. To assure healthy indoor air quality level for people, the typical outdoor ambient aerosol concentrations and size distribution as well as filtration technology should be taken into account in building ventilation

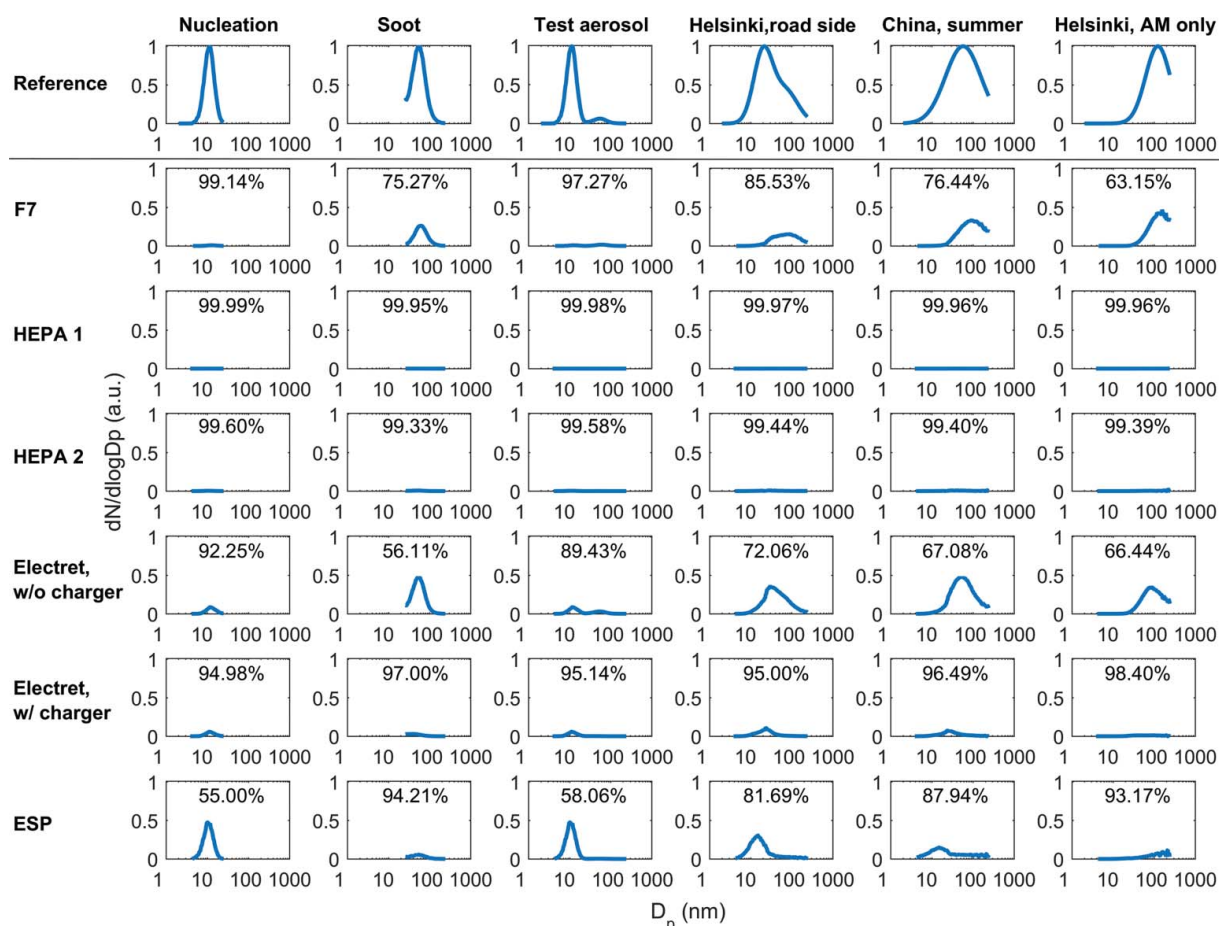


Figure 5. Uppermost row shows the normalized particle size distributions from the left: NM (this study), SM (this study), test aerosol (this study), Helsinki road side (Virtanen et al. 2006), Peking (Wu et al. 2008), Helsinki accumulation mode (AM) only (Hussein et al. 2004). The rows below indicate what size distribution exists indoor after row corresponding filtration, and the percentages indicate the total number filtration efficiency for the corresponding aerosol.

systems as well as in room air cleaners. Information on the filtration efficiency of commercial filters in the UFP size range is important, because health risks of these particles are high due to the high lung deposition probability, especially in the alveolar region (ICRP 1994). Thus, taken into account that particles smaller than 100 nm typically dominate vehicle exhaust particle number emissions and thus typically also the particle number concentration in urban air, it is reasonable to extend the particulate filter test standards in future to cover also the ultrafine particle size range also in other standards than ISO 29463.

Conclusions

We have developed a new method for particle generation for particle filtration efficiency tests of ventilation filters. The generation system reproduces a similar exhaust particle size distribution and characteristics as in typical real-world vehicles exhaust aerosol, and a typical size distribution observed next to a major road in Helsinki.

Different types of filters were tested in this study using a new particle generation system consisting of adjustable nucleation and soot particle generators. The nanocluster sized particles below ~ 3 nm were removed efficiently by the HEPA, F7 and electret filters, the ESP also showed relatively high filtration efficiencies but with increased uncertainty in the determination. For particles larger than 3 nm relatively large variations were observed in the ultrafine particle filtration efficiencies of the tested filter types. The HEPA filters were efficient in all particle sizes. The F7 filter was more efficient for the nucleation particles (below 30 nm), and in contrast, the ESP was more efficient for the soot particles (larger than 30 nm). The electret filter with charger using the advantages of F7 for small particles and the advantages of the ESP for larger particles was efficient in all the particle sizes studied but did not reach the HEPA filtration efficiency levels.

The filters tested in this study were based on very different operational principles. These operational principles practically determined the dominating mechanisms of particle collection into the filtering media or collection

plates, which was seen especially in size dependencies of filtration efficiencies. It can be concluded that for the smallest particles (nanoclusters) the diffusional collection of the particles increased the filtration efficiency, even in the case of the ESP, while for larger particles the use of electrophoresis was an efficient method to increase the filtration efficiency. This was seen especially in studies for the electret filter, which was tested with and without the charger. However, it should be noted that the filtration solutions utilizing electrophoresis may be more efficient for fresh traffic originated soot particles than e.g. for the long-range transported particles in ambient air due to the higher fraction of electrically charged particles in freshly emitted soot.

It should be kept in mind that the filtration efficiency curves were determined in this study under well-controlled laboratory conditions. The changes e.g. in temperature and humidity of air to be purified, filter clogging as well as air flow rate through filter media and maintenance of ventilation systems can affect the filtration efficiencies when these filters are used in real buildings and in real ventilation applications. Thus, the comprehensive understanding of filtration efficiencies requires studies in real-world environments too, such as made by Stephens and Siegel (2013).

Based on the results of this study, we suggest that the particulate filter test standards should be extended to cover more comprehensively also the particles smaller than 100 nm in diameter that dominate the vehicle exhaust particle emissions and are potentially hazardous for public health. In future studies, better understanding is needed on the filtration efficiency of ultrafine particles in various types of filtration systems, especially in real environments and with real ambient aerosols.

Acknowledgments

Authors acknowledge Matti Niemeläinen for his support in performing the experiments.

Funding

This work was made in the project “Finnish-Chinese Green ICT R&D&I Living Lab for Energy Efficient, Clean and Safe Environments,” financially supported by Finnish Funding Agency for Innovation (Tekes), and Ahlstrom Oy, FIAC Invest Oy, Green Net Finland Oy, Kauriala Oy, Lassila & Tikanoja Oy, Lifa Air Oy, MX Electrix Oy, Pegasor Oy and Sandbox Oy.

References

- Alderman, S. L., Parsons, M. S., Hogancamp, K. U., and Waggoner, C. A. (2008). Evaluation of the Effect of Media Velocity on Filter Efficiency and Most Penetrating Particle Size of Nuclear Grade High-Efficiency Particulate Air Filters. *J. Occupat. Environ. Hyg.*, 5(11):713–720.
- Arnold, F., Pirjola, L., Roönkkoö, T. et al. (2012). First Online Measurements of Sulfuric Acid Gas in Modern Heavy-Duty Diesel Engine Exhaust: Implications for Nanoparticle Formation. *Environ. Sci. Technol.*, 46(20):11227–11234.
- ASHRAE. (2012). *Standard 52.2-2012, Method of Testing General Ventilation Air-Cleaning Devices for Removal Efficiency by Particle Size (ANSI/ASHRAE Approved)*. American Society of Heating, Refrigerating and Air-Conditioning Engineers.
- Chang, D.-Q., Chen, S.-C., Fox, A. R., Viner, A. S., and Pui, D. Y. H. (2015). Penetration of Sub-50 nm Nanoparticles Through Electret HVAC Filters Used in Residence. *Aerosol Science and Technology*, 49(10):966–976.
- Chen, L., Ding, S., Liang, Z., Zhou, L., Zhang, H., and Zhang, C. (2017). Filtration Efficiency Analysis of Fibrous Filters: Experimental and Theoretical Study on the Sampling of Agglomerate Particles Emitted from a GDI Engine. *Aerosol Science and Technology*, in press. DOI: 10.1080/02786826.2017.1331293.
- EN 1822-1. (2009). *High Efficiency Air Filters (EPA, HEPA and ULPA). Part 1: Classification, Performance Testing, Marking*. European Committee for Standardization. ISBN 978 0 580 61789 8
- EN 1822-2. (2009). *High Efficiency Air Filters (EPA, HEPA and ULPA). Part 2: Aerosol Production, Measuring Equipment, Particle Counting Statistics*. European Committee for Standardization.
- Friedlander, S. K. (1958). Theory of Aerosol Filtration. *Ind. Eng. Chem.*, 50(8):1161–1164.
- Giechaskiel, B., Ntziachristos, L., Samaras, Z. et al. (2007). Effect of Speed and Speed-Transition on the Formation of Nucleation Mode Particles from a Light Duty Diesel Vehicle. *SAE Technical Papers*, 2007-01-1110. ISBN 978 0 580 61791 1
- Goodfellow, H. D., and Tähti, E. (Ed.). (2001). *Industrial Ventilation Design Guidebook: 13. Gas-Cleaning Technology*. California, Academic Press, p. 1199.
- Harris, S. J., and Maricq, M. M. (2001). Signature Size Distributions for Diesel and Gasoline Engine Exhaust Particulate Matter. *J. Aerosol Sci.*, 32 (6):749–764.
- Heywood, J. B. (1989). *Internal Combustion Engine Fundamentals*. McGraw-Hill, New York, p 930.
- Hinds, W. C. (1982). *Aerosol Technology: Properties, Behavior, and Measurement of Airborne Particles*. John Wiley & Sons, Hoboken, New Jersey.
- Huang, S. H., and Chen, C. C. (2002). Ultrafine Aerosol Penetration Through Electrostatic Precipitators. *Environ. Sci. Technol.*, 36(21):4625–4632.
- Hussein, T., Hämeri, K., Heikkinen, M., and Kulmala, M. (2005). Indoor and Outdoor Particle Size Characterization at a Family House in Espoo-Finland. *Atmos. Environ.*, 39:3697–3709.
- Hussein, T., Puustinen, A., Aalto, P. P., Mäkelä, J. M., Hämeri, K., and Kulmala, M. (2004). Urban Aerosol Number Size Distributions. *Atmospheric Chemistry and Physics*, 4(2): 391–411.
- Hussein, T., Wierzbicka, A., Löndahl, J., Lazaridis, M., and Hänninen, O. (2015). Indoor Aerosol Modeling for Assessment of Exposure and Respiratory Tract Deposited Dose. *Atmos. Environ.*, 106:402–411.
- Hussain, M., Winker-Heil, R., and Hofmann, W. (2011). Lung Dosimetry for Inhaled Long-Lived Radionuclides and

- Radon Progeny. *Radiation Protection Dosimetry*, 145(2–3):213–217.
- Hänninen, O., Knol, A. (ed.), Jantunen, M. et al. (2011). *European Perspectives on Environmental Burden of Disease: Estimates for Nine Stressors in Six Countries*. THL Reports 1/2011, Helsinki, Finland.
- International Commission on Radiological Protection (ICRP). (1994). *Human Respiratory Tract Model for Radiological Protection*. Publication 66. Elsevier Science, Oxford.
- Jaworek, A., Krupa, A., and Czech, T. (2007). Modern Electrostatic Devices and Methods for Exhaust Gas Cleaning: A Brief Review. *J. Electrostat.*, 65(3):133–155.
- Johnston, C. J., Finkelstein, J. N., Mercer, P., Corson, N., Gelein, R., and Oberdörster, G. (2000). Pulmonary Effects Induced by Ultrafine PTFE Particles. *Toxicol. Appl. Pharmacol.*, 168(3):208–215.
- Järvinen, A., Kuuluvainen, H., Niemi, J. V. et al. (2014). Monitoring Urban Air Quality with a Diffusion Charger Based Electrical Particle Sensor. *Urban Climate*. 14:441–456.
- Karjalainen, P., Pirjola, L., Heikkilä, J. et al. (2014a). Exhaust Particles of Modern Gasoline Vehicles: A Laboratory and an On-Road Study. *Atmos. Environ.*, 97:262–270.
- Karjalainen, P., Rönkkö, T., Pirjola, L. et al. (2014b). Sulfur Driven Nucleation Mode Formation in Diesel Exhaust Under Transient Driving Conditions. *Environ. Sci. Technol.*, 48(4):2336–2343.
- Keskinen, J., Pietarinen, K., and Lehtimäki, M. (1992). Electrical Low Pressure Impactor. *Journal of Aerosol Science*, 23:353–360.
- Ketzel, M., Wählin, P., Berkowicz, R., and Palmgren, F. (2003). Particle and Trace Gas Emission Factors Under Urban Driving Conditions in Copenhagen Based on Street and Roof-Level Observations. *Atmospheric Environment*, 37(20):2735–2749.
- Kim, C. S., Bao, L., Okuyama, K. et al. (2006). Filtration Efficiency of a Fibrous Filter for Nanoparticles. *J. Nanopart. Res.*, 8(2):215–221.
- Kim, S. C., Harrington, M. S., and Pui, D. Y. (2007). Experimental Study of Nanoparticles Penetration Through Commercial Filter Media. *J. Nanopart. Res.*, 9(1):117–125.
- Kim, S. C., Wang, J., Shin, W. G., Scheckman, J. H., and Pui, D. Y. (2009). Structural Properties and Filter Loading Characteristics of Soot Agglomerates. *Aerosol Sci. Technol.*, 43(10):1033–1041.
- Kittelson, D. B., Watts, W. F., and Johnson, J. P. (2004). Nanoparticle Emissions on Minnesota Highways. *Atmos. Environ.*, 38(1):9–19.
- Kulkarni, P., Baron, P. A., Willeke, K. (Eds.). (2011). *Aerosol Measurement: Principles, Techniques, and Applications*. John Wiley & Sons, Hoboken, New Jersey.
- Kuuluvainen, H., Rönkkö, T., Järvinen, A., Saari, S., Karjalainen, P., Lähde, T., Pirjola, L., Niemi, J. V., Hillamo, R., and Keskinen, J. (2016). Lung Deposited Surface Area Size Distributions of Particulate Matter in Different Urban Areas. *Atmos. Environ.*, 136:105–113.
- Lee, K. W., and Liu, B. Y. H. (1980). On the Minimum Efficiency and the Most Penetrating Particle Size for Fibrous Filters. *J. Air Pollution Control Assoc.*, 30(4):377–381.
- Lelieveld, J., Evans, J. S., Fnais, M., Giannadaki, D., Pozzer, A. (2015). The Contribution of Outdoor Air Pollution Sources to Premature Mortality on a Global Scale. *Nature*, 525(7569):367–371.
- Li, N., Sioutas, C., Cho, A. et al. (2003). Ultrafine Particulate Pollutants Induce Oxidative Stress and Mitochondrial Damage. *Environ. Health Perspect.*, 111:455–460.
- Lähde, T., Niemi, J. V., Kousa, A. et al. (2014). Mobile Particle and NO_x Emission Characterization at Helsinki Downtown: Comparison of Different Traffic Flow Areas. *Aerosol Air Quality Res.*, 14(5):1372–1382.
- Longley, I., Gallagher, M., Dorsey, J., Flynn, M., Allan, J., Alfara, M., and Inglis, D. (2003). A Case Study of Aerosol (4.6 nm < D_p < 10 μm) Number and Mass Size Distribution Measurements in a Busy Street Canyon in Manchester, UK. *Atmospheric Environment*, 37(12):1563–1571.
- Maricq, M. (2006). On the Electrical Charge of Motor Vehicle Exhaust Particles. *Journal of Aerosol Science*, 37(7):858–874.
- Morawska, L., Afshari, A., Bae, G. N. et al. (2013). Indoor Aerosols: From Personal Exposure to Risk Assessment. *Indoor Air*, 23: 462–487.
- Nazaroff, W. W., and Weschler, C. J. (2004). Cleaning Products and Air Fresheners: Exposure to Primary and Secondary Air Pollutants. *Atmospheric Environment*, 38(18):2841–2865.
- Oberdörster, G. (2001). Pulmonary Effects of Inhaled Ultrafine Particles. *Int. Arch. Occup. Environ. Health*, 74:1–8.
- Oberdörster, G., Oberdörster, E., and Oberdörster, J. (2005). Nanotoxicology: An Emerging Discipline Evolving from Studies of Ultrafine Particles. *Environmental Health Perspectives*, 113(7):823–839.
- Pirjola, L., Lähde, T., Niemi, J. et al. (2012). Spatial and Temporal Characterization of Traffic Emissions in Urban Microenvironments with a Mobile Laboratory. *Atmos. Environ.*, 63:156–167.
- PopeIII, C. A., Thun, M. J., Namboodiri, M. M. et al. (1995). Particulate Air Pollution as a Predictor of Mortality in a Prospective Study of US Adults. *Amer. J. Respirat. Crit. Care Med.*, 151(3_pt_1):669–674.
- Quang, T. N., He, C., Morawska, L., and Knibbs, L. D. (2013). Influence of Ventilation and Filtration on Indoor Particle Concentrations in Urban Office Buildings. *Atmos. Environ.*, 79:41–52.
- Romay, F., Liu, B. Y. H., and Chae, S. (1998). Experimental Study of Electrostatic Capture Mechanisms in Commercial Electret Filters. *Aerosol Sci. Technol.*, 28(3):224–234.
- Rostedt, A., Arffman, A., Janka, K. et al. (2014). Characterization and Response Model of the PPS-M Aerosol Sensor. *Aerosol Sci. Technol.*, 48(10):1022–1030.
- Rönkkö, T., Virtanen, A., Vaaraslahti, K. et al. (2006). Effect of Dilution Conditions and Driving Parameters on Nucleation Mode Particles in Diesel Exhaust: Laboratory and On-Road Study. *Atmospheric Environment*, 40:2893–2901.
- Rönkkö, T., Virtanen, A., Kannosto, J. et al. (2007). Nucleation Mode Particles with a Nonvolatile Core in the Exhaust of a Heavy Duty Diesel Vehicle. *Environ. Sci. Technol.*, 41:6384–6389.
- Rönkkö, T., Pirjola, L., Ntziachristos, L. et al. (2014). Vehicle Engines Produce Exhaust Nanoparticles Even When Not Fueled. *Environ. Sci. Technol.*, 48:2043–2050.
- Rönkkö, T., Kuuluvainen, H., Karjalainen, P., Keskinen, J., Hillamo, R., Niemi, J., Pirjola, L., Timonen, H., Saarikoski, S., Saukko, E., Järvinen, A., Silvennoinen, H., Rostedt, A., Olin, M., Yli-Ojanperä, J., Nousiainen, P., Kousa, A., and

- Dal Maso, M. (2017). Traffic is a Major Source of Atmospheric Nanocluster Aerosol. *Proc. Natl. Acad. Sci. USA*.
- Saarikoski, S., Timonen, H., Saarnio, K. et al. (2008). Sources of Organic Carbon in Fine Particulate Matter in Northern European Urban Air. *Atmos. Chem. Phys.*, 8 (20):6281–6295.
- Schauer, J. J., Kleeman, M. J., Cass, G. R., and Simoneit, B. R. T. (1999). Measurement of Emissions from Air Pollution Sources. 2. C1 Through C30 Organic Compounds from Medium Duty Diesel Trucks. *Environ. Sci. Technol.*, 33 (10):1578–1587.doi:10.1021/es980081n, 1999.
- Shi, B. (2012). *Removal of Ultrafine Particles by Intermediate Air Filters in Ventilation Systems. Evaluation of Performance and Analysis of Applications*. PhD Thesis, Chalmers University of Technology, Gothenberg, Sweden.
- Shi, B., Ekberg, L. E., and Langer, S. (2013). Intermediate Air Filters for General Ventilation Applications: An Experimental Evaluation of Various Filtration Efficiency Expressions. *Aerosol Sci. Technol.*, 47(5):488–498.
- Shi, J., Mark, D., and Harrison, R. (2000). Characterization of Particles from a Current Technology Heavy-Duty Diesel Engine. *Environ. Sci. Technol.*, 34:748–755.
- Schneider, J., Hock, N., Weimer, S., Borrmann, S., Kirchner, U., Vogt, R., and Scheer, V. (2005). Nucleation Particles in Diesel Exhaust: Composition Inferred from *in situ* Mass Spectrometric Analysis. *Environmental Science & Technology*, 39:6153–6161.
- Stephens, B., and Siegel, J. A. (2013). Ultrafine Particle Removal by Residential Heating, Ventilating, and Air-Conditioning Filters. *Indoor Air*, 23(6):488–497.
- Sinclair, David. (1976). Penetration of Hepa Filters by Submicron Aerosols. *J. Aerosol Sci.*, 7(2):175–179.
- Tobias, H. J., Beving, D. E., Ziemann, P. J. et al. (2001). Chemical Analysis of Diesel Engine Nanoparticles Using a NanoDMA/Thermal Desorption Particle Beam Mass Spectrometer. *Environ. Sci. Technol.*, 35:2233–2243.
- Valmari, T., Lehtimäki, M., and Taipale, A. (2006). Filter Clogging by Bimodal Aerosol. *Aerosol Sci. Technol.*, 40 (4):255–260.
- Vanhanen, J., Mikkilä, J., Lehtipalo, K., Sipilä, M., Manninen, H.E., Siivola, E., Petäjä, T., and Kulmala, M. (2011). Particle Size Magnifier for Nano-CN Detection. *Aerosol Science and Technology*, 45(4):533–542.
- Virtanen, A., Rönkkö, T., Kannosto, J. et al. (2006). Physical Characteristics of Winter and Summer Time Emissions of Busy Road at Helsinki. *Atmos. Chem. Phys. Discuss.*, 6:549–578.
- Wehner, B., Birmili, W., Gnauk, T., and Wiedensohler, A. (2002). Particle Number Size Distributions in a Street Canyon and Their Transformation into the Urban-Air Background: Measurements and A Simple Model Study. *Atmospheric Environment*, 36(13):2215–2223.
- WHO. (2012). *Report: Diesel engine exhaust carcinogenic*, International Agency for Research on Cancer. World Health Organization.
- Wichmann, H. E., and Peters, A. (2000). Epidemiological Evidence of the Effects of Ultrafine Particle Exposure. *Philos. Trans. R. Soc. Lond. A*, 358:2751–2768.
- Wu, Z., Hu, M., Lin, P., Liu, S., Wehner, B., and Wiedensohler, A. (2008). Particle Number Size Distribution in the Urban Atmosphere of Beijing, China. *Atmos. Environ.*, 42:7967–7980.

Measured performance of filtration and ventilation systems for fine and ultrafine particles and ozone in an unoccupied modern California house

Authors:

Brett C. Singer^{1,2,*}, William W. Delp^{1,2}, Douglas R. Black³, Iain S. Walker^{1,2}

¹Indoor Environment Group, ²Whole Building Systems Department, and ³Grid Integration Group Energy Technologies Area, Lawrence Berkeley National Laboratory, Berkeley, CA, U.S.

*Corresponding contact information: bcsinger@lbl.gov; Ph: 510-486-4779; Fax: 510-486-5928

**Energy Analysis and Environmental Impacts Division
Lawrence Berkeley National Laboratory**

December 2016

***Indoor Air* accepted manuscript online 05-Dec-2016**



This research was conducted for California Air Resources Board (CARB) Contract 11-311.

This work was supported by the U.S. Department of Energy under Lawrence Berkeley National Laboratory Contract No. DE-AC02-05CH11231.

ABSTRACT

This study evaluated nine ventilation and filtration systems in an unoccupied 2006 house located 250m downwind of the I-80 freeway in Sacramento, California. Systems were evaluated for reducing indoor concentrations of outdoor particles in summer and fall/winter, ozone in summer, and particles from stir-fry cooking. Air exchange rate was measured continuously. Energy use was estimated for year-round operation in California. Exhaust ventilation without enhanced filtration produced indoor PM_{2.5} that was 70% lower than outdoors. Supply ventilation with MERV13 filtration provided slightly less protection whereas supply MERV16 filtration reduced PM_{2.5} by 97-98% relative to outdoors. Supply filtration systems used little energy but provided no benefits for indoor-generated particles. Systems with MERV13-16 filters in the recirculating heating and cooling unit (FAU) operating continuously or 20 min/h reduced PM_{2.5} by 93-98%. Across all systems, removal percentages were higher for ultrafine particles and lower for black carbon, relative to PM_{2.5}. Indoor ozone was 3-4% of outdoors for all systems except an electronic air cleaner that produced ozone. Filtration via the FAU or portable filtration units lowered PM_{2.5} by 25-75% when operated over the hour following cooking. The energy for year-round operation of FAU filtration with an efficient blower motor was estimated at 600 kWh/year.

KEYWORDS

Residential filtration, PM_{2.5}, Ultrafine particles, Black carbon, Residential ventilation

PRACTICAL IMPLICATIONS

This study quantitatively demonstrates the potential for advanced filtration to reduce in-home exposures to outdoor air pollutants through engineered systems. It also demonstrates that high quality filtration is required on supply ventilation systems to achieve the same reductions of outdoor particles as exhaust ventilation in a moderately airtight home. Results from this work should help inform the setting of filtration requirements for high performance home standards and building codes.

INTRODUCTION

Extensive research links outdoor PM_{2.5} (US EPA, 2009) and ozone (US EPA, 2013) to increased risk of adverse human health outcomes. Black carbon (BC) is an indicator of diesel particulate matter (DPM), which has been associated with adverse health outcomes independently of PM_{2.5} mass (Cassee et al., 2013; Ristovski et al., 2012). Many studies have reported associations between ultrafine particles (UFP, smaller than 100 nm diameter) and health impacts (Beko et al., 2015; Wolf et al., 2015). While a recent expert review found the available evidence on the health effects of ultrafine particles UFP to be inconclusive (HEI Review Panel on Ultrafine Particles, 2013), significant concerns remain about UFP (Terzano et al., 2010)

Outdoor air pollutants are carried into homes with ventilation air entering through open windows, infiltrating through the building shell, and moving through supply ventilation fans. Mechanical systems that extract air from homes – including exhaust fans and venting

combustion appliances – increase outdoor air and pollutant entry. Particles (Chen and Zhao, 2011) and ozone (Stephens et al., 2012) may be removed as outdoor air infiltrates through the building shell. Particles are removed from indoor air through deposition (Nazaroff, 2004) and ozone is lost through reactions with surfaces (Weschler, 2000), further reducing indoor concentrations relative to those in outdoor air. The net result of these processes yields an infiltration factor (Allen et al., 2003; Bennett and Koutrakis, 2006; Chen and Zhao, 2011) that relates indoor to outdoor concentrations of outdoor pollutants.

In-home exposures to outdoor particles and ozone are reduced when homes are air-sealed to reduce uncontrolled infiltration as an energy efficiency measure. Indoor concentrations are reduced because entry is slowed in relation to indoor deposition. There is also evidence that removal rates during infiltration increase as air leakage is reduced (Stephens and Siegel, 2012b).

Traditionally, air infiltration provided substantial dilution of indoor-generated pollutants even when windows were closed. Concerns about increasing exposures to indoor-generated pollutants as homes were air-sealed led to the development of the ASHRAE 62.2 residential ventilation standard (Persily, 2015) and the adoption of mechanical ventilation requirements in building codes in California and some other U.S. states.

Air cleaning and filtration can be integrated into mechanical systems to reduce pollutant concentrations in residences (Siegel, 2016). A high performance filter in the forced air heating and cooling (HAC) system will remove particles when the system operates for thermal control and can be operated on a timer when no conditioning is needed. Filtration effectiveness has been investigated through measurement studies in homes (Batterman et al., 2012; Du et al., 2011; MacNeill et al., 2012; Noris et al., 2013; Spilak et al., 2014; Stephens and Siegel, 2013) and also via simulation studies that tend to focus on population-scale benefits (Azimi et al., 2014; MacIntosh et al., 2010; Zhao et al., 2015).

In this paper, filters are characterized by the Minimum Efficiency Reporting Value (MERV), determined by the ASHRAE Standard 52.2 test procedure (ASHRAE, 1999). The standard measures removal in 12 particle size bins then aggregates results in bins of 0.3–1, 1–3, and 3–10 μm diameter particles. Higher MERV filters remove higher percentages of particles. The lowest MERV designation that considers removal of 0.3–1 μm particles is MERV13. The ASHRAE 62.2 standard requires a MERV6 filter for recirculating forced air systems (ASHRAE, 2013). Stephens and Siegel have reported filter performance results for particles below the size range of the ASHRAE 52.2 test (Stephens and Siegel, 2012a; Stephens and Siegel, 2013). Installed filter performance can vary over time, depending on the media and type of charging (if any), the characteristics of the aerosol, the amount of loading, bypass, and other factors (Hanley et al., 1994; Hanley and Owen, 2003; Lehtimäki and Saamanen, 2005; Owen et al., 2013).

This study aimed to measure the performance of various ventilation and filtration system designs in an uninhabited house with a relatively airtight shell and a central forced air heating/cooling system as representative of modern construction. Systems were operated over multiday periods in two California seasons: very warm to hot conditions in summer and locally cool to cold in fall/winter. This paper focuses on performance of the systems for outdoor PM_{2.5}, UFP, BC, and ozone, and for indoor-generated particles from a scripted cooking procedure. Performance results for VOCs and additional analyses are included in the final project report (Singer et al., 2016).

MATERIALS AND METHODS

Overview

Systems of ventilation and filtration components were evaluated for pollutant removal and energy performance in an unoccupied house in Sacramento, California. The systems included variations in ventilation approach, filtration location, and filtration quality. Two sets of air pollutant analyzers were configured to continuously measure size-resolved indoor and outdoor concentrations of particles from 6 nm to 2.5 μm diameter, black carbon, and ozone. PM_{2.5} mass was estimated from size-resolved particle number concentrations. Data from the two monitoring apparatuses were analyzed to obtain continuous time series of indoor and outdoor concentrations, from which 24h and 1h running means were calculated. Indoor/outdoor (IO) ratios and percent reductions of indoors relative to outdoors were calculated. Systems were evaluated for indoor particle removal using a scripted cooking event. Energy impacts were estimated from measurements and rated power consumption of components and estimates of system run time.

Test House and Mechanical Systems

Experiments were conducted in a 2006-built, 106.7 m² (1148 ft²), detached house that was leased for the study from September 2013 to February 2015. A schematic is provided in Figure 1 and the house exterior is shown in Figure S.1 of the Supporting Information (SI). The house is typical for its vintage in California: single-story, concrete slab foundation, stucco exterior, and tile roofing. Ceiling heights were 2.75 m (9 ft) except for the great room, which had a sloped ceiling rising from 2.75 m at the back wall to 4 m (13 ft) in the center of the house. Envelope air leakage was measured as 438 L/s (928 cfm) at a 50 Pa indoor-outdoor pressure difference (ASTM E1827-11, 2011), equivalent to 5.0 ACH₅₀ at the calculated volume of 316 m³ (11,154 ft³). Heating and cooling were provided by a ducted forced air unit (FAU) with gas furnace and split air conditioner. The house is 250 m from Interstate 80, in the predominantly downwind direction.

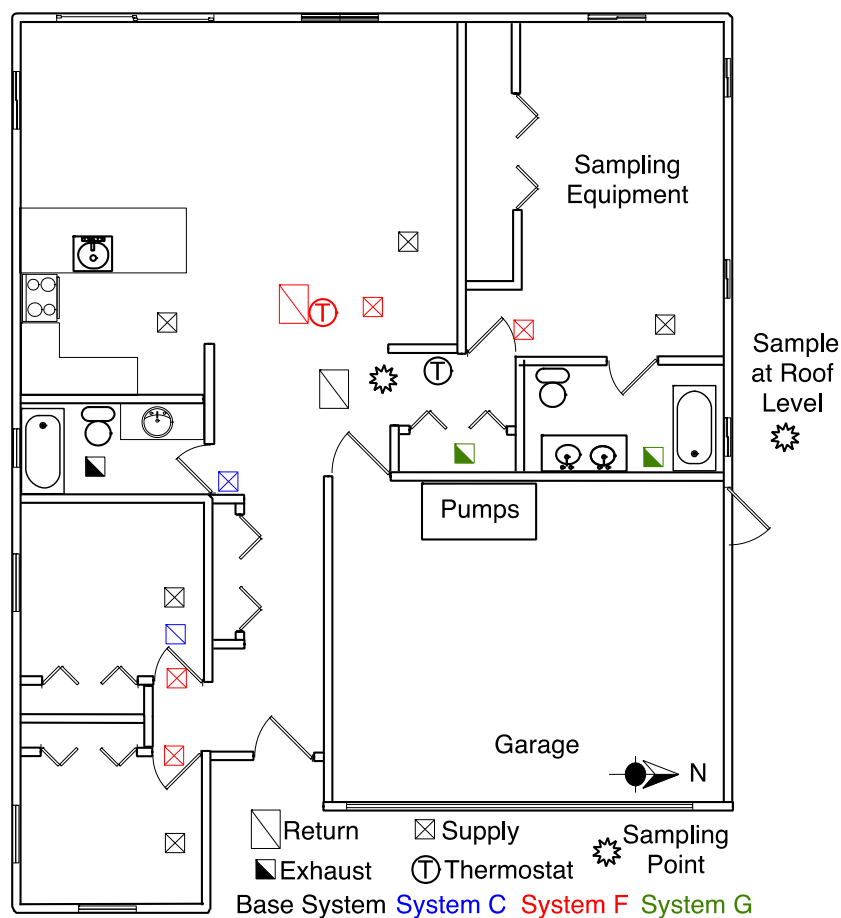


Figure 1. Schematic plan view of test house, drawn to scale.

Nine systems combining mechanical ventilation and air cleaning components were installed for evaluation. They are described in Table 1 and schematics are provided in Figure 2. The system selection process and details about system components are provided in the SI. Selected systems included variations for each major component: (a) exhaust, supply and balanced ventilation; (b) enhanced particle removal using MERV8, MERV13, MERV16, or HEPA filters or an electrostatic precipitator (ESP); (c) VOC removal using activated carbon, a chemisorbent, and a catalyst technology; (d) supply and balanced ventilation provided via the FAU or separate ductwork. A system with continuous exhaust ventilation and no enhanced filtration was designated as the Reference owing to its common use in California.

Table 1. Summary descriptions of system designs selected for testing.

System ID	Ventilation system description	Runtime control ¹	HAC return filtration	Filtration of ventilation air	VOC removal
Ref.	Exhaust, continuous	No	MERV4 ²	Building envelope ³	None
E	Exhaust, continuous	Yes	MERV13 (2.5 cm) at return grille	Building envelope ³	None
F	Exhaust, continuous	Yes ⁷	MERV13 at return of mini-split	Building envelope ³	None
Portables (+Ref)	Exhaust, continuous	No	MERV4 on FAU ² + 2 portable filtration units	Building envelope ³	None
A	Supply, continuous; distributed by FAU ducts or exiting at return grille	No	MERV4 ²	MERV13	None
B	Supply, continuous; distributed by FAU ducts or exiting at return grille	No	Electrostatic precipitator (ESP) ⁴	MERV13	None
C	Supply, continuous; separately ducted and blended	No	MERV4 ²	MERV16	Catalyst ⁵
D	Supply, on timer ¹ ; distributed by FAU ducts	Yes	Deep pleated MERV16 at FAU, on timer ⁶	MERV8 on supply, MERV16 on FAU	Chemisorbent ⁶
G	HRV, on timer ¹ , supplying into FAU	Yes	HEPA on bypass timed w/HRV + MERV4 on FAU	MERV8 on HRV + HEPA bypass	Activated Carbon

¹The runtime controller operates the forced air unit (FAU) for at least 20 min each hour. ²Installed as minimal protection for the furnace and coiling coils; not intended for removal of health relevant particles. ³Envelope can remove particles as air infiltrates to replace air being removed by the exhaust ventilation system; particle removal rates in building envelopes vary. ⁴Product marketed as an “electronic air cleaner”. ⁵Manganese oxide catalyst that oxidizes formaldehyde and other VOCs at room temperature (Sidheswaran et al., 2011). ⁶Purafil PuraGrid with IAQ Media Blend (PG20252-IAQ). ⁷The mini-split fan ran continuously on low speed to provide low pressure drop filtration and operated at higher speeds as needed for thermal conditioning.

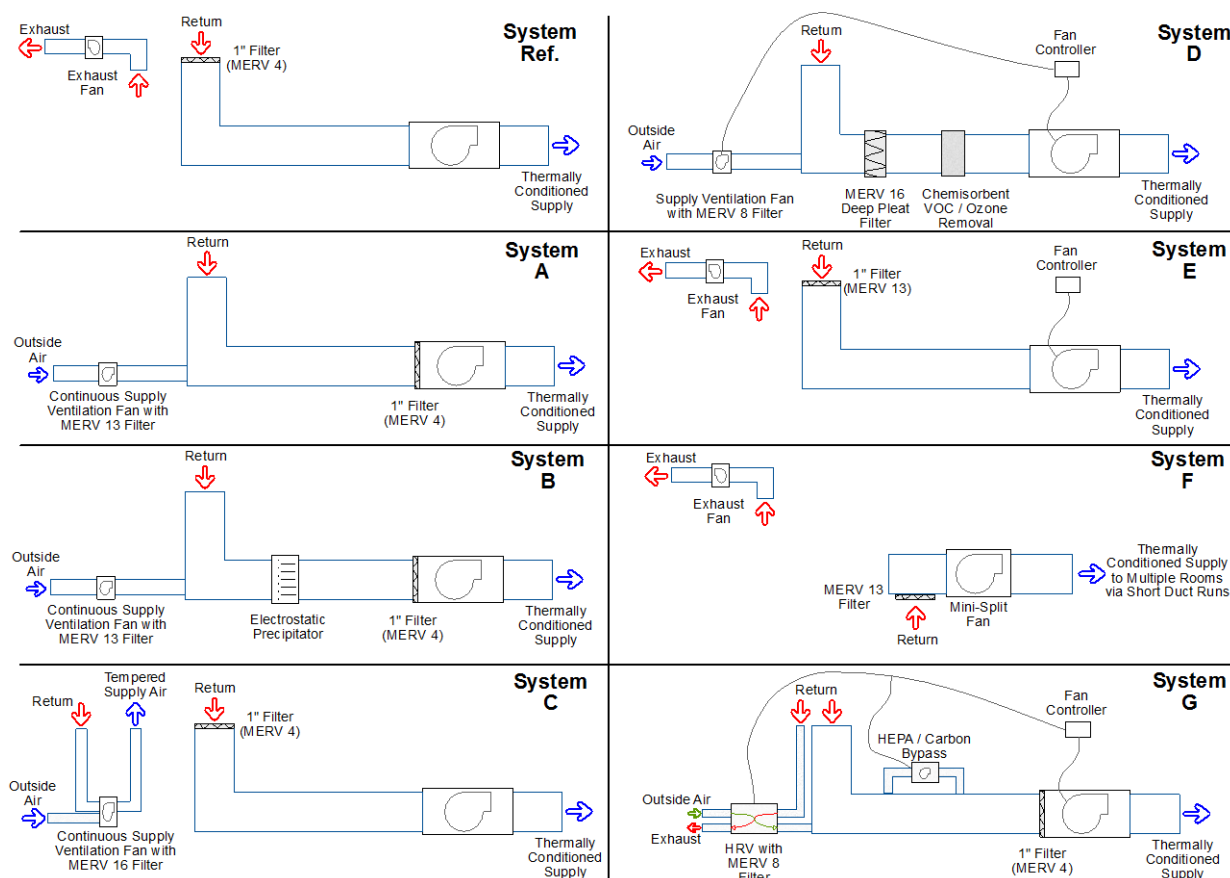


Figure 2. System schematics.

Systems were installed to enable quick switching for sequential operation during each season. The existing forced air heating and cooling system (FAU) was retained and ducting was modified to incorporate all system architectures. High-quality dampers established the flow paths shown in Figure 2. Testing confirmed low leakage rates. Supply and return register locations are shown in Figure 1. Most of the equipment was in the attic. The blending unit for System C was installed in the central hall closet and the HRV was installed in the garage. Supply ventilation air intakes were connected to a gable vent below the outdoor particle inlet (Figure S.1 of SI).

An Ecobee Smart SI Thermostat was installed to provide remote access and set with the schedule assumed in the Title 24-2013 Residential Alternative Calculation Method (SI Section S.1.4).

Airflow and power consumption were measured for each air-moving component and power consumption was measured for the ESP of System B. Methods and results of these measurements are provided in the SI.

Since pollutants inside the house were measured at only one location, the air was mixed to reduce spatial variations. Portable fans (AirKing Model 9102, rated at 439 L/s or 930 cfm) were installed by the front door, on the kitchen counter, and in the hallway near the return grille and operated continuously. In May, an additional mixing fan (FanTech FR-100) with ducting was installed to move air at 52 L/s (110 cfm) from the master bedroom to the great room. This also

moved heat generated by the instruments to other parts of the house. The effect of mixing fans on particle removal rates in the home was not determined. During all monitoring periods, blinds in all the windows and doors were angled to minimize incoming sunlight.

Environmental, air pollutant, and equipment monitoring

Wind speed and direction were measured with an anemometer (containing Met One 010C and 020C sensors) mounted above the roofline, adjacent to the air intakes for supply ventilation and outdoor particles, as shown in Figure S.1. Outdoor T and RH were measured and logged every 5 min using an Onset HOBO U23-001 placed on the north end of the house approximately 1 m above the ground. Precipitation and fog data were obtained from measurements at McClellan air force base, located approximately 5 km from the test house. Data were downloaded from www.weatherunderground.com.

Temperature and humidity inside the home were measured and logged every 5 min using ONSET HOBO loggers (model U12-012) and every 15 min by the ECOBEE thermostat. HOBOs were placed at 1 m height in the front bedroom and master bedroom, in the supply register in the master bedroom, in the return plenum, and in the garage.

The measurement system was designed for continuous, unattended monitoring of indoor and outdoor concentrations of particles from 6 nm to 2.5 μm , black carbon, and ozone. Instrument specifications are provided in Table S.3. Particle concentrations were resolved to the following size bins (in μm): 0.06–0.1, 0.1–0.3, 0.3–0.4, 0.4–0.5, 0.5–0.7, 0.7–1.0, and 1.0–2.5. The first bin was calculated as the difference between CPC 3787 (0.06–2.5 μm) and CPC 3781 (0.1–2.5 μm) measurements. The second bin was obtained as the difference between CPC 3781 data and the summed total of particle counts from the OPC channels between 0.3 and 2.5 μm . The other bins are those of the OPC.

Pairs of real-time monitoring instruments simultaneously measured indoor and outdoor air with functionally identical isokinetic sampling lines and manifold systems. Valves synchronously switched indoor and outdoor sample inlets between the two manifolds. This configuration was intended (1) to minimize errors in comparisons of indoor and outdoor particle levels that would result from drifts in instrument response, and (2) to reduce data loss by ensuring that at least a semi-continuous signal would be obtained for each location in the event of instrument failure. Ozone monitors were dedicated to indoor and outdoor air without switching. More details about the pollutant monitoring system are provided in the SI.

The air exchange rate was measured by continuous release and time-resolved measurement of sulfur hexafluoride (SF_6). Details are provided in the SI.

Monitoring Periods

Initial system operation and performance measurements occurred in January and February 2014, providing valid winter data for the Reference and System C (Table S.4). Instruments were powered down on March 19 and serviced as needed. Systems were restarted in May and operated through August to determine performance for outdoor particles and ozone during summer conditions and also for cooking particles (see below). Equipment was shut down August 6 for servicing then restarted in early October and operated through December 2014 to evaluate performance for outdoor particles during locally relevant fall and winter conditions. Table S.5 of the SI presents the monitoring dates for each system in each season.

Experiments to determine performance for indoor-generated particles

Performance for indoor-generated particles was assessed using a scripted cooking activity that generated particles from the ultrafine mode (<100 nm) to >1 µm. The activity involved stir-frying of string beans with oil, in a wok, over high heat for about 5 min (Lunden et al., 2014).

Cooking was synchronized with the start of a 20/60 operating cycle for Systems A, B, D, E, and G. This provided roughly 40 min for particles to mix throughout the house and be removed by ventilation and deposition before enhanced filtration operated for 20 min. Systems A and B operated through one hour-long cycle and Systems D, E, and G operated through two cycles. Continuous systems (C, F, Reference) were tracked for 80-90 min after cooking started. SF₆ was injected just before cooking to track outdoor air exchange during each experiment.

Following completion of each cooking experiment, a standalone 566 L/s (1200 cfm) fan (Dayton model 7M7T1) with HEPA filter unit (AirHandler model 2EJY3) and the two portable air cleaners were operated on high speed for 30-60 min. The supplemental fan-filter unit was in the great room at the back of the house. The intent was to remove particles that remained from cooking prior to starting an evaluation period for outdoor particles.

Data processing and analysis

Size resolved particle concentrations were used to estimate mass concentrations following the approach of (Sioutas et al., 1999), which was applied in field studies in Pittsburgh (Khlystov et al., 2004) and Los Angeles (Shen et al., 2002). Our application used the following assumptions: (1) all particles were spherical; (2) the mass mean diameter within each size bin was the midpoint diameter of the bin, and (3) all particles had the same seasonally-dependent density. Based on the first assumption, the volume of an individual particle was taken as $V_p = 4/3\pi(d/2)^3$ where d is particle diameter. Based on the second assumption, the total volume of the n_i particles within bin i , was calculated as $V_{bin} = n_i * V_{p,i}$. Volume estimates were converted to mass using the seasonally-dependent densities of 2.16 g cm⁻³ for winter and 1.43 g cm⁻³ for summer, as reported in Table 2 of (Hasheminassab et al., 2014).

Data from the two sets of instruments on the switching manifolds were processed to obtain continuous indoor and outdoor time series, as described in Section S.1.12 of the SI. These data were used to calculate running means for time windows of 1, 8 and 24 h. Since the home was unoccupied, system effectiveness for outdoor pollutants is indicated by the indoor to outdoor (IO) concentration ratio and as the percent reduction of indoor relative to coincident outdoor concentrations, calculated as 1–IO. Summary statistics were calculated for each diurnal interval and each monitoring period. Diurnal intervals were set to begin and end in the troughs of the outdoor particle profiles. Effectiveness for outdoor peaks was calculated by first identifying the highest 1h outdoor concentration each day, then finding the highest 1h indoor peak within the next 4 h and taking the IO ratio.

Performance for indoor-generated particles is presented as the reduction in time-integrated concentration when a system operated compared to the concentration with no system operation. To calculate this parameter, we used first order decay rates determined for each particle size bin over 15-min intervals after each cooking event because the decay rates in many cases changed over time. For intervals interrupted by a change of state (e.g. FAU turned on), shorter sections of data were used. The “as-tested” performance for each system was calculated as the reduction in

time-integrated concentration over the first hour following the peak from cooking. To account for variability in emissions from the scripted cooking event (Lunden et al., 2015), we calculated the reduction using the fitted decay rates for each system state of operation along with the actual operating schedule. The time-integrated concentration for the reference condition was based on the observed decay with no FAU operation. Potential reductions were calculated for each system assuming continuous operation and applying the fitted decay rates over a full hour of operation.

Estimation of Annual Energy Use

There is an energy cost to operating mechanical systems for ventilation and pollutant removal. We estimated the fan and air cleaner energy requirements for system to be deployed in California, including (1) extra hours of FAU operation for filtration and/or supply ventilation (but not the energy required for thermal conditioning), (2) changes in fan power as airflow resistance increases, and (3) operation of air cleaning devices including the ESP of System B and the HEPA + Activated Carbon unit of System G. We calculated incremental energy as the product of run time and power draw for each system component. Details are provided in the SI.

RESULTS AND DISCUSSION

Performance for Outdoor Particles

Tables S.7–S.8 in the SI provide summary statistics for outdoor conditions during each of the assessment periods for outdoor particles. PM_{2.5} levels generally were higher in fall/winter than summer, though there was substantial variability in each season.

Examples of the processed data analyzed to assess performance for outdoor particles are presented in Figures 3–4. These plots show outdoor and indoor time series of PM_{2.5} estimated from size-resolved particle counts, as described above. During both periods, outdoor concentrations varied by an order of magnitude with a diurnal pattern of peaks around midnight. Indoor concentrations followed outdoors with a delay of several hours and at substantially lower levels owing to particle losses during infiltration and from indoor deposition. There were large differences between the systems, with 24h indoor/outdoor (IO) ratios of 0.3–0.5 for System A and 0.04–0.06 for System F. Plots for all particle size bins during all assessment periods are included in appendices to the final project report at www.arb.ca.gov/research.

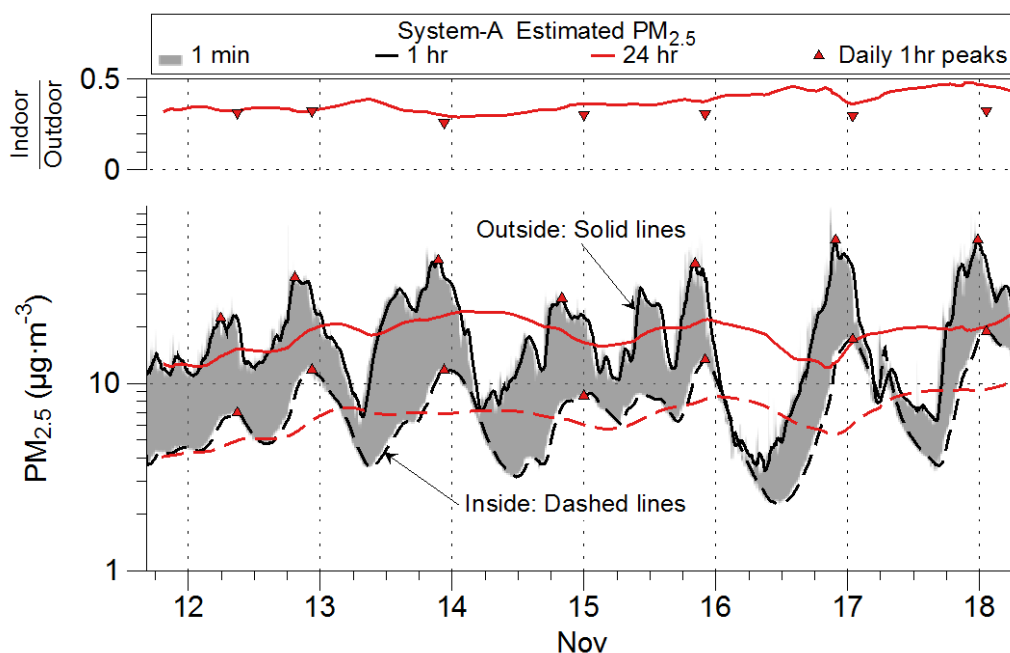


Figure 3. Estimated PM_{2.5} mass calculated from size-resolved particle number concentrations during operation of System A (continuous supply ventilation with MERV13 filtration), Nov 11-17, 2014. The top and bottom of the grey band are 1-minute outdoor and indoor concentrations. Black lines are running 1h averages and red lines are running 24h averages. Red triangles show the indoor highest 1h average during each day and the corresponding highest 1h average outdoors. The top section shows indoor / outdoor ratios.

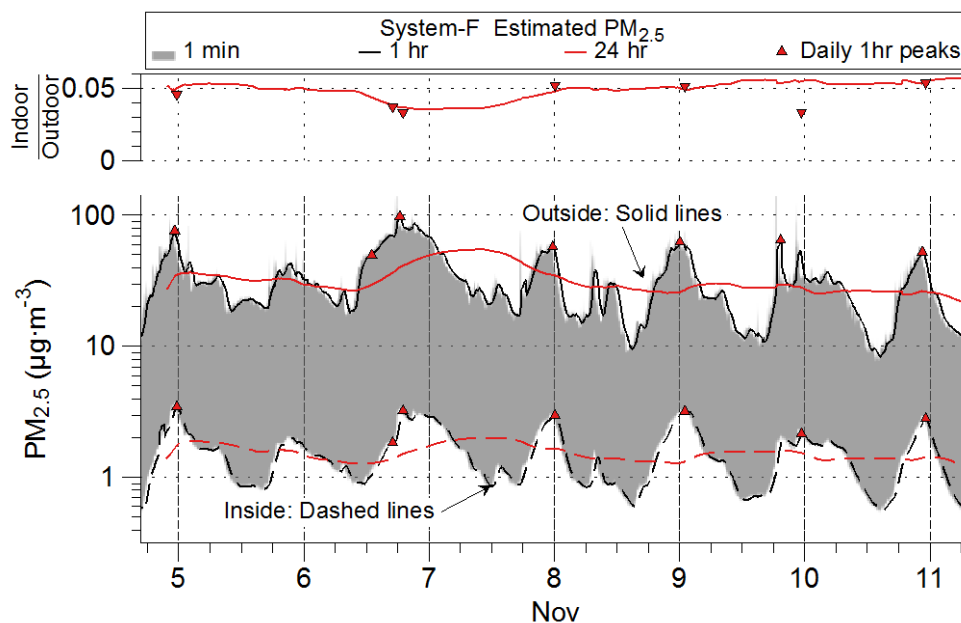


Figure 4. Estimated PM_{2.5} concentration calculated from size-resolved particle number concentrations during operation of System F (exhaust ventilation and MERV13 filtration on a mini-split heat pump operating continuously at low speed), Nov 4-10, 2014. See caption of Figure 3 for description of data plotted.

Effectiveness at reducing in-home concentrations of outdoor particles is indicated by the 24h average IO ratios for estimated PM_{2.5}, UFP, and BC, shown in Figure 5. The boxes present the interquartile range of all the IOs calculated for all minutes of each assessment period and whiskers show 1.5x the interquartile range. All systems performed better (lower IO) for UFP and worse (higher IO) for BC relative to PM_{2.5}. BC results for Systems C and D in both summer (SU) and fall/winter (FW) are biased toward lower performance as indoor concentrations were often below quantitation limits (QL) and set to half the QL when that occurred. The second (right) result for Systems A and E in FW is for monitoring that occurred with filter edges taped to minimize bypass. Consistency of these results with standard operation (left bars) suggests that bypass was not a factor. During the period when the portable air filters were set to “Auto” they mostly remained on low speed; hence the use of “low” to identify this period.

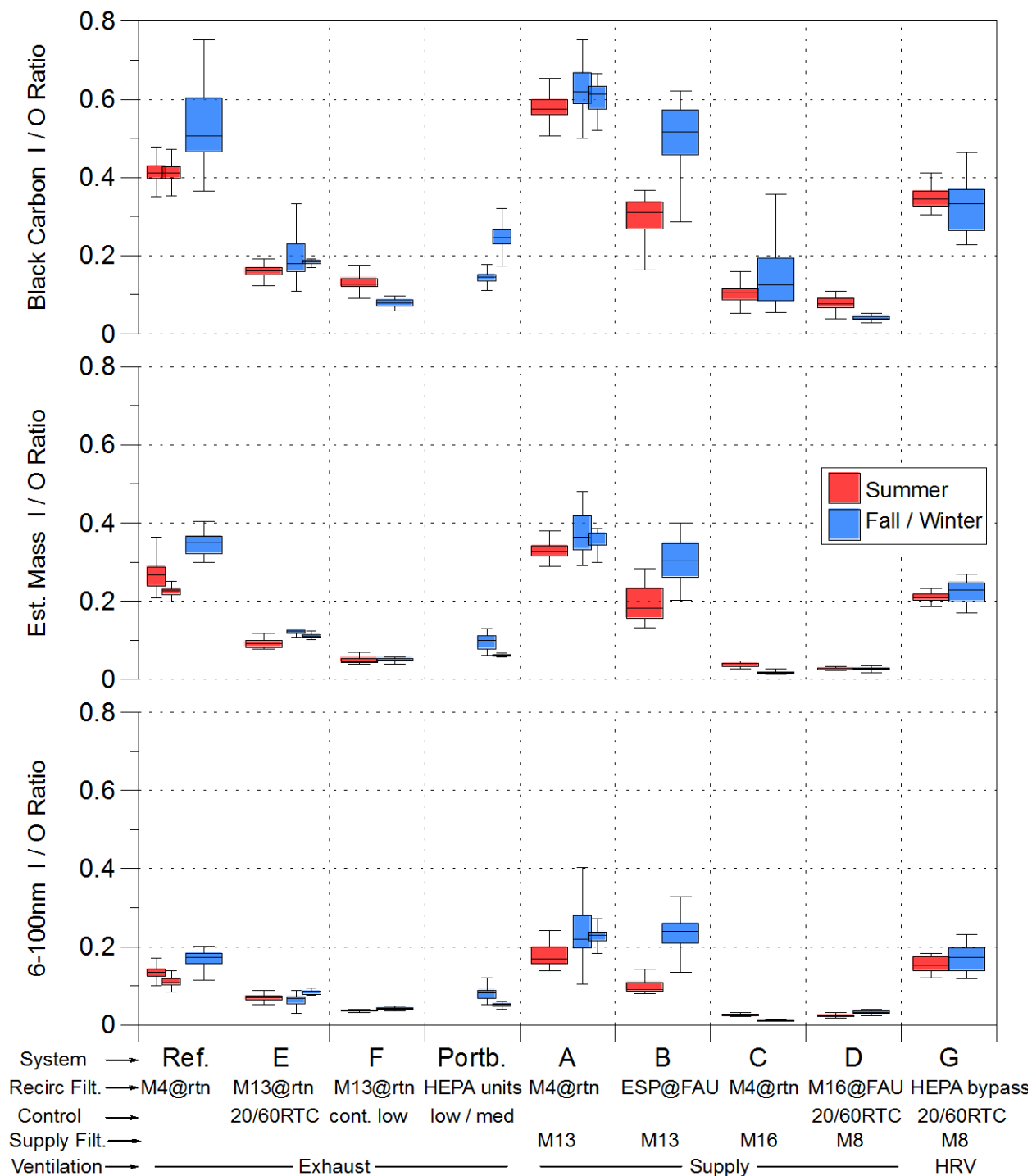


Figure 5. Running 24h mean indoor/outdoor ratios for black carbon, estimated PM_{2.5}, and ultrafine particles (6-100 nm) for systems operating over multi-day periods in fall/winter (FW) and summer (SU). The Reference was assessed over two distinct periods in SU. For Systems E and A, the right bar in FW presents results for operation with tape around the filter to ensure no bypass and the left bar represents the standard weeklong assessment period. Bars present the interquartile range (IQ) and whiskers are 1.5x the IQ. SI Table S.10 provides the days of data for each system and season.

Though we did not conduct a systematic analysis of this relationship, a visual review of the data suggests that PM_{2.5} IO ratios were relatively insensitive to outdoor concentrations. As an example, the first and third diurnal intervals for System A in FW (Figure 3) had outdoor PM_{2.5} of 14 and 24 $\mu\text{g m}^{-3}$, respectively, and the IO ratios were 0.33 and 0.30 on these days.

Table 2 presents the percent reductions of indoor 24h mean concentrations relative to coincident outdoor 24h means. Results in this table are the mean and standard deviation across daily intervals set according to the diurnal pollutant pattern.

Table 2. Percent reduction in 24h mean indoor PM_{2.5} mass, ultrafine particles (UFP) and black carbon (BC), relative to outdoors for each evaluation period, presented as mean (SD) across distinct diurnal periods [days].¹ Mean of daily air exchange rates (AER) also shown.

System Description (M=MERV)	N [days]		PM _{2.5}		UFP		BC		AER [h ⁻¹]	
	SU	FW	SU	FW	SU	FW	SU	FW	SU	FW
Exhaust Ventilation										
Ref: M4@rtn	13	7	75 (3)	65 (3)	87 (2)	84 (3)	57 (6)	47 (8)	0.29	0.22
E: M13@rtn	6	3-7 ³	93 (2)	88 (1)	93 (2)	95 ³ (3)	91 (3)	81 (6)	0.27	0.35
E: w/o bypass	nd ²	4	nd ²	88 (1)	nd ²	91 (1)	nd ²	81 (2)	nd ²	0.27
F: M13 on mini-split	4	7	95 (1)	95 (1)	96 (0)	96 (0)	87 (2)	92 (1)	0.31	0.30
Portables on Auto / Low	nd ²	4	nd ²	90 (2)	nd ²	92 (1)	nd ²	85 (3)	0.31	0.31
Portables on Medium	nd ²	3-4 ⁴	nd ²	94 (0)	nd ²	95 (1)	nd ²	79 ⁴ (5)	nd ²	0.35
Supply Ventilation										
A: M13@Supply	4-5 ⁵	7	67 (2)	63 (5)	82 (3)	77 (8)	45 ⁵ (3)	39 (6)	0.29	0.28
A: w/o bypass	nd ²	4	nd ²	64 (2)	nd ²	77 (2)	nd ²	39 (4)	nd ²	0.31
B: M13@Supply/ESP@FAU	7	7	82 (7)	69 (5)	90 (4)	76 (5)	75 (9)	50 (9)	0.21	0.28
C: M16@Supply	7	7	96 (1)	97 (3)	97 (1)	99 (0)	91 (3)	84 (10)	0.23	0.22
D: M8@Supply/M16@FAU	7	7	97 (0)	97 (1)	98 (0)	97 (1)	93 (2)	96 (1)	0.25	0.34
Balanced Ventilation										
G: M8@Sup/HEPA bypass	5	6	79 (1)	78 (3)	84 (2)	83 (3)	66 (2)	68 (5)	0.27	0.35

¹Diurnal periods did not start at the same time as monitoring. Some days have <24h of data; but no day has <10h of data. ²No data. ³UFP based on 3d of data; both CPC-3787 instruments failed during other days. ⁴BC based on 3 days of data; 4th day was outlier (>3 σ from mean). ⁵BC based on 4 days of data; 5th day was outlier (>3 σ from mean).

Despite having no enhanced pollutant removal technology beyond a modestly tight shell to limit infiltration with windows and doors closed, the Reference system had indoor concentrations much lower than outdoors. System A, with MERV13 filtration on continuous supply ventilation, performed a bit worse than the Reference for all three parameters. System B, which had the same ventilation system as System A along with an ESP on the FAU, performed similarly and perhaps slightly better than System A in fall/winter. In summer, the ESP operated several hours per day as the FAU provided cooling and the performance of System B was clearly better. The systems that provided the best protection for outdoor particles were C, D, and F. These systems – which included two with MERV16 filtration on supply ventilation (C and D) and one with MERV13 filtration on a continuous recirculating flow through the mini-split fan unit (F) – yielded reductions in indoor concentrations, relative to outdoors, by 95-97% for PM_{2.5}, 96-99% for UFP, and at least 84-96% for BC across SU and FW seasons. The next-best system was E, with

MERV13 filtration through the FAU operating intermittently with a fan timer. System G, with supply ventilation and a HEPA bypass on the FAU return operating intermittently with timer, performed similarly to the Reference for UFP, but showed moderate improvements for PM_{2.5} and BC. During limited testing in FW, the two portable HEPA air filtration units lowered UFP and PM_{2.5} similarly to System F when the portables operated continuously on medium setting. When operated on automatic setting, performance was similar to System E for UFP, PM_{2.5} and BC.

Table 2 also presents the measured AERs for the outdoor particle mitigation evaluation periods. There were variations in AER, even for systems that used the same ventilation equipment (e.g. Ref, E, and F) caused by variations in temperature and wind driving forces impacting the infiltration component of outdoor air exchange. Higher AER tends to increase IO ratios when other parameters are unchanged. It is thus notable that systems D, E, F, and the Portable HEPA units achieved low IO ratios despite having higher AERs relative to the Reference in fall/winter. Higher AERs may have contributed to the slightly worse performance of Systems A and B relative to Reference in winter.

Performance for Indoor-Generated (Cooking) Particles

Example data from a cooking experiment are provided in Figures S.10–S.11 of the SI.

Summary results for cooking particle removal are provided in Figure 6, which presents the reduction in time-integrated PM_{2.5} relative to the baseline condition of no FAU operation. An analogous plot of UFP results is provided in the SI. The “As Tested” performance of System A is expected to be the same as the Reference (within experimental error) because it has no recirculation filtration. And the recirculation flow through System C (for tempering) is too small to provide noticeable benefit. Systems D, E, and G all provide moderate improvements over the Reference system. A much larger benefit was observed for System F and for the Portables, which operated continuously for the hour after cooking. As Tested results represent a minimum benefit because intermittent systems operated only at the end of the hour. For the first 40 min, intermittent systems were identical to the Reference.

Figure 6 also presents calculated reductions for systems operating over the entire hour (Always On). For intermittent systems (B, D, E, and G) the reduction was estimated by calculating the concentration over the hour assuming the first order removal rate observed during intermittent system operation. For the Reference and System A, reductions for Always On are assumed to result from deposition of large particles in the FAU and ductwork. When operated continuously, Systems B, D, E, and G provide large reductions for the indoor-generated particles.

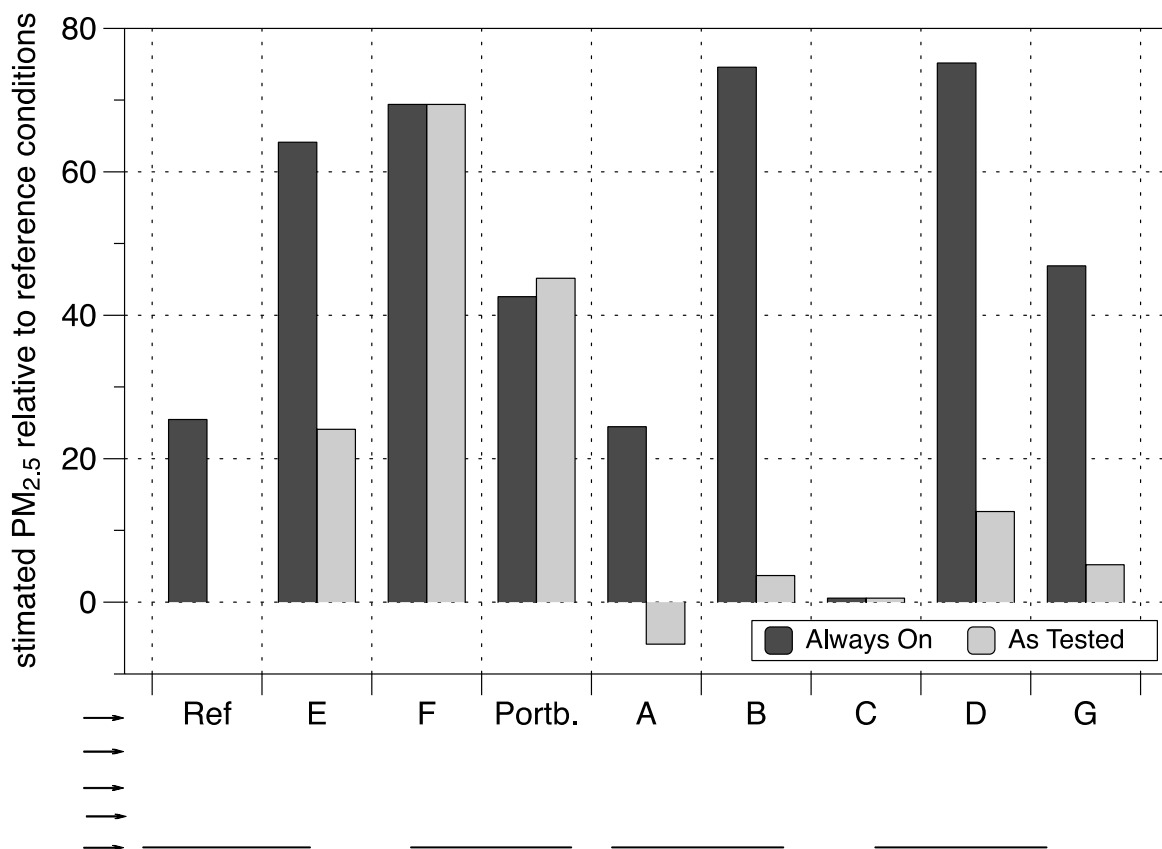


Figure 6. Reductions in estimated PM_{2.5} concentrations over 1h following an indoor cooking event, relative to Reference system. For systems with intermittent FAU operation, cooking occurred at the start of the 40 min interval between FAU operating periods. “Always on” is the estimated reduction with the recirculating filtration system operating continuously for the hour.

Performance for Ozone

Example ozone data are provided in SI Figure S.13. Summary results for measured concentrations and system performance for ozone during summer are presented in Table 3. Performance was similar for all systems other than System B, which had substantially higher IO ratios and thus a lower protection factor. The IO ratios of 0.03–0.04 for the highest daily 8h and 1h concentrations for the Reference and Systems C and D are calculated using mean indoor concentrations below the nominal single measurement quantitation limit. Only System B had indoor daily high concentrations mostly above the QL. The higher IO ratios for System B result from ozone production in the ESP, as shown in Figure S.14 of the SI. Ozone production by an ESP has been reported previously (Poppendieck et al., 2014).

Table 3. Summary results for ozone.¹

System ² (start)	Days	Highest 8h Outdoor		Highest 8h Indoor		High 1h Outdoor		Highest 1h Indoor		I/O ratio of highest 8h		I/O ratio of highest 1h	
		Mn	SD	Mn	SD	Mn	SD	Mn	SD	Mn	SD	Mn	SD
Ref (7/2)	7	60	10	1.9	0.2	72	9	2.0	0.2	0.03	0.00	0.03	0.00
Ref (7/16)	6	37	6	1.6	0.1	44	8	1.6	0.1	0.04	0.01	0.04	0.01
B	7	50	12	5.9	1.3	59	16	7.4	1.5	0.12	0.02	0.13	0.03
C	7	55	12	1.7	0.2	64	17	1.9	0.3	0.03	0.00	0.03	0.01
D	7	53	11	1.5	0.1	64	19	1.7	0.3	0.03	0.01	0.03	0.00
G	3	59	11	2.5	0.6	68	15	2.5	0.6	0.04	0.00	0.04	0.01

¹Data unavailable for Systems E and F because of instrument problems. ²Ref = Reference, exhaust ventilation with no enhanced filtration. B has supply ventilation with MERV13 filtration and electrostatic precipitator on FAU return controlled by thermostat. C has MERV16 filtration on a blended supply ventilation system. D has supply ventilation with MERV8 filter and MERV16 filtration on the FAU operating on a 20/60 cycle. G has an HRV with MERV8 filter on the supply and a bypass with HEPA filtration on the FAU.

Power and Energy Use

Annual energy use estimates, presented in Figure 7, are for systems installed in mid-2000s, code-compliant homes in California. Actual incremental energy use would vary somewhat by climate zone, specific characteristics of the home, and thermostat settings, which impact both the baseline operating schedule of the forced air system and extra operation for air cleaning. The left panel of Figure 7 is for a conventional permanent split capacitor (PSC) FAU motor, as found in the test house. The panel at right is for a brushless permanent magnet (BPM) fan motor. These results demonstrate the increased energy required when the FAU is operated year-round for filtration (e.g., for D, E, and G). Systems with filtration only on supply fans (A-C) have much smaller energy requirements. The Portable HEPA filtration units, which reduce exposure to both indoor and outdoor particles, require only a modest increase in energy use. The right panel shows that an efficient blower motor reduces energy use for all systems, with the largest impact on systems that use the FAU for ventilation and/or filtration.

We do not provide a quantitative estimate the incremental energy requirement of System F because the mini-split heat pump cannot be assumed to have the same base operation schedule as the conventional FAU. Since mini-splits operate at varying capacity over many more hours in both heating and cooling seasons, there would be less operation expressly for the purpose of filtration. Since these devices are also more efficient at part-load, the incremental energy required for System F is likely to be much less than for D and E, i.e. <600 kWh/y.

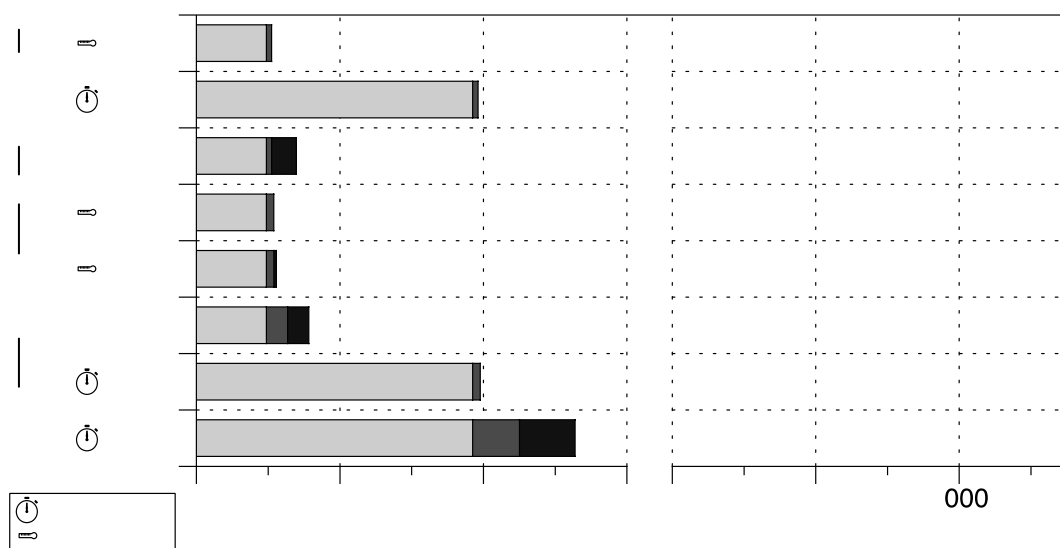


Figure 7. Estimated fan energy use for ventilation and air recirculation for filtration.

Results for the Reference system include the FAU fan energy required for thermal conditioning of the extra outdoor air brought in by the mechanical ventilation system along with energy to power the ventilation fan. The energy required to thermally condition the ventilation air is not included. Results for other systems include FAU fan energy for heating and cooling distribution plus any additional operation for enhanced pollutant removal. The panel at right presents estimates for a system with an efficient, variable speed brushless permanent magnet motor.

The higher MERV filters tested in this study had small impacts on airflow and power. The deep-pleated MERV16 filter of System D reduced FAU flow by 2.7% and power consumption by 2%. The 1" MERV13 filter of System E reduced FAU flow and power by roughly the same amount, 5%. Details are provided in SI Section S.2.5.

Considerations for Low Energy Homes

Many new homes in California and elsewhere are tighter than the test house (Chan et al., 2013), and high performance home standards require even tighter construction. With less air entering via infiltration, ventilation design (exhaust vs. supply/balanced) and the quality of supply filtration will have a larger impact on indoor concentrations of outdoor particles. There is evidence that tighter homes have lower penetration rates for submicron particles (Stephens and Siegel, 2012b). Results for System A in this study suggests that a MERV13 or better filter is needed on supply ventilation to avoid increasing in-home levels of outdoor particles relative to exhaust ventilation for a moderately airtight home.

Changes to heating and cooling (HAC) equipment designs and operation in energy efficient homes will impact the costs and benefits of central FAU filtration. An increase in the availability and use of multistage, variable output HAC equipment that also has sophisticated controls could lead to more opportunities to modulate and manage filtration airflow for lower energy operation.

Caveats and Other Considerations

There are several important caveats to the results presented in this paper. The first is that all filters were installed and used without preconditioning or preloading. Even accounting for the higher loading rate associated with 20/60 or continuous operation, filters were used over short durations relative to recommended service lifetimes in residences. Except for the filter on the mini-split unit (System F), all filters were replaced at the start of each season. Results thus reflect performance of filters that were used for less than 3 weeks total run time. There were no obvious indications – such as dramatic shifts in IO ratios – that any of the filters saw sharp performance degradations that can occur as charged media filters load or performance enhancements that can occur as fiberglass media filters load (Hanley et al., 1994; Hanley and Owen, 2003; Lehtimäki and Saamanen, 2005; Owen et al., 2013).

The second caveat is that there is variability in the performance of filters with any given MERV designation. It is therefore possible that different filters with the same MERV designations would have produced different results for one or more of the systems.

Conditions in the test house differed from occupied homes in ways that could bias particle deposition and affect IO ratios. The lack of furnishings and much lower surface to volume ratios in the test house reduced particle deposition rates relative to an inhabited home, while the higher air velocities from the mixing fans pushed deposition rates higher (Thatcher et al., 2002).

As with all experimental studies, results of this study are based on a limited set of conditions. The test house FAU and the local outdoor air pollution are relevant to many homes throughout California. Assessment during both summer and fall/winter provides results for outdoor pollutant mixes with distinctly different characteristics and patterns. Scripted cooking experiments were included to raise the issue that filtration can be used to protect occupants from indoor-generated particles in addition to those from outdoors; however, effectiveness for the cooking particles should not be construed as predictive of performance for all indoor aerosols.

PM_{2.5} estimated from size resolved particle concentrations may differ from gravimetric measurements. The estimate will be biased if the midpoint bin sizes are very different from the mass mean diameters by bin, or if the effective density differs substantially from assumed values. If selective removal of particles changes either of these parameters between outdoors and indoors, the IO ratio analysis would be impacted. Use of density values from Los Angeles (Hasheminassab et al., 2014) is reasonable as Sacramento has a similar mix of ambient pollutant sources and similar climate, but the lack of coincident density data is a potential source of error.

CONCLUSIONS

Results indicate that houses with moderately airtight shells and continuous exhaust ventilation provide substantial protection from outdoor PM_{2.5}, UFP, BC, and ozone, even without enhanced filtration. To achieve a roughly similar level of protection with supply ventilation requires MERV13 filtration or better. In-home concentrations of outdoor particles can be reduced to <10% of outdoors using MERV13 filtration on a timer-controlled FAU and exhaust ventilation, and to <4% using MERV16 filtration either inline with supply ventilation or on the FAU with timer if using exhaust ventilation. Supply filtration is an energy efficient approach to addressing outdoor pollutants but does nothing for indoor-generated pollutants. The lowest energy solution for reducing in-home exposures to both outdoor- and indoor-origin particles is MERV13 (or

better) filtration on an FAU with efficient fan motor or efficient portable air cleaners, with exhaust ventilation.

ACKNOWLEDGMENTS

This research was conducted for California Air Resources Board (CARB) Contract 11-311; the assessments presented in this paper are those of the authors and not necessarily those of CARB. Manuscript preparation was supported by the U.S. Department of Energy under Contract DE-AC02-05CH11231. Peggy Jenkins, Michael Gabor, Zoe Zhang, Hyung-Joo Lee and the project's technical advisors provided reviews of the research plan and draft reports. Gavin Healy and Dan Perunko of Balance Point Home Performance installed the ventilation and filtration systems. Melissa Lunden and Tosh Hotchi helped design and assemble the pollutant monitoring and data acquisition systems. Frank Hammes of IQAir provided the filter used in System C.

REFERENCES

- Allen, R., Larson, T., Sheppard, L., Wallace, L. and Liu, L.J.S. (2003) Use of real-time light scattering data to estimate the contribution of infiltrated and indoor-generated particles to indoor air, *Environ. Sci. Technol.*, **37**, 3484-3492.
- ASHRAE (1999) Standard 52.2-1999. Method of testing General Ventilation Air-Cleaning Devices for Removal Efficiency by Particle Size, Atlanta, GA.
- ASHRAE (2013) Ventilation and Indoor Air Quality in Low-Rise Residential Buildings, Standard 62.2-2010, Atlanta GA, ASHRAE.
- Astm E1827-11 (2011) Standard Test Method for Determining Airtightness of Buildings Using an Orifice Blower Door West Conshohocken, PA, <http://www.astm.org>, ASTM International.
- Azimi, P., Zhao, D. and Stephens, B. (2014) Estimates of HVAC filtration efficiency for fine and ultrafine particles of outdoor origin, *Atmos. Environ.*, **98**, 337-346.
- Batterman, S., Du, L., Mentz, G., Mukherjee, B., Parker, E., Godwin, C., Chin, J.Y., O'toole, A., Robins, T., Rowe, Z. and Lewis, T. (2012) Particulate matter concentrations in residences: an intervention study evaluating stand-alone filters and air conditioners, *Indoor Air*, **22**, 235-252.
- Beko, G., Kjeldsen, B.U., Olsen, Y., Schipperijn, J., Wierzbicka, A., Karotki, D.G., Toftum, J., Loft, S. and Clausen, G. (2015) Contribution of various microenvironments to the daily personal exposure to ultrafine particles: Personal monitoring coupled with GPS tracking, *Atmos. Environ.*, **110**, 122-129.
- Bennett, D.H. and Koutrakis, P. (2006) Determining the infiltration of outdoor particles in the indoor environment using a dynamic model, *J. Aerosol Sci.*, **37**, 766-785.
- Cassee, F.R., Heroux, M.E., Gerlofs-Nijland, M.E. and Kelly, F.J. (2013) Particulate matter beyond mass: recent health evidence on the role of fractions, chemical constituents and sources of emission, *Inhal Toxicol.*, **25**, 802-812.
- Chan, W.Y.R., Joh, J. and Sherman, M.H. (2013) Analysis of air leakage measurements of US houses, *Energy Build.*, **66**, 616-625.
- Chen, C. and Zhao, B. (2011) Review of relationship between indoor and outdoor particles: I/O ratio, infiltration factor and penetration factor, *Atmos. Environ.*, **45**, 275-288.
- Du, L., Batterman, S., Parker, E., Godwin, C., Chin, J.Y., O'toole, A., Robins, T., Brakefield-Caldwell, W. and Lewis, T. (2011) Particle concentrations and effectiveness of free-

- standing air filters in bedrooms of children with asthma in Detroit, Michigan, *Build. Environ.*, **46**, 2303-2313.
- Hanley, J.T., Ensor, D.S., Smith, D.D. and Sparks, L.E. (1994) Fractional Aerosol Filtration Efficiency of in-Duct Ventilation Air Cleaners, *Indoor Air-International Journal of Indoor Air Quality and Climate*, **4**, 169-178.
- Hanley, J.T. and Owen, M.K. (2003) Developing a new loading dust and dust loading procedures for the ASHRAE filter test standards 52.1 and 52.2 - Final Report for ASHRAE Project No. 1190-RP, Research Triangle Park, NC 27709, RTI.
- Hasheminassab, S., Pakbin, P., Delfino, R.J., Schauer, J.J. and Sioutas, C. (2014) Diurnal and seasonal trends in the apparent density of ambient fine and coarse particles in Los Angeles, *Environ. Pollut.*, **187**, 1-9.
- Hei Review Panel on Ultrafine Particles (2013) Understanding the Health Effects of Ambient Ultrafine Particles. HEI Perspectives 3. , Boston, MA., Health Effects Institute.
- Khlystov, A., Stanier, C. and Pandis, S.N. (2004) An algorithm for combining electrical mobility and aerodynamic size distributions data when measuring ambient aerosol, *Aerosol Sci. Technol.*, **38**, 229-238.
- Lehtimäki, M. and Saamanen, A. (2005) Investigation of mechanisms and operating environment that impact the filtration efficiency of charged air filtration media. Final report to the American Society of Heating, Refrigerating, and Air-Conditioning Engineers (ASHRAE 1189-RP 2005).
- Lunden, M.M., Delp, W.W. and Singer, B.C. (2015) Capture efficiency of cooking-related fine and ultrafine particles by residential exhaust hoods, *Indoor Air*, **25**, 45-58.
- Macintosh, D.L., Minegishi, T., Kaufman, M., Baker, B.J., Allen, J.G., Levy, J.I. and Myatt, T.A. (2010) The benefits of whole-house in-duct air cleaning in reducing exposures to fine particulate matter of outdoor origin: A modeling analysis, *Journal of Exposure Science and Environmental Epidemiology*, **20**, 213-224.
- Macneill, M., Wallace, L., Kearney, J., Allen, R.W., Van Ryswyk, K., Judek, S., Xu, X. and Wheeler, A. (2012) Factors influencing variability in the infiltration of PM_{2.5} mass and its components, *Atmos. Environ.*, **61**, 518-532.
- Nazaroff, W.W. (2004) Indoor particle dynamics, *Indoor Air*, **14**, 175-183.
- Noris, F., Adamkiewicz, G., Delp, W.W., Hotchi, T., Russell, M., Singer, B.C., Spears, M., Vermeer, K. and Fisk, W.J. (2013) Indoor environmental quality benefits of apartment energy retrofits, *Build. Environ.*, **68**, 170-178.
- Owen, K., Pope, R. and Hanley, J. (2013) How do pressure drop, efficiency, weight gain, and loaded dust composition change throughout filter lifetime, Atlanta GA, ASHRAE, Submitted by RTI International, Research Triangle Park NC.
- Persily, A. (2015) Challenges in developing ventilation and indoor air quality standards: The story of ASHRAE Standard 62, *Build. Environ.*, **91**, 61-69.
- Poppendieck, D.G., Rim, D. and Persily, A.K. (2014) Ultrafine particle removal and ozone generation by in-duct electrostatic precipitators, *Environmental Science & Technology* **48**, 2067-2074.
- Ristovski, Z.D., Miljevic, B., Surawski, N.C., Morawska, L., Fong, K.M., Goh, F. and Yang, I.A. (2012) Respiratory health effects of diesel particulate matter, *Respirology*, **17**, 201-212.
- Shen, S., Jaques, P.A., Zhu, Y.F., Geller, M.D. and Sioutas, C. (2002) Evaluation of the SMPS-APS system as a continuous monitor for measuring PM_{2.5}, PM₁₀ and coarse (PM_{2.5-10}) concentrations, *Atmos. Environ.*, **36**, 3939-3950.

- Sidheswaran, M., Destailats, H., Sullivan, D.P., Larsen, J. and Fisk, W.J. (2011) Quantitative room-temperature mineralization of airborne formaldehyde using manganese oxide catalysts, *Applied Catalysis B: Environmental* **107**, 34-41.
- Siegel, J.A. (2016) Primary and secondary consequences of indoor air cleaners, *Indoor Air*, **26**, 88-96.
- Singer, B.C., Delp, W.W., Black, D.R., Destailats, H. and Walker, I.S. (2016) Reducing In-Home Exposures to Air Pollution. Final Report to California Air Resources Board for Contract 11-311. , Sacramento, CA.
- Sioutas, C., Abt, E., Wolfson, J.M. and Koutrakis, P. (1999) Evaluation of the measurement performance of the scanning mobility particle sizer and aerodynamic particle sizer, *Aerosol Sci. Technol.*, **30**, 84-92.
- Spilak, M.P., Karottki, G.D., Kolarik, B., Frederiksen, M., Loft, S. and Gunnarsen, L. (2014) Evaluation of building characteristics in 27 dwellings in Denmark and the effect of using particle filtration units on PM_{2.5} concentrations, *Build. Environ.*, **73**, 55-63.
- Stephens, B., Gall, E.T. and Siegel, J.A. (2012) Measuring the Penetration of Ambient Ozone into Residential Buildings, *Environ. Sci. Technol.*, **46**, 929-936.
- Stephens, B. and Siegel, J.A. (2012a) Comparison of Test Methods for Determining the Particle Removal Efficiency of Filters in Residential and Light-Commercial Central HVAC Systems, *Aerosol Sci. Technol.*, **46**, 504-513.
- Stephens, B. and Siegel, J.A. (2012b) Penetration of ambient submicron particles into single-family residences and associations with building characteristics, *Indoor Air*, **22**, 501-513.
- Stephens, B. and Siegel, J.A. (2013) Ultrafine particle removal by residential heating, ventilating, and air-conditioning filters, *Indoor Air*, **23**, 488-497.
- Terzano, C., Di Stefano, F., Conti, V., Graziani, E. and Petroianni, A. (2010) Air pollution ultrafine particles: toxicity beyond the lung, *European Review for Medical and Pharmacological Sciences*, **14**, 809-821.
- Thatcher, T.L., Lai, A.C.K., Moreno-Jackson, R., Sextro, R.G. and Nazaroff, W.W. (2002) Effects of room furnishings and air speed on particle deposition rates indoors, *Atmos. Environ.*, **36**, 1811-1819.
- Us Epa (2009) Final Report: Integrated Science Assessment for Particulate Matter, Washington, DC, U.S. Environmental Protection Agency.
- Us Epa (2013) Integrated Science Assessment for O₃ and Related Photochemical Oxidants: Final, Research Triangle Park, NC, U.S. Environmental Protection Agency.
- Weschler, C.J. (2000) Ozone in indoor environments: Concentration and chemistry, *Indoor Air-International Journal of Indoor Air Quality and Climate*, **10**, 269-288.
- Wolf, K., Schneider, A., Breitner, S., Meisinger, C., Heier, M., Cyrus, J., Kuch, B., Von Scheidt, W., Peters, A. and Grp, K.S. (2015) Associations between short-term exposure to particulate matter and ultrafine particles and myocardial infarction in Augsburg, Germany, *International Journal of Hygiene and Environmental Health*, **218**, 535-542.
- Zhao, D., Azimi, P. and Stephens, B. (2015) Evaluating the Long-Term Health and Economic Impacts of Central Residential Air Filtration for Reducing Premature Mortality Associated with Indoor Fine Particulate Matter (PM_{2.5}) of Outdoor Origin, *International Journal of Environmental Research and Public Health*, **12**, 8448-8479.

Measured Performance of Filtration and Ventilation Systems for Fine and Ultrafine Particles and Ozone in an Unoccupied Modern California House – SUPPORTING INFORMATION

Brett C. Singer^{1,2,*}, William W. Delp^{1,2}, Douglas R. Black³, Iain S. Walker^{1,2}

¹Indoor Environment Group, ²Whole Building Systems Department, and ³Grid Integration Group Energy Technologies Area, Lawrence Berkeley National Laboratory, Berkeley, CA, USA

*Corresponding contact information: bcsinger@lbl.gov; Ph: 510-486-4779; Fax: 510-486-5928

Contents

<i>S.1 Methods and Materials</i>	23
S.1.1 Test House	23
S.1.2 System Selection Considerations	23
S.1.3 Selection of Components to Meet Design Objectives	24
S.1.4 Thermal Conditioning Schedule and Equipment	25
S.1.5 Specifications of Installed Ventilation Systems	26
S.1.6 Specifications of Particle Removal Technologies	28
S.1.7 Measurements of Envelope and Duct Air-tightness Between Summer and Fall Monitoring.	30
S.1.8 Supplemental Cooling for Manifold Pumps (Summer Only)	30
S.1.9 Details of Time-Resolved Pollutant Monitoring Systems	30
S.1.10 Details of SF ₆ Release and Measurement	33
S.1.11 Experimental Schedule	33
S.1.12 Data Processing and Analysis	34
S.1.12.1 Processing to produce time series of indoor and outdoor concentrations	34
S.1.12.2 Screening of data impacted by activities inside the home	39
S.1.12.3 Calculation of 24h, 8h and 1h running averages	39
S.1.12.4 Selection of dividing time for statistics by day	40
S.1.13 Estimation of Annual Energy Use	40
<i>S.2 Results</i>	43
S.2.1 Assessment Periods for Outdoor Particles	43
S.2.2 Performance for Outdoor Particles	45
S.2.3 Performance for Indoor Particles	46
S.2.4 Performance for Ozone	48
S.2.5 Filter Impacts on Airflow and Power Consumption	50
<i>S.3 References</i>	52

S.1 Methods and Materials

S.1.1 Test House



Figure S.8. Weather station and air intakes for supply ventilation and outdoor particle sampling.

The meteorology tower is visible above the roofline. Just above the apex of the roof is the outdoor aerosol sample inlet. Outdoor air inlets for supply ventilation systems were connected to the gable end vent. The sample inlet for outdoor ozone was just outside the master bathroom window.

S.1.2 System Selection Considerations

The first stage of mechanical system selection involved specification of seventeen candidate systems followed by a semi-quantitative evaluation of each system on the eleven criteria noted in Table S.4 below. The systems included various combinations of ventilation approaches (exhaust, supply, balanced), particle filtration locations (as part of supply ventilation, as part of forced air heating and cooling system, standalone), particle filtration quality (MERV8 through HEPA), VOC removal technologies (physical sorbents, chemisorbents, photocatalytic oxidation, etc.), and operational approaches (continuous, minimum of 20 min of every 60, only when heating or cooling required, etc.). The categorical scoring approach was designed primarily to elucidate strengths and weaknesses of the systems rather than to provide a firm priority order for testing.

Table S.4. Assessment criteria for system selection.

Evaluation Criterion	Weight	Considerations
Outdoor-generated particle removal efficiency	10	Filter rating and configuration. Building shell filtration with exhaust ventilation assumed to be equivalent to MERV8.
Outdoor VOC/ozone removal effectiveness	8	Available product information (limited)
Energy Performance	8	Based on residential energy model simulations, power ratings from manufacturer specs, and engineering estimates
Indoor-generated particle removal efficiency	7	Filter efficiency rating and configuration
Noise	5	Home Ventilating Institute (HVI) product database and contractor input
Suitability for California climate and construction practices	5	Contractor input and researcher assessment
Maintenance requirements	4	Manufacturer's recommended maintenance schedules and contractor input
Component availability	3	Contractor input and product searches on internet
Durability (including performance with imperfect maintenance)	3	Assessment based on system complexity, how long technology available; contractor input
Initial cost of equipment and installation	3	Contractor estimated costs
Annual operating costs in addition to energy	2	Maintenance kit costs as provided by on-line vendors

S.1.3 Selection of Components to Meet Design Objectives

(a) Ventilation. There were 4 systems with supply ventilation specified, including three (A-C) with continuous supply fans and one that operated intermittently with a run-time controller (D). All provided enhanced filtration on the supply air, with MERV13 on the supply duct of A and B; MERV16 on C, and the timer-coordinated supply ventilation and AHU with MERV16 filter for D. The airtight envelope was thought to provide something akin to supply filtration but the effectiveness was unknown. System G used an HRV linked to the central system air handler, with enhanced filtration provided by the HEPA bypass that was designed to operate whenever the HRV was operating.

(b) Particle removal. For the Reference system having no enhanced filtration, we specified a low-efficiency filter of the type that has been used historically to reduce dust accumulation on cooling coils. This corresponds to MERV4. This filter was used in the return of several other systems that featured enhanced filtration at another location. System A had enhanced particle filtration only for ventilation supply air. System B had additional filtration with an ESP in the FA system, but that was designed to operate only when heating or cooling was needed. System C was primarily a supply filtration design but also provided filtration to the indoor air that was blended into the supply for tempering (the blending air was roughly twice the mechanical ventilation air flow rate). System G had a MERV8 filter on the supply, with higher performance HEPA bypass filtration at the central system return. The bypass unit directs a portion of the air moving through the FAU ductwork through the HEPA filter assembly; the remainder of the air moving through the AHU passes through the low efficiency filter only. The other three systems featured high performance filters on a central forced air system return: MERV16 for D, MERV13 for E and F. Systems D-G were designed to provide regular filtration for particles

already in the house owing to programmed operation of the system for at least 20 min of each hour with the runtime controller (D-E) and continuous, lower speed/flow operation of System F. Any system with enhanced filtration on a recirculation loop (B, D-G) could be operated on demand when indoor particle sources are known to be present.

(c) VOC removal. We selected three technologies for VOC removal. For System C, we specified inclusion of a recently developed (by LBNL) manganese oxide catalyst that oxidizes formaldehyde and other VOCs at room temperature (Sidheswaran et al., 2011). For System D, the intent was to use a chemisorbent that removes formaldehyde (and potentially also nitrogen dioxide) in addition to other VOCs. For System G, we specified activated carbon, which is the most common of the technologies available for VOC removal in residential HVAC systems and is known to remove some VOCs, such as the BTEX compounds, but is not very effective for removal of formaldehyde.

(d) Design of supply ventilation. There were two systems (D and G) in which outdoor air was supplied via the central forced air ducting system with intermittent operation of the AHU. There were three supply systems (A-C) featuring continuous supply ventilation that did not rely on the central blower. These designs were selected in place of the more common intermittent supply using the AHU to avoid the energy costs of running the typically much larger, and higher power consumption AHU blower. To avoid pushing supply air back through the central system filter that is used to protect equipment, the system protection filter was moved from the return grille to a slot just before the AHU for systems A and B.

(e) Systems that are low-cost. Systems A, B, E, and F are all relatively simple and should be relatively low initial cost (with the exception of the ESP on system B).

(f) System for low-load homes. System F explores a technology combination – ducted mini-split heat pump with a custom, low pressure drop MERV13 filter compartment – that is applicable to low-load homes including homes that have undergone energy efficiency retrofits to achieve very low loads.

(g) Low-energy pollutant removal. Systems A and F should incur relatively low energy costs as they use low resistance filtration with efficient fans. System C may also be low energy provided a low resistance MERV16 filter is available.

S.1.4 Thermal Conditioning Schedule and Equipment

Title 24 has two pathways for compliance, prescriptive or performance. The performance pathway is model based, and the prescribed model inputs are covered in the Alternative Calculation Methods (ACM) manual. The schedules are shown in Figure S.9 below.

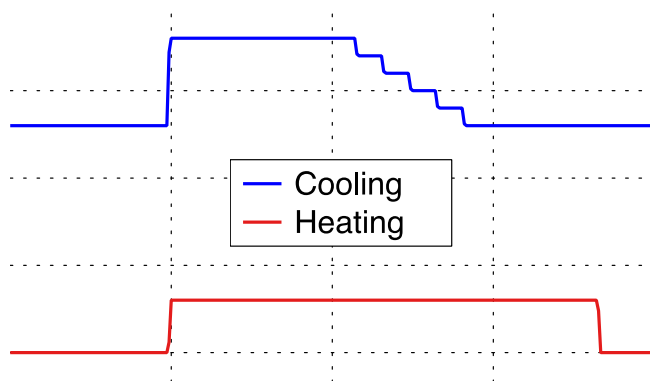


Figure S.9. Thermostat daily schedule based on California Title 24 design standard.

The thermal conditioning system for the home included a single-stage 75,000 Btu/h, 80% AFUE furnace; a 2.5 ton, an air conditioning unit with seasonal energy efficiency rating (SEER) of 13; and a blower with a nominal 600 W permanent split capacitor (PSC) motor. The return duct was located in the ceiling of the central hallway, at 2.75 m (9 ft) height and insulated flex duct distributed conditioned air to registers located in each room. Measurements of airflows at all heating/cooling supply registers were used to determine the total system airflow of 566 L/s (1200 cfm).

For System F, heating and cooling were provided by a mini-split heat pump (Daikin SkyAir 18 kbtu Minisplit with ducts & control) with the fan-coil unit mounted on scaffolding that was installed in the large common room for the duration of all experimental periods. A manifold at the outlet of the fan-coil unit fed smooth, sheet metal (for low pressure drop) duct runs to each of the three bedrooms. The mini-split was rated at 20 kbtuh for heating and (HSPF 10.6), 18 kbtuh for cooling (SEER 17.5). The instrument's native control system was programmed to operate on the Title 24 schedule described above.

S.1.5 Specifications of Installed Ventilation Systems

Specifications for ventilation system components are provided in Table S.5.

The exhaust fan used in Systems Ref, E and F (Panasonic model FV-08VKS3) was a “double-duty” fan installed in the bathroom. The double-duty refers to the fan providing continuous exhaust ventilation at the rate required to meet Title 24 / ASHRAE 62.2-2010, 17.5 L/s (37cfm) while having a higher speed of 41.5 L/s (88cfm) that can be manually initiated when needed for bathroom humidity or odor control.

All of the systems that provided ventilation through a dedicated supply fan (including A, B, C, D, and G) pulled outdoor air from the same location (the gable end vent on the north end of the house), which was nearby to the sampling point for outdoor air.

The same supply fan was used for Systems A, B, and D (Fantech model FR125). For System D the fan speed was set to provide a flow rate of 51.4 L/s (109 cfm) to meet the Title 24 / ASHRAE 62.2-2010 airflow requirement when operated for 20 min of each hour. A balancing damper just downstream of the fan was used to reduce the airflow rate for continuous operation

for Systems A and B. The damper position that provided the desired continuous airflow (the same flow as that used for the exhaust fan) was determined and marked prior to the start of multi-day experiments and the damper was set to this position when System A or B was tested. The actual flows achieved with the damper were not precisely 1/3 of the intermittent rate.

The blended supply ventilation for System C was provided by a commercially available product (American Aldes Model BV120). This product blended 16.5 L/s (35 cfm) indoor air drawn from the one of the small bedrooms and 28.3 L/s (60 cfm) of outdoor air drawn from the same location as the other supply fans, and supplied this mixture to the hallway in front of the main bathroom. The blending unit was mounted on the ceiling in the hallway closet.

The heat recovery ventilator (Fantech model FLEX 100H) used in System G was installed in the garage. It pulled outdoor air from the common intake used for all supply systems and provided that ventilation air to the return side of the FAU after heat exchange. The exhaust side of the HRV pulled indoor air from the laundry and master bathrooms, and exhausted that airstream to under an eave on the side of the house. Active flow-capture measurements using an Energy Conservatory Duct Blaster confirmed the supply and exhaust airflows were balanced at 52.9 L/s (112 cfm).

Airflow and power consumption were measured for each air-moving component and power consumption was measured for the ESP of System B. FAU airflow was measured as the sum of all supply register flows, after the distribution system was balanced according to industry standard Manual J HAC load calculations. Airflows were measured using the Energy Conservatory DuctBlaster™ and the active flow method outlined in the product manual. The nominal accuracy for this measurement is $\pm 3\%$. For components with plugs, spot power measurements were made using a plug-through power meter (WattsUp PRO, www.wattsupmeters.com), with nominal accuracy $\pm 1.5\%$. For components without plugs, power consumption was measured with WattNode model WNB-3Y-208P current transducers (www.onsetcomp.com), with nominal accuracy of $\pm 0.5\%$. Performance measurements of installed system components are summarized in Table S.2.

Energy use and operating patterns of mechanical systems were monitored using WattNode current transducers (model WNB-3Y-208P) connected to a PointSix wireless data logging system. The following systems were monitored: FAU; exhaust fan used by Systems Ref, E, F; Supply fan used by Systems A, B, D; the mini-split unit of System F; the HRV of System G; and the HEPA bypass of System G. The ECOBEE thermostat system logged set points and system operation at 15 min resolution.

Table S.5. Airflows and power consumption of system components.

Component, Setting	Airflow ² [L/s]	Measured Power ³ [W]	Catalog Power [W]	Notes
Exhaust fan for Systems E, F, Ref. (continuous)	17.5	4.2	3.7	Catalog power for 18.9 L/s @ 25 Pa
Supply fan, continuous setting for Systems A-B	17.5	17.7	18	Flow set with balancing damper. May have varied each time System A or B was set up.
Supply fan, intermittent setting for System D	51.4	18.0	18	
Blending supply fan for System C	44.8	33.8	43	Flow from outdoors = 17.4 L/s Flow from indoors = 27.4 L/s
HRV for System G, during intermittent operation	52.9	111.3	102	Catalog power for 46.7 L/s
HRV for System G, standby mode	No flow	10.1	N/A ¹	
AHU, high speed w/MERV4	566	660	N/A ¹	Cooling mode, sum of flows measured at supply registers
AHU, high speed w/MERV13	NM ¹	627	N/A ¹	System E; flow not measured in this configuration
AHU, high speed w/ESP	NM ¹	659	N/A ¹	System B; flow not measured in this configuration
AHU, high speed w/MERV16 + VOC	NM ¹	605	N/A ¹	System D; flow not measured in this configuration
AHU, medium high speed w/MERV4	500	N/A	N/A ¹	Heating mode, sum of flows measured at supply registers
AHU, standby mode	No flow	7.6	N/A	
System F mini-split, continuous setting for filtration	282	106.5	N/A ¹	Power measured by WattNode.
Electronic air cleaner (ESP) for System B	NR ¹	23.8	36	Catalog lists 36W as the maximum power
HEPA bypass for System G	85	121.1	125	Flow from manufacturer spec sheet.
Portable air filtration devices (n=2), Auto setting (~99% Low)	55	8.2	N/A ¹	Flow from manufacturer spec sheet (Low speed). Power measured over operating period
Portable air filtration devices (n=2), Medium setting	106	19.7	N/A ¹	Flow from manufacturer spec sheet (Medium speed). Power measured over operating period

¹ NM = Not measured in this configuration; N/A = not available; NR = not relevant to equipment. ² Unless otherwise noted in the last column, all airflows measured with Ductblaster method noted in the text. The nominal accuracy of this measurement is $\pm 3\%$. ³ The nominal accuracy of power measurements is $\pm 0.5\%$ to $\pm 1.5\%$.

S.1.6 Specifications of Particle Removal Technologies

Specifications for particle removal technology components are provided in Table S.5.

The Reference system featured a nominal 1-inch (2.5 cm) thick, 50 x 76 cm (20 x 30 in.) filter (Purolator F312) installed at the return grille. The design intent was to use a low-efficiency (i.e., low MERV) filter that protects the heating and cooling equipment from dust but does not provide any benefit of enhanced particle removal. The decision to use the F312, which is rated as MERV4, instead of a MERV6 filter as specified by ASHRAE62.2, was based on input from HVAC and home performance contractors who conveyed to us that the lower quality filter is much more widely available and more commonly used. The same filter was installed at the return grille for System C and an appropriately sized 51 x 63 cm (20 x 25 in.) version of this product was installed at the AHU for System A, B and G.

Systems A and B both included a nominal 2-inch (5cm) thick, 41 x 34 cm (16 x 14 in.) MERV13 filter installed at the junction of the supply ventilation duct and the return air duct. Since this was not a commonly available size, the local filter vendor (Air Filter Supply in Sacramento, CA) fabricated these filters from media that met the MERV13 specification (Airguard DP-g13een). System B additionally incorporated an ESP, marketed as an Electronic Air Cleaner (Honeywell model F300A2025/U), installed between the supply air junction and the central heating and cooling equipment. The ESP only operated when the central FAU was operating for thermal control.

System C utilized the same MERV4 filter at the FAU return grill as the Reference system, but also included a MERV16 filter on the blended air system. The MERV16 filter was a specially modified IQAir model HyperHEPA cartridge. The filter was downstream of the blending, and the fan was always on.

System D included a nominal 1-inch (5cm) thick, 41 x 36 cm (16 by 14 in.) MERV8 filter installed at the junction of the supply ventilation duct and the return air duct. As with the supply filter for Systems A and B, this filter was fabricated as a special order by Air Filter Supply in Sacramento CA using media that met the MERV8 specification (AirGuard DP-Max). System D also included a nominal 5-inch (13 cm) thick, 51 x 63 cm (20 x 25 in.) MERV16 filter (Lennox model X8313). Both the ventilation fan and the FAU were controlled by an AirCycler controller (model g2) serving as a runtime controller to ensure that the FAU with this filter in-line operated for at least 20 min of each hour, irrespective of cooling or heating demand.

System E provided the simplest filtration upgrade, relative to the Reference, with a nominal 1-inch (2.5 cm) thick, 50 x 76 cm (20 x 30 in.) MERV13 filter (FiltersFast model FFM1361) installed at the return air grille and the AirCycler controller (model g2) serving as a runtime controller to ensure that the FAU with this filter in-line operated for at least 20 min of each hour, irrespective of cooling or heating demand.

System F incorporated a nominal 1-inch (2.5 cm) thick, 81x 63 cm (32 x 25 in.) MERV13 filter (FiltersFast model FFM1361) into a custom-built sheet-metal box that was attached to the return side of the mini-split evaporator and fan unit. The purpose of the custom box was to enable use of a high quality filter with low enough pressure drop to meet the mini-split's pressure tolerance limits. The outlet of the mini-split was directed through smooth, low-pressure drop ductwork to deliver filtered and conditioned (when needed) air to the living space and three bedrooms.

System G had the previously described MERV4 filter installed at the AHU. It also included a HEPA bypass unit (Lennox model HEPA-20 with optional 94X98 carbon canister). The bypass unit drew 85 L/s (180 cfm) from the return plenum downstream of where the HRV airstream

entered, and discharged the filtered air just upstream of the FAU. The AirCycler controller (model g2) served as a runtime controller to ensure that the FAU with the bypass filter and HRV operated for at least 20 min of each hour, irrespective of cooling or heating demand.

The portable air filters were RabbitAir model SPA-780A (A2-minus) with a HEPA main filter and the “pet / allergy” pre-filter. One was set up in the living room and the other was in the front hallway by the entry door. For one of the two test periods the units were operated in an AUTO mode where the speed of the fan increases if the unit senses high particle concentrations. The other week had the units running at a fixed medium speed. Both weeks had the air ionizer turned off but main filter and pre-filters in place.

S.1.7 Measurements of Envelope and Duct Air-tightness Between Summer and Fall Monitoring.

Prior to the start of the fall monitoring campaign, we again measured the envelope air tightness and also measured air leakage in the FAU ductwork configured for the Reference system. The envelope air leakage was 5.0 ± 0.2 air changes per hour at 50 Pascal indoor-outdoor pressure difference. Duct leakage was determined by a “Delta-Q” test (Walker et al., 2001) to be 4.2 ± 0.5 % of system flow on the return side and 3.8 ± 0.5 % on the supply side of the FAU. Here the uncertainty reflects the precision of the measured value. Measurements of air exchange rates in the house with and without the FAU operating during the cooking experiments suggest lower duct leakage than implied by these measurements. This is possible because the relative accuracy of the Delta-Q test decreases as duct leakage airflows become small relative to envelope leakage airflows.

S.1.8 Supplemental Cooling for Manifold Pumps (Summer Only)

The two large diaphragm pumps that pulled air through the instrument manifolds were located in the garage to reduce heat gain to the house interior. This appeared to be sufficient during the winter operation period; but we observed when restarting the systems in May that heating of the garage by the pumps would have a substantial impact on cooling demand and AHU operation for cooling.

To solve this problem, we constructed a chamber to house the pumps and provided supplemental mechanical cooling to this chamber. The chamber, situated in the garage, close to the common wall with the house, was constructed of wood and measured 1.2 m high by 2.4 m wide by 0.8 m deep. Cooling was provided by a 2.7 kW (9300 Btu/h) portable air conditioner (Friedrich model P09B) located in the garage with the hose for venting the condenser heat connected to the outdoors through the side door of the garage.

S.1.9 Details of Time-Resolved Pollutant Monitoring Systems

Sample air was drawn at 0.28 L/s (0.59 cfm) through each sample line using vacuum pumps in the garage. The outdoor air inlet for particles was 0.5 m above the apex of the roof just above the supply air inlet and the indoor air inlet was in the central hallway at 1.5 m height. The aerosol inlet assembly (BGI, Inc.) on each sampling line comprised a PM₁₀ inlet with rain shield coupled with a sharp cut 2.5 μ m cyclone. Sample lines connected to indoor and outdoor inlets had identical lengths of conductive tubing and similar bends to arrive at a set of switching valves that connected the two air streams to manifolds from which aerosol instruments sampled. The main

sampling lines – from inlet assemblies to switching system leading into instrument manifolds – were 7 m long. The lines used for winter 2014 monitoring had internal diameters (ID) of 11.1 mm (0.436 in.). Prior to the start of summer monitoring, we changed sample inlet tubing for both indoor and outdoor inlets, using larger diameter samples lines. The sample lines used in summer and fall 2014 had ID of 14.1 mm (0.555 in.). The larger diameter sampling lines were expected to yield lower particle deposition losses with negligible impact on the analysis of system performance since indoor and outdoor sampling lines were identical both before and after the switch.

Valves synchronously switched indoor and outdoor sample inlets between the two manifolds. The switching interval was 10 min during monitoring in Jan-Feb 2014 that included fall/winter evaluation of the Reference system and System C. The switching interval was changed to 15 min on March 6, 2014 and this interval was used for all subsequent measurement periods. This change was made to reduce the fraction of samples that had to be removed because they straddled a switch and thus reflected a combination of both indoor and outdoor air.

Table S.6 lists the instrumentation used to measure each pollutant parameter. All instruments other than the aethalometer were set to calculate and record 1-min average values. The Aethalometers were initially set to record 1-min average values then reset on March 6, 2014 to record 3-min running averages. The longer sample time provided a lower minimum quantitation limit and improved resolution for systems with high efficiency filters.

Air pollutant monitoring instruments and switching valves were located in the master bedroom. The layout of the instruments is shown in Figure S.10. Aerosol and ozone analyzers were sent for manufacturer calibration prior to first deployment.

Ozone monitors were dedicated to indoor and outdoor air without switching. The outdoor sample was drawn from 2.5 m below the outdoor aerosol inlet and 0.5 m from the exterior wall. The indoor sample location was at the indoor aerosol inlet. Air was pulled from these locations through 5 m lengths of 3.2 mm ID Teflon tubing to ozone instruments in the master bedroom. Ozone instruments were installed prior to the start of hot weather monitoring in June 2015.

Table S.6. Measured air pollutant parameters and monitoring equipment.

Parameter	Device	Quantitation limit (QL)	Calibration and nominal accuracy.
Number conc. of particles ≥ 6 nm	TSI Condensation Particle Counter (CPC) Model 3781	Max. QL 500,000 particles cm^{-3}	Manufacturer calibrated before deployment.
Number conc. of particles ≥ 100 nm	TSI CPC Model 3787 with TSI particle size selector	Max. QL 500,000 particles cm^{-3}	Manufacturer calibrated before deployment.
Number conc. of particles in 6 bins from $>0.3\mu\text{m}$ to $>2.5\mu\text{m}^1$	MetOne Optical Particle Counter (OPC) Model BT-637S	Max. QL 10^7 particles cm^{-3}	Manufacturer calibrated before deployment. Accuracy: $\pm 10\%$ to calibration aerosol.
PM _{2.5} mass estimated by forward light scattering	TSI DustTrak II 8530	Min. QL $4\mu\text{g m}^{-3}$ for 1h avg ²	Manufacturer calibrated before deployment.
Mass concentration of black carbon aerosol (BC)	Magee Scientific Aethalometer AE22	Min. QL 30 ng m^{-3} for 3 min sample ³	Manufacturer calibrated before deployment.
Ozone (O ₃)	2BTech Model 202 UV-absorbance analyzer	Min. QL 4.5 ppb ⁴	Manufacturer calibrated before deployment. Nominal accuracy: larger of 1.5 ppb or 2% of reading;

¹Bins defined by lower size cut, e.g. >0.3 , >0.4 , >0.5 , >0.7 , >1.0 , $>2.5\mu\text{m}$. ²Reported by (Wallace et al., 2011).

³Estimated based on visual review of data. Estimated min. QL of 90 ng m^{-3} for 1-min sample duration. ⁴Based on manufacturer precision (1σ) of 1.5 ppb.

**Figure S.10. Layout of instrumentation in master bedroom.**

The photo shows the two manifolds with identical particle instrumentation. Aethalometers are the large blue boxes at the bottom left of the photo. Moving up and to the right, there are CPC 3781s with water bottles on top, CPC 3787s without covers, MetOne OPCs, and DustTraks (small, dark blue cases). Switching valves are visible at the inlet of the manifold, toward the right edge of the photo. In the back corner are two 2BTech ozone analyzers sitting atop an API NO_x analyzer (not discussed in this paper), and the B&K instrument used to monitor SF₆ (far corner).

S.1.10 Details of SF₆ Release and Measurement

SF₆ was released at the kitchen peninsula counter and at 1 m height in the nook just outside of the two smaller bedrooms. At each location the tracer was released using a peristaltic pump connected to a Tedlar bag containing pure SF₆ and a 30 cm axial fan was positioned to blow the tracer outward for mixing. Concentrations of SF₆ were measured with ~1 min resolution in the central hallway, near the FAU return, at a height of 2 m using a Bruel & Kjaer (now Innova) 1312 photoacoustic infrared analyzer. The instrument was zero-checked between most monitoring intervals and a span calibration was conducted at the start of each seasonal campaign. The time-resolved air exchange rate was calculated by the constant injection method in ASTM Standard E741-11.

S.1.11 Experimental Schedule

We started with a series of “shakedown” and pilot experiments conducted from mid-January through the first few weeks of February 2014, as summarized in Table S.7. These mostly used the Reference system. One objective was to confirm performance of the switching, parallel manifold systems and all instrumentation for unattended monitoring periods lasting approximately one week. Another objective was to develop and test algorithms for a remote, daily review of data to affirm proper operation and to generate data that was used to develop processing and analysis algorithms for assessing enhanced particle removal. During two of these early monitoring periods we obtained data sets that were complete enough to use for the analysis of system performance under winter conditions. All systems and instruments were powered down on March 19 and instruments were serviced as needed.

Table S.7. Winter 2014 “Shakedown” and pilot experiments to identify and resolve challenges related to weeklong, unattended monitoring.

Dates	System	Data Notes
1/15–1/22	Reference	Monitoring systems operating in parallel, no switching. Outdoor 3781 and Aeths offline for repairs. DustTraks off manifolds.
1/23–1/29	Reference	Outdoor 3781 offline for repairs. Switching started. AER 2x design b/c bath fan set too high. DustTraks off manifolds.
1/29–2/6	Reference	Outdoor 3781 offline for repairs. AER still 2x design. DustTraks off manifolds.
2/6–2/12	C: Blended Supply, MERV16	Outdoor 3781 offline for repairs. DustTraks off manifolds. Indoor DustTrak and BC below QL much of week.
2/12–2/19	Reference	No data from 3781s starting 2/13; pump failure. Indoor BC below QL for much of week. Response shift of 3781s on 2/16.
2/20–2/27	Reference ¹	DustTraks on manifolds; curious data 2/20-2/22. Increase Aeth flow to 4 L/min. Other instruments and systems operating as designed.
2/27–3/6	C: Blended Supply, MERV16 ¹	No AER data from 2/28; B&K problem. Other instruments and systems operating as designed.
3/6–3/12	A: Cont. Supply w/MERV13.	One 3781 not operating; take offline to repair. Computer down 3/7-3/8.
3/13–3/19	E: MERV13 on return	Lost power to one manifold on 3/16. Various other problems.
3/19	Shutdown	Power down all equipment for service.

¹Data collected in this period used for system performance analysis.

Table S.8. Monitoring periods to assess system performance for outdoor particles in fall/winter and outdoor particles and ozone in summer.

Fall/Winter Performance		Summer Performance	
Dates (2014)	System	Dates (2014)	System
2/21–2/27	Ref: Continuous exhaust ventilation; no enhanced filtration	6/6–6/12	E: Continuous exhaust ventilation; MERV13 on FAU, 20/60 fan timer
2/27–3/6	C: Continuous blended supply w/MERV16	6/12–6/17	A: Continuous supply w/MERV13
10/28–11/4	E: Continuous exhaust ventilation; MERV13 on FAU, 20/60 fan timer	6/18–6/22	F: Continuous exhaust ventilation; Cont. MERV13 on mini-split fan unit
11/4–11/10	F: Continuous exhaust ventilation; Cont. MERV13 on mini-split fan unit	6/25–7/2	G: Supply ventilation + HEPA bypass on FAU, 20/60 fan timer
11/11–11/17	A: Continuous supply w/MERV13	7/2–7/9	Ref: Continuous exhaust ventilation; no enhanced filtration
11/18–11/25	B: Continuous supply w/MERV13; ESP on FAU, thermostat control.	7/9–7/16	D: Supply ventilation + MERV16 on FAU, 20/60 fan timer
11/25–12/2	D: Supply ventilation + MERV16 on FAU, 20/60 fan timer	7/16–7/23	Ref: Continuous exhaust ventilation; no enhanced filtration
12/2–12/8	G: Supply ventilation + HEPA bypass on FAU, 20/60 fan timer	7/23–7/30	C: Continuous blended supply w/MERV16
12/8–12/12	Portable air filtration unit set to Auto operation mode	7/30–8/6	B: Continuous supply w/MERV13; ESP on FAU, thermostat control.
12/12–12/15	Portable air filtration unit set to Medium speed operation mode		
12/16–12/19	E: Continuous exhaust ventilation; MERV13 on FAU, 20/60 fan timer		
12/19–12/23	A: Continuous supply w/MERV13		

S.1.12 Data Processing and Analysis

S.1.12.1 Processing to produce time series of indoor and outdoor concentrations

The first step of pollutant data analysis was to filter/remove data points from the measurements that were recorded just after the two manifolds synchronously switched between indoor and outdoor inlets. During the first two months of sampling in Jan-Feb, 2014, the manifolds switched on 10 min intervals. On March 6, the switching interval was changed to 15 min. Measurements just after switching reflect a combination of air from indoors and outdoors, and are thus not valid as indicators of concentrations in either location. For the instruments that were on the manifolds and that recorded measurements at 1 min intervals, i.e. CPCs, Optical particle counters (OPCs), and DustTraks, it was typically the case that only the first data point after the switch was invalid as a measurement of either indoor or outdoor air. However, in a non-

negligible number of cases, the first data point was so close in time to the switch that a second measurement was impacted. For consistent and efficient data handling, two data points were filtered from the time series from these instruments following each synchronous manifold switch. Starting on March 6, only one point was filtered from aethalometer time series data because that instrument was configured to switch every 3 minutes. Prior to March 6, the aethalometers sampled every 1 min; so two aethalometer measurements were removed following manifold switching for data collected prior to March 6.

An example of after-switching data filtering is shown in the two figures below. Figure S.11 displays particle number concentration time series that include all of the measurements output by the two CPCs; data from one instrument are shown in blue, the other in red. The instruments sampled from manifolds that switched every 15 min between indoor and outdoor inlets. At many of the manifold switches, there are two blue and two red data points that reflect a combined indoor and outdoor air sample. The time series with these points removed are shown in Figure S.12.

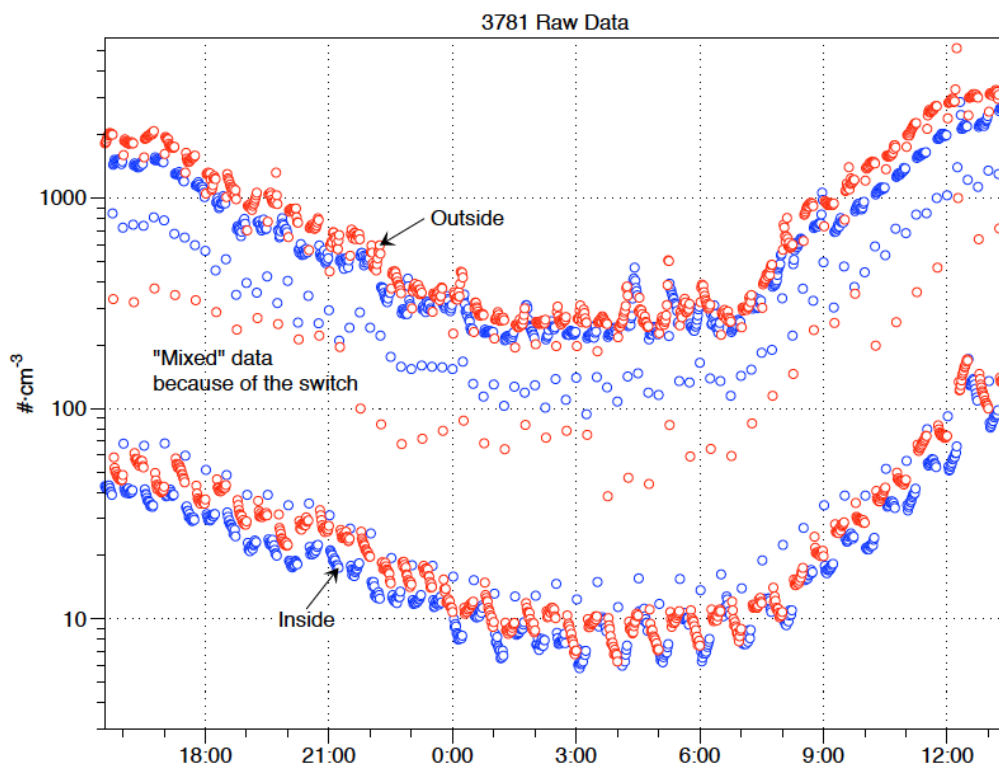


Figure S.11. Time series of measurements from two CPC3781 units (shown as red and blue circles) switching synchronously, on a 15-min interval, between indoor and outdoor sample inlets.

Units of y-axis are particles cm⁻³ for size range of 100 nm to 2.5 μ m diameter particles. Concentrations at top are outside and at bottom are indoors. Points between the outdoor and indoor series occur just after the switch and reflect measurements in air samples drawn partly from each location.

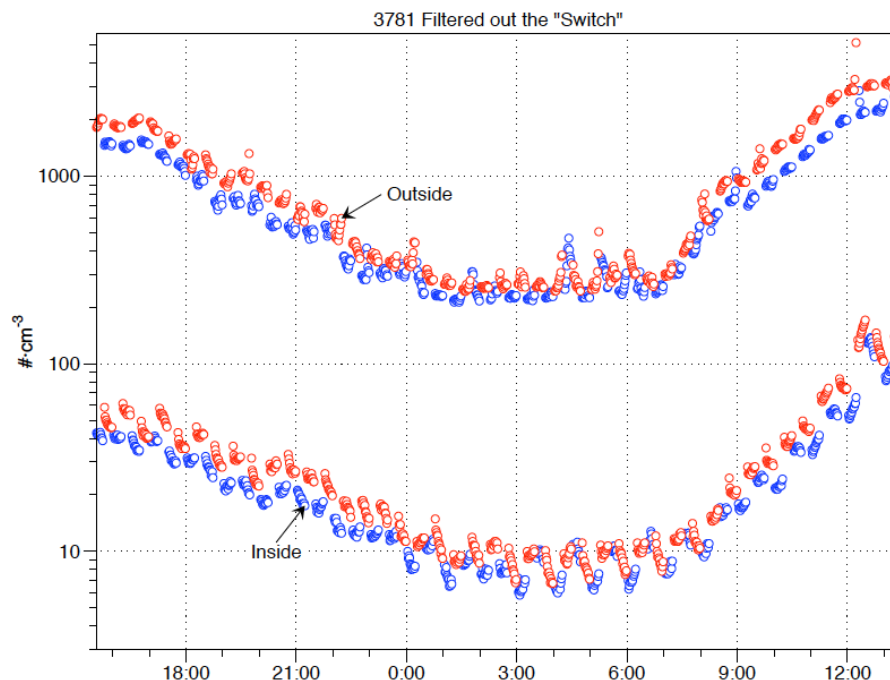


Figure S.12. Time series data shown in Figure S.11 with post-switching points removed. Units of y-axis are particles cm^{-3} for size range of 100 nm to 2.5 μm .

The next step in the analysis was to align the indoor and outdoor data from the two instruments to create nearly continuous data series for indoor and outdoor sampling locations. To accomplish this alignment, we compared the indoor time series of the two instruments as a form of cross-calibration; then used the relative responses to adjust both indoor and outdoor data. The cross-calibration and adjustment is needed because instrument responses drift apart over time and field calibration of particle instrumentation is not practical. Alignment was accomplished as follows. We first applied a locally weighted scatterplot-smoothing algorithm to the available indoor data for each instrument. The available data excluded the post-switching data points and any missing data. We used an open source python implementation¹ of the LOESS² algorithm that is based on methods first proposed by Cleveland (1979) and further developed in Cleveland (1981) and Cleveland and Devlin (1988). A good description of the method is available via Wikipedia³. Briefly, the algorithm uses near-neighbor data points, weighted by proximity, to develop a low order polynomial fit to the data around each point. When applied across a time series, the algorithm produces a smoothed series with 1-min time resolution. At each time

¹http://statsmodels.sourceforge.net/devel/generated/statsmodels.nonparametric.smoothers_lowess.lowess.html.

²LOESS, in capital letters, is a particular form of the smoothing algorithm. It is not an acronym.

³As of Oct 2015, a good description of method is presented on Wikipedia:

http://en.wikipedia.org/wiki/Local_regression

interval, the two LOESS-smoothed indoor time series were compared to the mean of the two series to determine a scaling factor to align the time series from each instrument to the mean of the two instruments. This provides a one-min resolution time-series of a scaling factor that was applied to the data from both instruments to create merged indoor and outdoor time series. The following three figures demonstrate this procedure. Linear interpolation was used to impute concentrations for the two-min period following each switching event.

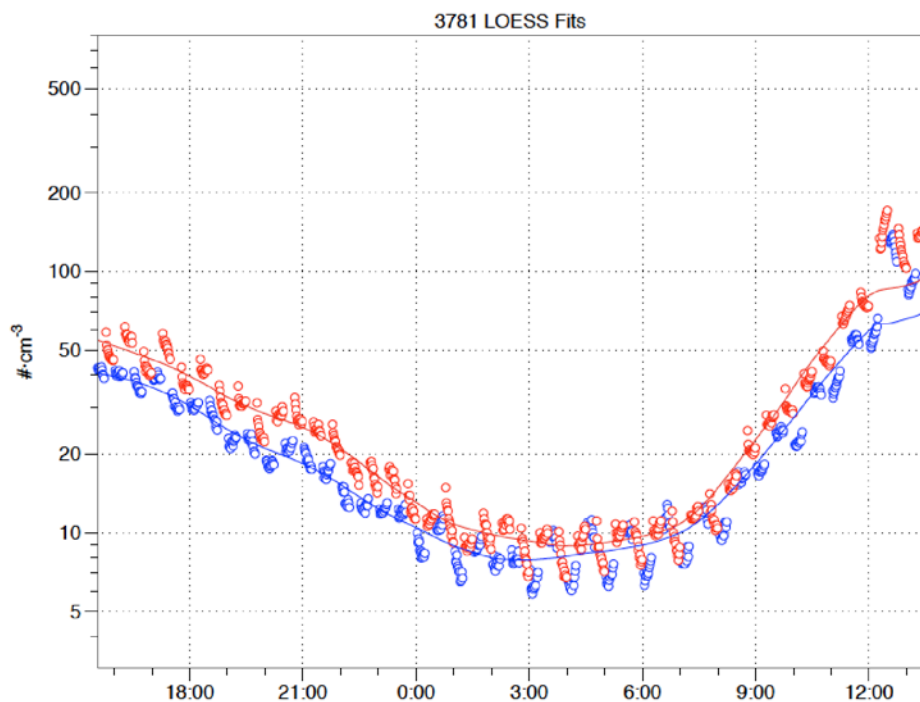


Figure S.13. Smoothed time series of indoor measurements from each of two CPCs obtained by applying a python implementation of the LOESS algorithm to data series of each CPC.

Units of y-axis are particles cm^{-3} for size range of 100 nm to 2.5 μm .

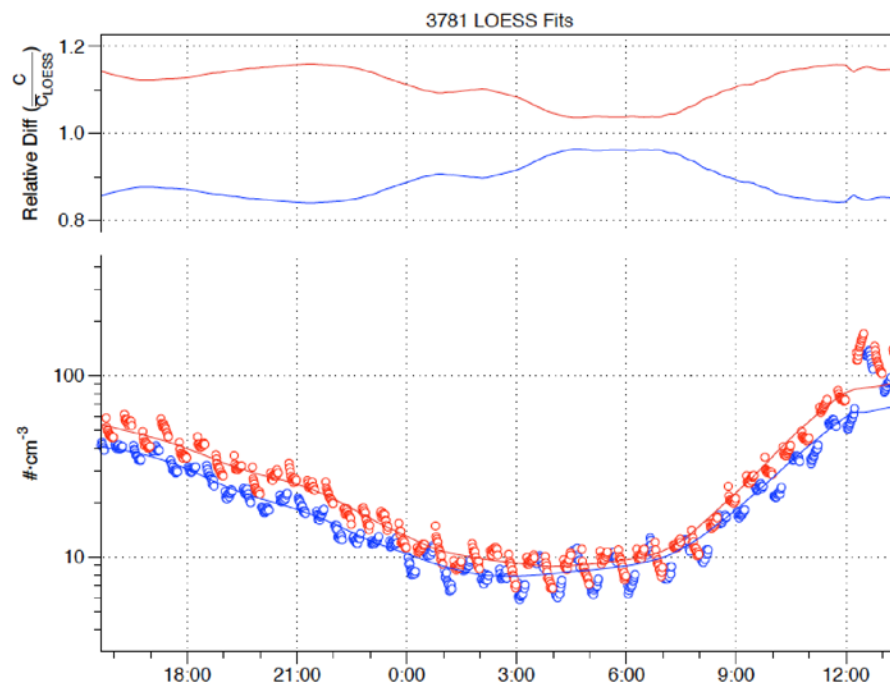


Figure S.14. Relative difference (top) of smoothed indoor time series (bottom) for each CPC 3781 relative to the mean of the two time instruments.

The time-resolved relative difference functions are used to align the indoor and outdoor time series for the two instruments. Units of y-axis on bottom panel are particles cm^{-3} for size range of 100 nm to 2.5 μm .

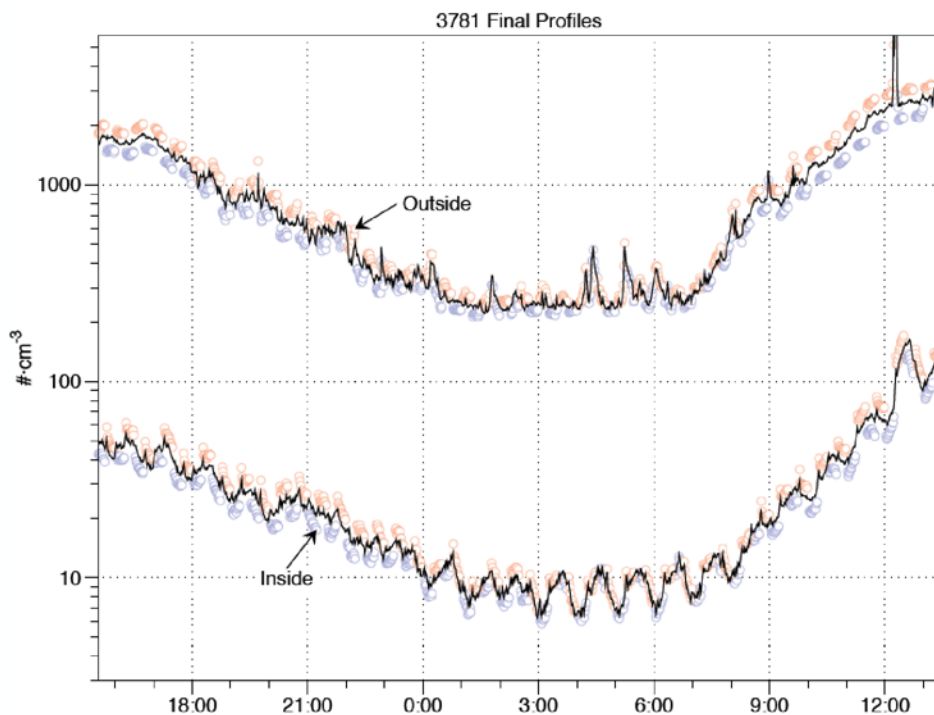


Figure S.15. Indoor and outdoor time series constructed by aligning data from two instruments alternately measuring indoors and outdoors at 15 min intervals via synchronously switching.

Raw data show as partially opaque red and blue open circles. Units of y-axis are particles cm^{-3} for size range of 100 nm to 2.5 μm . The saw tooth pattern indoors (e.g. during the hours of 3:00 to 8:00) results from intermittent operation of a filtration system.

For UFP, we first developed continuous time series for total particles 6nm–2.5 μm and for 100nm–2.5 μm , using data from the two pairs of instruments. We then subtracted the latter from the former to obtain the number concentration of 6–100nm particles.

S.1.12.2 Screening of data impacted by activities inside the home

For multi-day monitoring periods, a screen was applied to the start of the time series data to avoid any biases from field technician impacts on indoor particle levels, typically this was 3–4 h after the field technician exited the test house. A varying delay was applied to the start of the running 24h averages, with the delay determined from a visual review of data. For each week of monitoring, we applied the same initial delay to all pollutant parameters. This screening was not applied to the highest daily 1h outdoor and indoor values because the short-term running averages were not as impacted by earlier activity in the homes.

Additional masking of 24h running average time series data was done on monitoring days when the house was accessed by a field technician. These included set-up of VOC samples and a system check by the HVAC contractor on 19-Jun. Additional details are provided in the Appendix results for each system in the final project report (Singer et al., 2016).

S.1.12.3 Calculation of 24h, 8h and 1h running averages

After screening the data as described in the preceding sub-section, we calculated running statistics (mean, median, standard deviation) from the 1-min data for each of the measured

parameters (and 3 min data for BC). Running statistics were calculated for time windows of 1, 8, and 24 hours. When calculating summary statistics for a monitoring period, we did not use running 8h and 24h mean values until a sufficient amount of time had elapsed that these means were representative. This initial delay varied from a few hours to nearly 24h.

S.1.12.4 Selection of dividing time for statistics by day

Distinct 24h diurnal periods (“days”) within a monitoring period were set by selecting a daily dividing time, with the intent that this would be at a time of low outdoor concentrations. The diurnal patterns varied seasonally, across weeks within a season and sometimes even across days within a monitoring period. A daily dividing time was selected for each multi-day monitoring period by visual review of the time series for all measured parameters. Summary statistics were then calculated for all data available during each specified day during the monitoring period. The dividing time for each period is specified at the front of the appendix that presents data from the period in the final project report.

S.1.13 Estimation of Annual Energy Use

Incremental fan energy requirements for each system, relative to the Reference, were calculated for deployment across California using equipment runtime estimates and component power consumption. Actual energy consumption during the limited monitoring periods in the test house is not reported because they are not representative of annualized impacts.

Incremental fan energy requirements result from the following: (1) extra hours of FAU operation for filtration and/or supply ventilation; (2) increased or decreased fan power as airflow resistance increases, (3) operation of air cleaning devices including the ESP of System B and the HEPA + Activated Carbon unit of System G.

To calculate the energy for extra central air handler operation, we used baseline heating and cooling system runtimes developed for studying the impacts of ventilation requirements in California’s Title 24 building code (Walker and Sherman, 2006). That analysis used a heat transfer, airflow, and moisture simulation model to determine FAU operating times attributed to heating, cooling and ventilating. Simulations were conducted for Title 24 prototype homes, including a 1761 ft² home, under various ventilation configurations in several California climate zones. Although the simulated house is larger than the test house, FAU runtimes should be similar since heating and cooling systems are sized to demand. The simulated home had a typical efficiency (2 cfm/W) air handler and fan power varied by climate zone according to industry standards for equipment sizing. Simulations assessed the effect of the supply fan and central blower fan heat on heating and cooling loads. Simulations were conducted for California climate zones 3, 10, 13, 15 and 16. California’s climate zones are shown in Figure S.16. For this assessment, we analyzed simulations for a Central Fan Integrated Supply (CFIS) system that operates for a minimum of 20 min each hour (20/60).

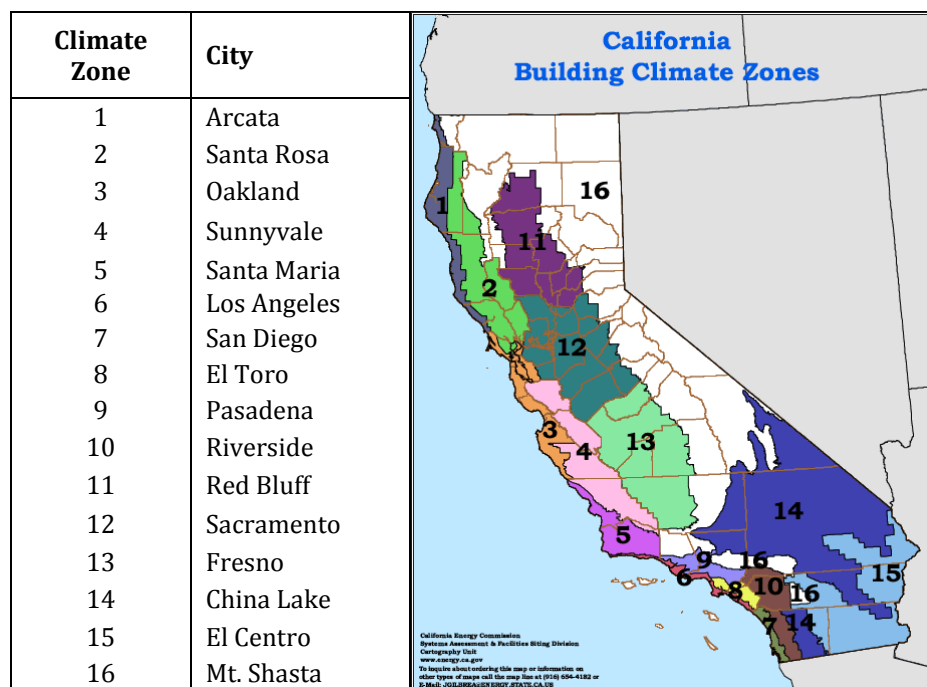


Figure S.16. California climate zone map.

To estimate incremental runtime for 20/60 operation, we start with the Reference system operating hours for heating and cooling only. We compare this to the total hours of FAU operation for the CFIS system, which includes additional runtime to thermally condition the extra airflow for ventilation, and all hours of 20/60 operation. Table S.9 breaks out these components. Despite large variations in Reference system runtimes for heating and cooling, the relative variation of incremental runtime is small across climate zones. From this analysis, we used an incremental runtime of 2400 hours per year for the FAU to run on a 20/60 cycle to provide enhanced filtration or supply ventilation.

Operating the FAU continuously for pollutant removal requires an additional 7949 hours of operation (8760 total – 811 for heating + cooling).

Table S.9. Simulation based estimates of annual operating hours for central forced air system in typical new California homes in various California climate zones.¹

Climate Zone	City	Reference heating + cooling hours	Total CFIS runtime, hours	CFIS heating + cooling hours	CFIS ventilation, hours	Incremental runtime of CFIS, hours
3	Oakland	606	3056	616	2440	2450
10	Riverside	709	3191	752	2439	2482
13	Fresno	882	3278	928	2351	2397
15	El Centro	988	3332	1046	2287	2345
16	Mt. Shasta	870	3187	887	2300	2318
Mean		811	3209	846	2363	2398

¹ From Walker and Sherman (2006).

The energy for additional FAU fan operation was calculated as the product of the incremental run time and 600 W, the actual power consumption of the test house FAU (Table S.5); this

corresponds to 0.5 W/cfm, a typical efficacy for a permanent split capacitor (PSC) motor. Incremental power needs were also calculated for an efficient, brushless permanent magnet (BPM) FAU motor. These fans operate more efficiently in low speed continuous mode – as used in the System F mini-split F – than intermittently at higher speed. For the FAU with BPM, we assumed that the schedule and airflow did not change from the Reference system and assumed an efficacy of 0.375 W/cfm, corresponding to 450 W for all HAC operation. For an FAU operating continuously at low speed, we assumed airflow of 188 L/s (400 cfm) and an efficacy of 0.175 W/cfm as measured for the mini-split in System F. For this situation, a power draw of 70 W was assumed to occur 7949 hours per year. For System G, we assumed the BPM motor operating at the higher flow rate on a fan cyclor to keep energy use estimates consistent with pollutant removal performance. If the System G bypass were operated continuously it would have higher energy consumption but also better pollutant removal.

The fan power to overcome airflow resistance of higher performance filters was treated as follows. For the PSC motor, we assumed no change in power. In fact, there may be a small decrease in power as the higher resistance leads to lower airflows. For the BPM motor, we estimated a power increase proportional to those reported by Lutz et al. (2006). For the MERV16 filter of System D, we assumed an 8W increase (11.4% increase) and for the MERV13 filter of System E, we assumed a 4W increase (5.7%) increase.

We accounted for filtration energy costs on the supply ventilation systems by assuming that, in the absence of enhanced filtration, the fan efficacy would be the same as for exhaust fans: 0.11 W/cfm. For the supply systems with MERV13 filtration, the incremental energy attributed to filtration was 2.2 W ($0.17 - 0.11 = 0.06 \text{ W/cfm} \times 17 \text{ cfm}$) for continuous operation and 6.7 W for intermittent operation. We used the supply fan efficacy measured for System D because the lower flow for Systems A and B was obtained by partially closing a damper to increase duct pressure. The energy cost for MERV16 filtration on the blended (higher airflow) System C was 22.8W ($0.35 - 0.11 = 0.24 \text{ W/cfm} \times 95 \text{ cfm}$).

The energy costs of operating the ESP and HEPA bypass were calculated from the component power consumption data presented in Table S.5.

S.2 Results

S.2.1 Assessment Periods for Outdoor Particles

Table S.10. Outdoor conditions during fall/winter monitoring periods assessing performance for outdoor particles

Dates (2014)	System	Period mean PM _{2.5} mass (µg/m ³)	Period mean dry-bulb temp. (°C)	Mean daily low/high temp. (°C)
2/21–2/27	Ref: Continuous exhaust ventilation; no filtration	21	11.7	5.7 / 19.3
2/27–3/6	C: Continuous blended supply w/MERV16	12	13.8	10.4 / 17.2
10/28–11/4	E: Cont. exhaust ventilation; MERV13 on FAU, 20/60 timer	15	14.4	9.1 / 21.0
11/4–11/10	F: Cont. exhaust vent.; Cont. MERV13 on mini-split fan unit	31	14.9	9.0 / 21.9
11/11–11/17	A: Continuous supply w/MERV13	19	12.3	8.1 / 17.3
11/18–11/25	B: Cont. supply w/MERV13; ESP on FAU, t-stat control.	22	10.9	7.0 / 15.3
11/25–12/2	D: Supply ventilation + MERV16 on FAU, 20/60 fan timer	25	11.6	8.1 / 17.3
12/2–12/8	G: Supply ventilation + HEPA bypass on FAU, 20/60 fan timer	12	14.6	11.8 / 17.7
12/8–12/12	Portable air filtration unit set to Auto operation mode	18	12.6	10.3 / 15.5
12/12–12/15	Portable air filtration unit set to Medium speed operation mode	12	9.8	8.3 / 13.1
12/16–12/19	E: Cont. exhaust ventilation; MERV13 on FAU, 20/60 timer; tape around edges of filter to ensure no bypass.	8.3	11.5	9.6 / 14.3
12/19–12/23	A: Continuous supply w/MERV13; tape around edges of filter to ensure no bypass.	8.1	13.0	10.5 / 15.9

Table S.11. Outdoor conditions during summer monitoring periods assessing performance for outdoor particles

Dates (2014)	System	Period mean PM _{2.5} mass (µg/m ³)	Period mean dry-bulb temp. (°C)	Mean daily low/high temp. (°C)
6/6–6/12	E: Cont. exhaust ventilation; MERV13 on FAU, 20/60 timer	15	27.0	16.5 / 40.5
6/12–6/17	A: Continuous supply w/MERV13	12	22.2	14.2 / 33.0
6/18–6/22	F: Cont. exhaust vent.; Cont. MERV13 on mini-split fan unit	12	24.9	15.5 / 39.1
6/25–7/2	G: Supply ventilation + HEPA bypass on FAU, 20/60 fan timer	10	26.7	17.6 / 40.2
7/2–7/9	Ref: Continuous exhaust ventilation; no enhanced filtration	16	27.5	17.9 / 41.2
7/9–7/16	D: Supply ventilation + MERV16 on FAU, 20/60 fan timer	9.4	26.6	18.5 / 38.1
7/16–7/23	Ref: Continuous exhaust ventilation; no enhanced filtration	6.3	23.8	17.7 / 34.8
7/23–7/30	C: Continuous blended supply w/MERV16	12	28.3	19.7 / 40.6
7/30–8/6	B: Cont. supply w/MERV13; ESP on FAU, t-stat control.	12	25.8	19.3 / 34.3

Table S.12. Median and mean of continuous air exchange rate measurements during each assessment period for outdoor particles.

Summer			Fall/Winter		
Sys	Median	Mean	Sys	Median	Mean
Ref	0.278	0.290	Ref	0.218	0.218
Ref	0.283	0.292			
A	0.208	0.218	A	0.268	0.275
			A taped	0.267	0.267
B	0.213	0.226	B	0.274	0.277
C	0.232	0.250	C	0.217	0.219
D	0.262	0.276	D	0.337	0.339
E	0.292	0.306	E	0.347	0.347
			E taped	0.352	0.352
F	0.265	0.268	F	0.303	0.303
G	0.298	0.313	G	0.352	0.353
			Port auto/low	0.302	0.312
			Port medium	0.304	0.307

S.2.2 Performance for Outdoor Particles

Table S.13 presents the days of monitoring data and the days of 1-minute resolved running 24h mean indoor/outdoor ratios (IOs) presented in Figure 5 in the main paper.

Table S.13. Days of data presented in Figure 5 in main paper.¹

System Description	Days of monitoring data		Days of 1-minute resolved running 24h mean IOs in Figure 5	
	SU	FW	SU	FW
(M=MERV)				
<i>Exhaust Ventilation</i>				
Ref: M4@rtn	6.7, 6.7	6.5	6.3, 6.4	5.5
E: M13@rtn	6.0	7.0	5.7	2.4
E: w/o bypass	nd ²	2.7	nd ²	2.3
F: M13 on mini-split	4.5	6.8	4.0	6.4
Portables on Auto / Low	nd ²	3.7	nd ²	3.4
Portables on Medium	nd ²	3.8	nd ²	3.4
<i>Supply Ventilation</i>				
A: M13@Supply	5.2	6.7	4.3	6.5
A: w/o bypass	nd ²	4.0	nd ²	3.8
B: M13@Supply/ESP@FAU	6.7	6.7	5.7	6.4
C: M16@Supply	6.8	6.8	5.7	5.6
D: M8@Supply/M16@FAU	6.7	6.7	6.5	6.4
<i>Balanced Ventilation</i>				
G: M8@Sup/HEPA bypass	5.0	5.7	4.7	5.2

¹Each data point is an IO ratio calculated from minute-by-minute running 24h mean indoor and outdoor concentrations. The running 24h concentrations start 5-24h after the start of the monitoring period in almost all cases. ²No data collected

To address system performance for reducing the highest short-term exposures, Table S.11 presents the protection factors for the highest 1h outdoor-origin PM_{2.5} mass and UFP. Hourly results are not presented for BC because those data are not as well resolved for short time duration analysis. The IO ratios for the highest daily 1h concentrations were lower than the 24h IO ratios for almost all systems and parameters. For the Reference system, the highest indoor hourly PM_{2.5} concentrations were lower than the highest outdoor hourly PM_{2.5} concentrations by 77-78% on average for each season. The supply ventilation & filtration of System A had somewhat higher 1h IO ratios compared to the Reference, corresponding to a 70% reduction. System B had lower 1h IO ratios in SU than FW, corresponding to 85% and 71% reductions of outdoor PM_{2.5}. The better performance in summer resulted from the ESP operating with the FAU for cooling. As with the longer time-averaged performance, the best systems for reducing short-term indoor concentrations of outdoor particles were C, D, and F, followed by System E and the portables.

Table S.14. Percent reduction in highest daily 1 h indoor concentrations compared to corresponding highest daily 1h outdoor concentration of outdoor-origin PM_{2.5} mass and ultrafine particles (UFP) over each evaluation period; mean and standard deviation across distinct 24h diurnal periods of analysis within each period.

System	PM _{2.5}				UFP			
	SU		FW		SU		FW	
	Mean	SD	Mean	SD	Mean	SD	Mean	SD
Ref	78	3	77	5	89	2	90	2
A	70	7	70	2	86	3	81	6
B	85	10	71	5	86	4	84	3
C	95	2	98	1	98	1	99	1
D	97	1	98	0	98	0	97	1
E	92	1	89	1	94	2	92	8
F	95	0	96	1	97	1	96	1
G	81	3	81	3	85	0	86	3
Port	nd ¹	nd ¹	93	2	nd ¹	nd ¹	96	2

¹ No data.

S.2.3 Performance for Indoor Particles

Example data from an experiment assessing performance for indoor-generated particles are provided here for System D (supply ventilation and MERV16 filtration on the FAU return on 20/60 operation). The figures show the time series of SF₆ (indicating AER) and calculated PM_{2.5} from before cooking through two cycles of FAU operation. The SF₆ tracer time series in Figure S.17 shows the higher AERs that occurred during system operation and the lower AERs during the intervals without mechanical ventilation.

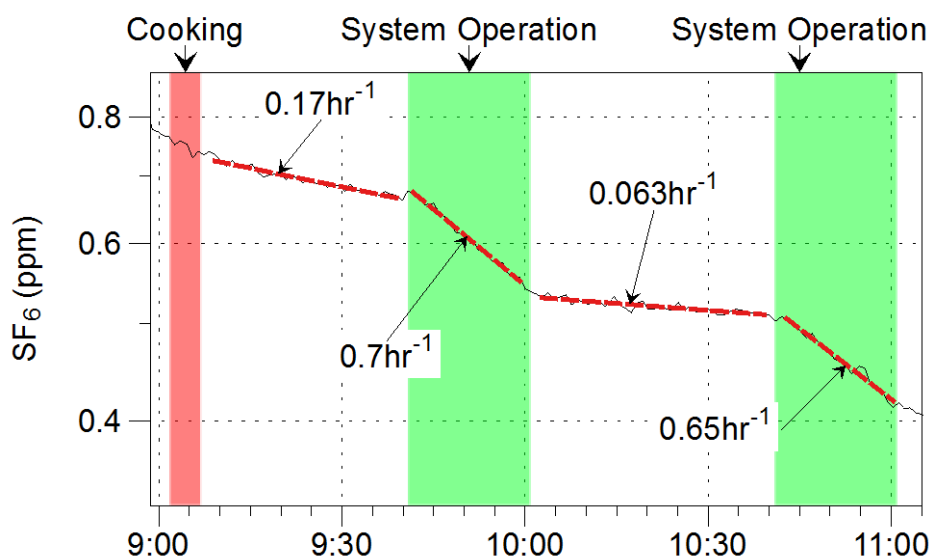


Figure S.17. Time series of SF₆ tracer concentrations during cooking experiment with System D on July 16, 2014. Refer to text for a detailed description.

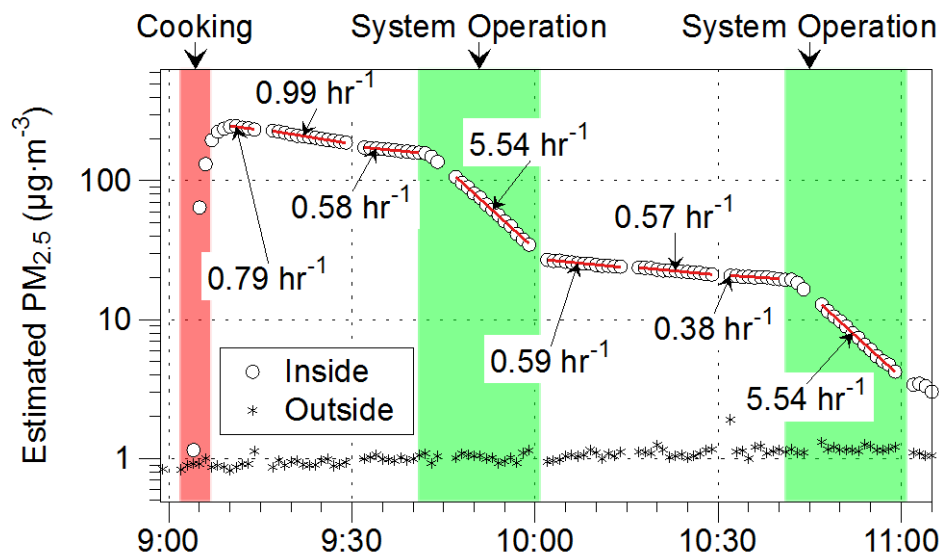


Figure S.18. Time series of estimated PM_{2.5} concentration calculated from size-resolved particle number concentrations during cooking experiment with System D on July 16, 2014.

Refer to Methods for details on this calculation. Fitted decay rates during each period reflect sum of all particle transformation and removal mechanisms including growth, ventilation, deposition and filtration.

Figure S.18 presents PM_{2.5} mass estimated from particle number concentrations. In this experiment, indoor PM_{2.5} from cooking reached a peak that was more than two orders of magnitude higher than outdoor levels. Over the two hourly cycles of intermittent system operation, indoor concentrations dropped to within 2x outdoor levels. PM_{2.5} decay rates during both periods of system operation were 5.5 h⁻¹, which is 4.8 h⁻¹ higher than the AER of 0.7 h⁻¹. Results for all particle size fractions will be included as appendices to the final project report at <https://www.arb.ca.gov/html/publications.htm>.

Figure 6 presents the reduction in time-integrated UFP relative to the baseline condition of no FAU operation. UFP data were missing from several of the experiments. “As tested” results represent a minimum benefit because intermittent systems operated only at the end of the hour. For the first 40 min, intermittent systems were identical to the Reference. Figure 6 also presents calculated reductions for systems operating over the entire hour (“Always On”). For intermittent systems (B, D, and G) the reduction was estimated by calculating the concentration over the hour assuming the first order removal rate observed during intermittent system operation. For the Reference, reductions for Always On are assumed to result from deposition of large particles in the FAU and ductwork.

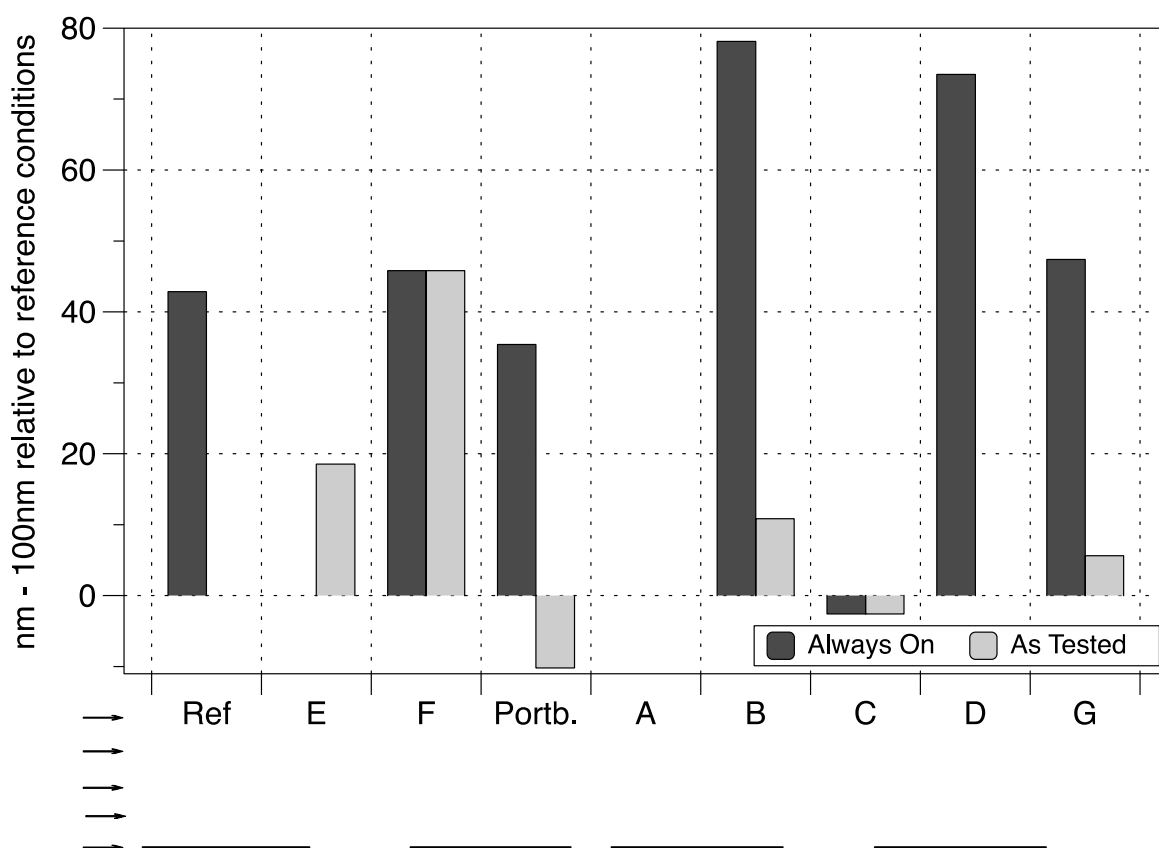


Figure S.19. Reductions in estimated UFP concentrations over 1h following an indoor cooking event, relative to Reference system. Systems with intermittent filtration were tested at the start of a cycle, i.e., with cooking occurring at the start of the 40 min interval between air handler operating periods. “Always on” is the estimated reduction with the recirculating filtration system operating continuously for the hour.

S.2.4 Performance for Ozone

Figure S.20 presents an example plot of processed ozone data from Reference system operation during the summer. During this period, outdoor ozone varied diurnally with daily 1h peaks of 30-60 ppb and troughs between 10 and 20 ppb. Indoor ozone determination was limited by instrument sensitivity, causing uncertainty in the 24h and 1h IO ratios.

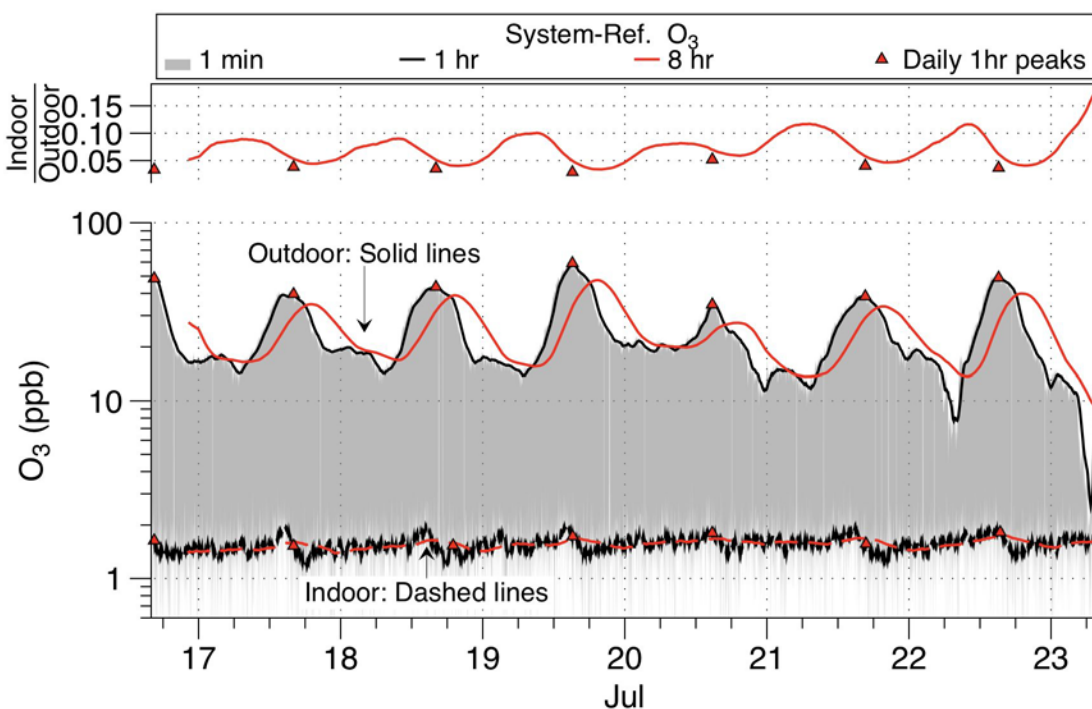


Figure S.20. Ozone concentrations measured outdoors and indoors during operation of Reference System, July 16-22, 2014.

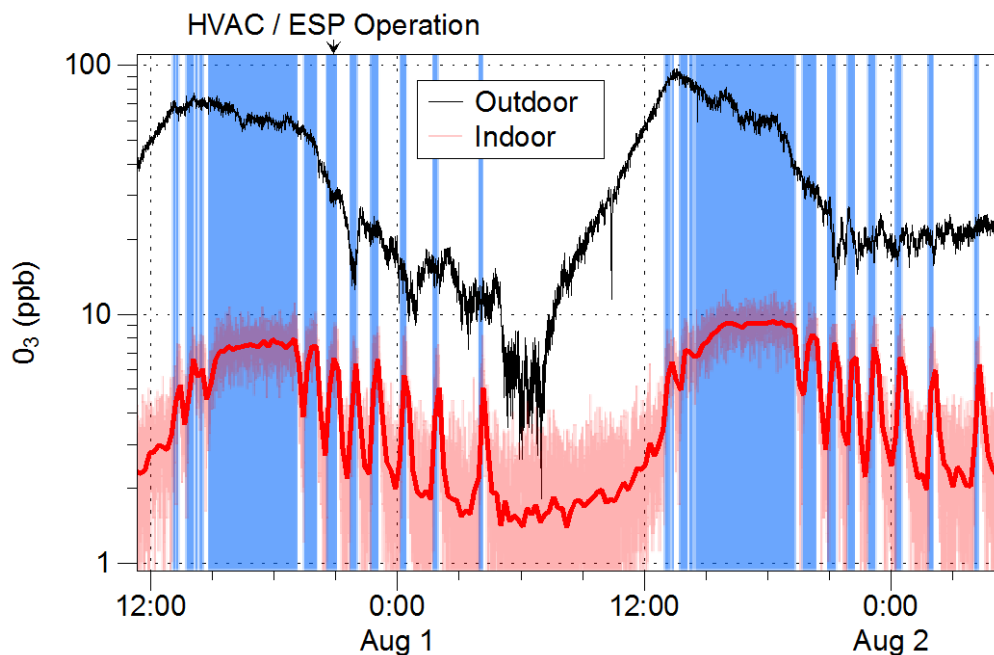


Figure S.21. Time series of ozone concentration for System B indicating ozone production when the FAU with electronic air cleaner operated (shown in blue shading).

For indoor data, the figure shows both the minutely measurements – which are noisy because the concentrations are close to the quantitation limit – and a smoothed fit.

S.2.5 Filter Impacts on Airflow and Power Consumption

The effect of filter resistance on airflow and power consumption is displayed in Figure S.22, which shows the FAU fan curves along with system curves representing the various filters. The two fan curves represent the two operating speeds of the FAU. Typical for this type of system, the fan was set at a higher speed for cooling than for heating. Fan curve data were obtained from the manufacturer's specification sheet. The system curves represent the combined resistance of the ductwork, FAU cabinet, cooling coils, and the filters. The actual flow delivered by a system is the intersection of the system and fan curves. We used filter curves from manufacturer specification sheets and adjusted the other resistance such that the combined resistance profile of the system curve matched the measured flow at the intersection with the fan curve for cooling mode. The close agreement between the measured heating mode airflow and the intersection of the fitted system curve with the heating fan curve provides some assurance that the system curve is correct.

The effect of resistance on airflow and power is presented in Table S.12. The PSC-motor used in the FAU is essentially a constant speed motor. Adding resistance to this system produces lower flows. The least restrictive system was the MERV4 filter. The ESP had very little internal resistance (which, for an ESP, is determined by the distance between the charging grids), and it had essentially the same effect as the MERV4 filter on system performance. We show for comparison purposes the calculated airflow and fan efficacy of the MERV16 filter without the PuraGrid product, even though we did not test pollutant removal of this configuration. The 2.5 cm MERV13 filter was more restrictive than the deep pleat MERV16 and it cut the flow by 4.9%. Combining the PuraGrid cartridge with the MERV16 filter created the highest resistance, which cut the flow by 12.3%. The drop in flow (determined from system and fan curves) caused a drop in power consumption (measured) and the fan efficacy remained nearly constant.

It is important to note that for some FAU fans and installed ducting, the increase in resistance of a higher rated filter could result in a larger reduction in airflow. In cooling mode, a drop in flow causes a drop in cooling coil temperatures and cooling efficiency. If flow drops too much the coil temperature can drop below freezing and block airflow. Concerns about these effects inhibit HVAC contractors from installing or recommending filters that are rated for higher fine PM removal. While use of low resistance filters mitigates the risk of a problem developing, it is important and valuable to design or retrofit ductwork for low resistance irrespective of filtration.

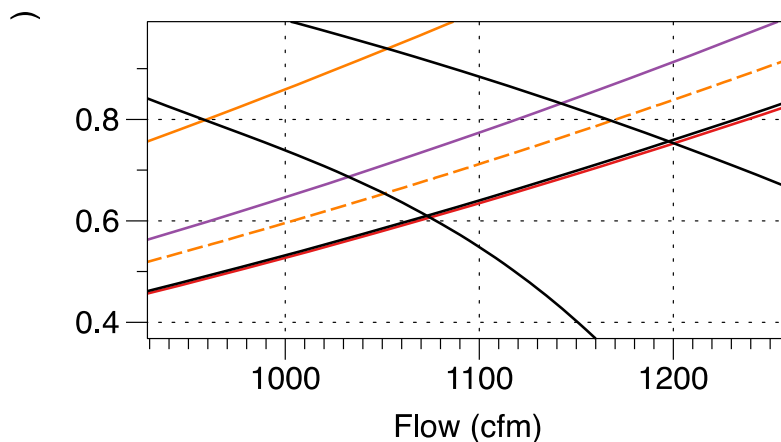


Figure S.22. Intersections of forced air unit (FAU) fan curves and inferred systems curves based on product specification sheets and measured airflows.

Table S.15. Calculated effect of filters on airflow, power, and fan efficacy.

Filter	System	Flow (cfm) ¹	Change in flow (%)	Power (W)	Change in Power (%)	Efficacy (cfm/W) ¹
MERV4	Ref, A, C, G	1200	-	660	-	1.82
ESP	B	1198	-0.2%	659	-0.2%	1.82
MERV16 (deep pleat) only	Not tested ²	1168	-2.7%	647	-2.0%	1.81
MERV13 (2.5 cm)	E	1142	-4.9%	626	-5.1%	1.82
MERV16 (deep pleat) + PuraGrid	D	1052	-12.3%	605	-8.4%	1.74

¹ Flow and fan efficacy provided in units most commonly used for evaluation of home and HVAC energy efficiency.

² Flow and power for the MERV16 filter without PuraGrid provided as relevant to system configuration without VOC removal media; this study did not test that configuration independently of System D.

S.3 References

- Cleveland WS, Devlin SJ. 1988. Locally-Weighted Regression: An Approach to Regression Analysis by Local Fitting. *Journal of the American Statistical Association* 83 (403): 596–610. doi:10.2307/2289282
- Cleveland WS. 1981. LOWESS: A program for smoothing scatterplots by robust locally weighted regression. *The American Statistician* 35 (1): 54.
- Cleveland WS. 1979. Robust Locally Weighted Regression and Smoothing Scatterplots. *Journal of the American Statistical Association* 74 (368): 829–836. doi:10.2307/2286407
- Lutz J, Franco V, Wong-Parodi G. 2006. ECM motors in Residential Furnaces: What are the Savings. Proceedings of ACEEE Summer Study 2006, Washington, DC.
- Sidheswaran M, Destailats H, Sullivan DP, Larsen J, Fisk WJ. 2011. Quantitative room-temperature mineralization of airborne formaldehyde using manganese oxide catalysts. *Applied Catalysis B: Environmental* 107: 34-41.
- Singer, B.C., Delp, W.W., Black, D.R., Destailats, H. and Walker, I.S. (2016) Reducing In-Home Exposures to Air Pollution. Final Report to California Air Resources Board for Contract 11-311. , Sacramento, CA.
- Walker, I.S. and Sherman, M.H. (2006) Evaluation of existing technologies for meeting residential ventilation requirements., Berkeley, CA, Lawrence Berkeley National Laboratory, LBNL-59998.
- Walker IS, Sherman MH. 2006. Evaluation of existing technologies for meeting residential ventilation requirements. LBNL-59998. Berkeley, CA: Lawrence Berkeley National Laboratory. Also published as California Energy Commission Report Number CEC-500-2007-051 (<http://www.energy.ca.gov/2007publications/CEC-500-2007-051/CEC-500-2007-051.pdf>).